Title Study of moisture in concrete utilizing the effect on the electromagnetic fields at UHF frequency on an embedded transmission line

Name Francois S. Malan

University of Luton

STUDY OF MOISTURE IN CONCRETE UTILISING THE EFFECT ON THE ELECTROMAGNETIC FIELDS AT UHF FREQUENCY ON AN EMBEDDED TRANSMISSION LINE

Francois S Malan

A thesis submitted to
the Faculty of Creative Arts and Technologies,
University of Luton,
in partial fulfilment of the requirements for the degree
Doctor of Philosophy.

Date: 4th September 2002

ABSTRACT

The aim of the research was to find an effective, reliable and cost-effective method for long-term monitoring of moisture in concrete structures. The slow diffusion rate of moisture through concrete requires that monitoring should be done over time scales of several years without periodic re-calibration. The solution arrived at was to use a quasi-coaxial transmission line, termed a cage-coaxial transmission line, as the sensing element. The transmission line, terminated in a short circuit, is encapsulated in a porous dielectric medium. It was found that the microstructure of the encapsulating medium had to be similar to the concrete in terms of capillary characteristics in order to track the moisture content of the material under test. The moisture in the encapsulating medium would change the electrical length of the transmission line by increasing the relative permittivity of the medium.

The method used makes it possible to measure moisture levels to full saturation. Moisture content can be measured in terms of a percentage of saturation, which will be of considerable help as an early warning system of possible frost damage.

A mathematical model was derived to calculate the relative permittivity in terms of moisture content in concrete. It was shown that to calculate the total permittivity of a solid porous medium with a dielectric mix formula, the formula must be expanded to include air, water and solid, before realistic values for the permittivity of the ingredients could be assigned. A dielectric mix formula was derived to account for the liquid to solid boundary effect on the permittivity of water in a solid porous material.

The foundations were laid for the development of a reliable and cost-effective probe based on an oscillator, operating around 1 GHz, using the transmission line as a tuning element. The frequency of oscillation is a function of the apparent length, determined by the permittivity and therefore the moisture content, in the transmission line dielectric material. A method to convert this frequency to a format that can be monitored on a data logger system is described. The high oscillation frequency eliminates the effect of ionic conduction from dissolved substances.

Acknowledgements

The author would like to express his deep appreciation for the help and guidance given by Dr Kemal Ahmet who acted as Director of Studies. His unswerving enthusiasm helped to add interest as well as depth to the work.

I would like to thank Dr Rob Hearing, head of the Department of Electronics at Luton University for his considerable help and suggestions that is much appreciated. My thanks to Dr Andrew Dunster of Building Research Establishment for his help on concrete technology. Also Mr Richard Tomlin for the preparation of test samples.

Dedication

This work is dedicated to my wife Evelyn for her support and encouragement.

List of Contents

List of Figures

List of Tables

Preface

This study was undertaken as partial fulfilment of the requirements for the degree of Doctor of Philosophy at the University of Luton in the Moisture Research Group (MORG) in the Faculty of Creative Arts and Technologies.

Monitoring the moisture content levels in concrete over long periods of several decades is important as moisture plays a pivotal role in the chemical reactions of the corrosion processes in concrete. It is an aid in the determination of the condition of concrete structures to plan remedial actions before permanent damage is caused. An investigation and literature search into present methods of detecting moisture in concrete indicated that there was a definite requirement for a reliable, non-destructive and cost effective method to determine moisture in concrete at specific points inside the concrete and not only on the surface or close to the surface. There is a requirement to measure moisture levels over the full range to saturation. A solution was found in the form of an embedded transmission line that serves as the tuning element of a sensing oscillator.

The University of Luton funded the study as a research studentship bursary. The work done had been presented at the Institute of Materials (IOM) Conference in Sheffield, September 2000, the Fourth International Conference on Electromagnetic Wave Interaction with Water and Moist Substances, Weimar, Germany, March 2001 as well as a paper presented at the 9th DBMC (Durability of Building Materials Conference) in Brisbane, Australia, March 2002.

Considerable interest was shown at the 9th DBMC Conference from various parts of the world due to the cost effectiveness and the unique capability of the sensor to measure moisture from a very low moisture content to a region above the hygroscopic range including saturation. Discussions with interested parties is currently ongoing.

DECLARATION

I declare that this thesis is my own unaided work. It is being submitted for the degree of Doctor of Philosophy at the University of Luton. It has not been submitted before for any degree or examination in any other University.

Francois S. Malan

11th day of September, 2002

Glossary of Terms

AC	Alternating current
Aquametry	Moisture measurement
BRE	Building Research Establishment
C_2S	Dicalcium Silicate
C_3S	Tricalcium Silicate
CH	Calcium Hydroxide
CRI	Complex refractive index
C-S-H or CSH	Calcium Silicate Hydrate
DC	Direct current
EM	Electromagnetic
FFT	Fast Fourier transform
GHz	Gigahertz 1×10^9 Hertz
HP	Hewlett Packard
IOM	Institute of Materials
IR	Infrared
LMS	Least mean square
MC or MC_v	Percentage of moisture content per unit volume
MC_g	Percentage of moisture content as a mass ratio
MORG	Moisture Research Group
MUT	Material under test
NMR	Nuclear magnetic resonance
OSA-NMR	One sided access nuclear magnetic resonance

Permeability	Defined by equation 3-3, used for hydrodynamic permeability unless specified as magnetic permeability
ps	pico second 1×10^{-12} seconds
PTFE	Teflon™, polytetrafluoroethylene
PVC	Polyvinyl chloride
RF	Radio frequency
RH, RH_v	Relative humidity percentage volumetric
SAW	Surface acoustic wave
SEM	Scanning electron microscope
SG	Specific gravity
Spice	General-purpose circuit simulation software. Originated at the University of California at Berkley.
TDR	Time domain reflectometry
TDRI	Time domain reflectometry imaging
w/c ratio	Water to cement ratio

Chapter 1. Introduction. Measurement of moisture in concrete.

This chapter gives a general background to the work carried out in the MORG group at University of Luton. It explains why the measurement of moisture in concrete is important, gives a general overview of microwave aquametry and summarises the findings of the study.

It is important to emphasise that the work carried out was of a multi-disciplinary nature. The work is unique in the way it combined various disciplines to provide an insight into the behaviour of moisture in concrete and the effect on the dielectric properties of concrete in the presence of moisture. Dielectric properties were studied with the aid of a unique design of transmission line called a cage-coaxial transmission line embedded in the concrete. The basis on which the electronic circuitry can be designed to develop and manufacture a cost effective moisture probe is discussed in some detail.

1.1. Background

Previous research carried out by the Moisture Research Group (MORG) of the University of Luton concentrated on the measurement of moisture in timber, using resistivity and capacitive measurement techniques (Dai, 1999, Jazayeri, 1999 respectively).

Considering the requirements for the long term monitoring of moisture in concrete, it was realised that methods suitable for timber did not suit the requirements for long term measurement in concrete structures. For example the surface conditions on exposed concrete structures are very different from the conditions inside the concrete matrix. Any sensor on the surface would be

subjected to large variations in the ambient conditions. As the aim was to find a method to measure the moisture content which in turn had to serve as an early warning system of potential damage to the concrete, it was a requirement that the moisture content could be measured at any selected point in the concrete. Surface measurements of either capacitance or resistance were therefore ruled out. Resistance measurements in drilled cavities as used by Dai (1999) for timber could conceivably be adapted for the measurement of moisture in concrete, but the method was rejected as will be explained in section 2.2.3. The work described here would indicate the reasons why microwave aquametry was the method finally chosen.

1.2. Importance of measuring moisture in concrete

Fagerlund (1996) states that a service life prediction of buildings often requires a calculation or measurement of the moisture level and moisture variation in the structure. This requires knowledge of the properties of the materials both with regard to critical moisture levels and with regard to moisture transport properties as well as the role that moisture levels play in the durability, or lack of, in concrete. The harmful chemical reactions in concrete all require the presence of moisture, which makes moisture the only common denominator in chemical attack. Water serves as the medium in which degradation takes place. A meaningful method of measurement that would serve the required purpose as an early warning system also requires some knowledge of the nature of the chemical attack and how moisture affects it. Chapter 3 investigates the physical characteristics of moisture in concrete, the pore structure and how moisture interacts with chemical substances to affect durability.

The normal rate of diffusion of moisture through concrete is extremely slow (Neville, 1995). The variation in moisture at a depth greater than a few millimetres (10 to 50 mm) would be very slow under normal circumstances. Relatively sudden changes could only be caused by some abnormal change in the structure, like the appearance of cracks, other mechanical damage or even chemical attack. Continuous monitoring of the moisture level over the lifetime of the structure should give an early indication of potential damage mechanisms

developing and remedial action could then be taken well before serious structural damage has taken place. It requires the use of a measuring system capable of reliable continuous monitoring over many years. The system does not have to be able to measure the moisture content as a quick one-off check at different points.

Extensive literature reviews concluded that there is an acute requirement in the construction industry for such a reliable, non-destructive and cost-effective method to track moisture variations in concrete and to monitor the moisture content over many years or even decades. See for example Parrott (1990) and Ahmet *et al.* (1999). It is recognised that while a range of methods exists for the monitoring of moisture in construction materials, whether based on the determination of moisture content or the relative humidity, these methods are predominantly aimed at either one-off measurements, or relatively short term monitoring over a few weeks or months. Measurements should be made at various key points within the concrete structure and not confined to surface or near-surface monitoring. Further, sensors should be capable of functioning reliably over the long-term without the need for re-calibration and must be low-cost to enable employment in large numbers. It should be capable of functioning as a stand-alone device connected to a data-logger and with the power supplied from a central point when readings are taken or through a remote radio frequency link with appropriate coding to extract data (see section 7.4.1). An external power supply is essential if the probe is to function over long periods or is embedded permanently into the structure.

Moisture measurement of concrete is required in three distinct phases of concrete use:

1. To determine the water content during mixing in a concrete mix when the correct water to cement ratio has an important bearing on the quality of the concrete.
2. To determine whether the concrete is dry enough to apply a final coating or flooring
3. To monitor and determine the condition of the mature set concrete in a structure over a number of decades.

The first case falls outside the scope of this research. Considerable work is being carried out in this field because of the importance of the water cement ratio in a concrete mix. The water cement ratio has a direct influence on the pore system of the cement paste (see section 3.2) and will determine the ultimate strength of the concrete. In the second case the actual moisture content is not very important. It is important however to be able to decide if the setting and drying out process is completed. Water combines with the cement particles to form the cement hydration product that hardens to form the cement paste (see section 3.2.1). Sufficient water must be available to complete the cement hydration process – otherwise the cement will not set properly. On the other hand, excess water not taken up by the hydration process will increase the porosity of the final matrix, which also has some effect on the strength or hardness of the concrete. A typical application is in floor slabs where water can only be evaporated from the upper surface. Flooring material is often waterproof and should not be applied until the floor is dry enough. The trapped moisture may adversely affect the covering. The third case is the topic of this investigation and will be examined in detail.

As concrete is a porous material, it takes up moisture from the atmosphere as well as from direct contact with water. The pore system of cement will be discussed in some detail in sections 3.2.2 to 3.2.4 as the pore system has a direct influence on the way moisture is absorbed by the material. Although water cannot damage concrete directly, it is the only common denominator in all chemical deterioration mechanisms in concrete (see section 3.3.2 on chemical attack and the durability of concrete). Damage to concrete can be pure physical damage or it can be a chemical reaction in the concrete matrix, which reduces the strength of the cement paste. The complex chemical reactions involved fall outside the scope of this work and will not be dealt with in any detail. It is sufficient to note that the normally high pH of around 14 of cement paste prevents corrosion of the steel reinforcement (section 3.3.3), which provides tensile strength to the concrete. Any corrosion of the steel will have a major impact on the strength of the structure. Corrosion of the steel could also cause spalling (see Figure 3-7). There are other chemical reactions in the concrete that affects the hardness of the cement paste itself and therefore the compressive strength of the concrete (section 3.3.2).

Present methods employed to monitor the moisture content of concrete, for example by monitoring the relative humidity in the concrete, are not suitable for long term and cost effective monitoring.

The main thrust of this investigation is towards the long term monitoring of moisture in concrete. It was considered important to gain an insight into and understanding of the way that moisture behaves in concrete, which in turn is closely related to the pore structure of the concrete matrix. This is then used as a foundation on which such an instrument or system can be designed, and the feasibility of the design principles for long term monitoring at relatively low cost can be tested.

1.3. Overview and general discussion. Microwave aquametry.

1.3.1. Microwave aquametry

The chair of the *Fourth International Conference on Electromagnetic Wave Interaction with Water and Moist Substances*, Weimar, Germany, Dr. Klaus Kupfer (Kupfer K, 2001), stated in his opening address that "Microwave Aquametry is the wide area of metrology that includes science and technology applied in Microwave Sensing of moist materials, foods, and other dielectrics".

There are a number of reasons why a high frequency (microwave) is advantageous for the determination of moisture in a number of applications.

1. Not affected by ion concentration and thus measures the free water only.
2. Can be used to measure the full complex permittivity, real and imaginary, of a dielectric substance (expressed in section 4.2.2), that in turn can help to determine the moisture level independent of the density of the mixture. The density independence is of major importance in the moisture measurement of grain and foodstuffs for example.
3. Sensor components can be made small enough to enable localised measurements to be taken.

The high relative permittivity of water due to the dipolar character of the water molecule (see section 4.2.1) increases the relative permittivity of a porous

material containing moisture. The picture is complicated by the way the water molecules behave at the boundary of solid and liquid. The theory on dielectrics applicable to this work will be discussed in more detail in Chapter 4.

1.4. Main findings of the thesis.

The multi-disciplinary nature of this study is unique in the way it utilises various disciplines to provide a foundation for further work in sensor design to measure moisture in concrete and other solid porous substances, notably various building materials and soil.

1.4.1. Transmission line sensor

Of the various methods used in microwave aquametry discussed in Chapter 2, it was decided to use a transmission line in a novel way. After early attempts to measure the influence of the concrete on the transmission line characteristics, as would be the normal practice in microwave aquametry, it was decided to change the approach completely and limit the electromagnetic field to a 'cage-coaxial'. This 'cage' is filled with an appropriate filler material, placed in close contact with and in moisture equilibrium with the surrounding concrete matrix. A typical filler material would be either cement paste or mortar produced from a mix of cement and fine aggregate (sand). The advantages and disadvantages of this approach will be discussed in more detail in Chapter 6.

The transmission line sensor studied in this work developed into different versions depending on the application (see Chapter 6). The porous ceramic clay that appeared to be the ideal as a general purpose filler material turned out to be entirely unsuitable. This however led to a better understanding of the behaviour of moisture in a solid porous medium and more importantly where there is a mix of materials, which is a situation often encountered in practice especially in building technology (see section 3.4). It highlighted the importance of a thorough understanding of the characteristics of the pore system and its effect on the behaviour of moisture in concrete. In section 3.2, the pore system in concrete and how it is formed by the process of cement hydration is discussed.

The study provides a solid basis on which to develop the transmission line moisture sensor further into a final practical model. Section 7.4 discusses the ways it could be developed. It gives an indication of the potential of a final product and a monitoring system based on this work.

1.4.2. New findings

The new findings can be summarised as:

a. A novel method to measure the moisture in concrete to overcome some of the disadvantages of current methods.

b. A more suitable mathematical model to calculate the total relative permittivity of concrete as a function of the moisture content.

c. The basis for a low component count and therefore reliable and cost effective electronic circuit to monitor the relative permittivity of the material in the probe.

d. Measurement of moisture as a percentage of the maximum full saturation moisture content made possible by the method employed and a first in this field.

The new method of measuring moisture in concrete was developed to overcome a number of problems encountered in practice. The 'cage-coaxial' transmission line filled with an appropriate filler material uses the advantages of a closed electromagnetic field in a coaxial type of transmission line and yet is able to measure the moisture in the surrounding concrete matrix (see section 4.4.2). Other workers in microwave aquametry have used transmission lines as a resonant cavity or using the material under test as a load impedance at the end of a transmission line or waveguide (see section 2.2.6). In this study the transmission line is used as an inductive tuning element in an oscillator circuit. It allows a much shorter transmission line to be used thus reducing the depth over which measurements are taken (better depth resolution) whilst still remaining in a frequency band that can be handled with ease with cheap electronic components (see section 7.3). Further work can be done to determine the minimum practical length of transmission line that can be used as circuit simulations showed that the

oscillator could handle frequencies at least twice as high as those achieved with the 30 mm transmission line. It would mean a transmission line of only 15 mm in length. Apart from better depth resolution a smaller transmission line, material volume would reach equilibrium with the surrounding matrix sooner. The very slow rate of moisture diffusion[1] through concrete (see section 3.3.1) means that the distance over which moisture must diffuse into the sensor transmission line filler material should be kept as small as possible.

A mathematical model to calculate the permittivity of concrete as a function of moisture level was developed (see section 5.3). Such a model is useful in calculating the predicted permittivity with changes in the dielectric mix. There are a number of dielectric mixing formulae in the literature and most of them are only valid for a certain range of moisture content (refer to section 5.3.1). This model is unique because it is linear and covers the whole range of moisture content from dry to saturation with an error of less than ±0.1% moisture content. The fact that, like all the other models it tends to be material specific and only applies to concrete of a certain type, is quite acceptable. The adjustment that had to be made to the model was to allow for the reduction in the relative permittivity of water from that of bulk water to a lower value to allow for the fact that some water molecules are bound to the solid of the pores walls (see section 5.2.3). That is why it can only be applied to the specific pore system of concrete with a specific total pore surface (about 200 m^2/g in the case of cement paste, refer to section 3.2.2).

A search of current literature indicated that the proposed use of a modified Collpits oscillator to determine the change in the electrical length of an embedded transmission line appears to be a first in the field of microwave aquametry. As mentioned previously such a circuit does not use the transmission line as a pure quarter wave resonator, but uses the equivalent inductive impedance of a short-circuited transmission line at a frequency for which the transmission line is shorter than ¼ wavelength. Although not used in this study, this arrangement has the potential to measure both the real and imaginary part (frequency and amplitude of oscillation, see section 7.1) of the complex permittivity. This is done in

[1] Diffusion at low MC is mostly through the diffusion of water vapour and dominated by capillary action at higher MC

microwave aquametry to reduce the effect of density of the material on the final value of moisture content (see section 2.1.1).

Finally, phase velocity measurements in concrete and specifically cement paste showed up some important characteristics of the apparent permittivity at different discrete frequencies around the frequency band of interest (see section 4.5.4). The variation in apparent permittivity could not be explained but was thought to be due to the effect of the non-ideal short circuit of the transmission line resulting from the fact that it is not a pure coaxial transmission line.

1.5. Layout of Thesis

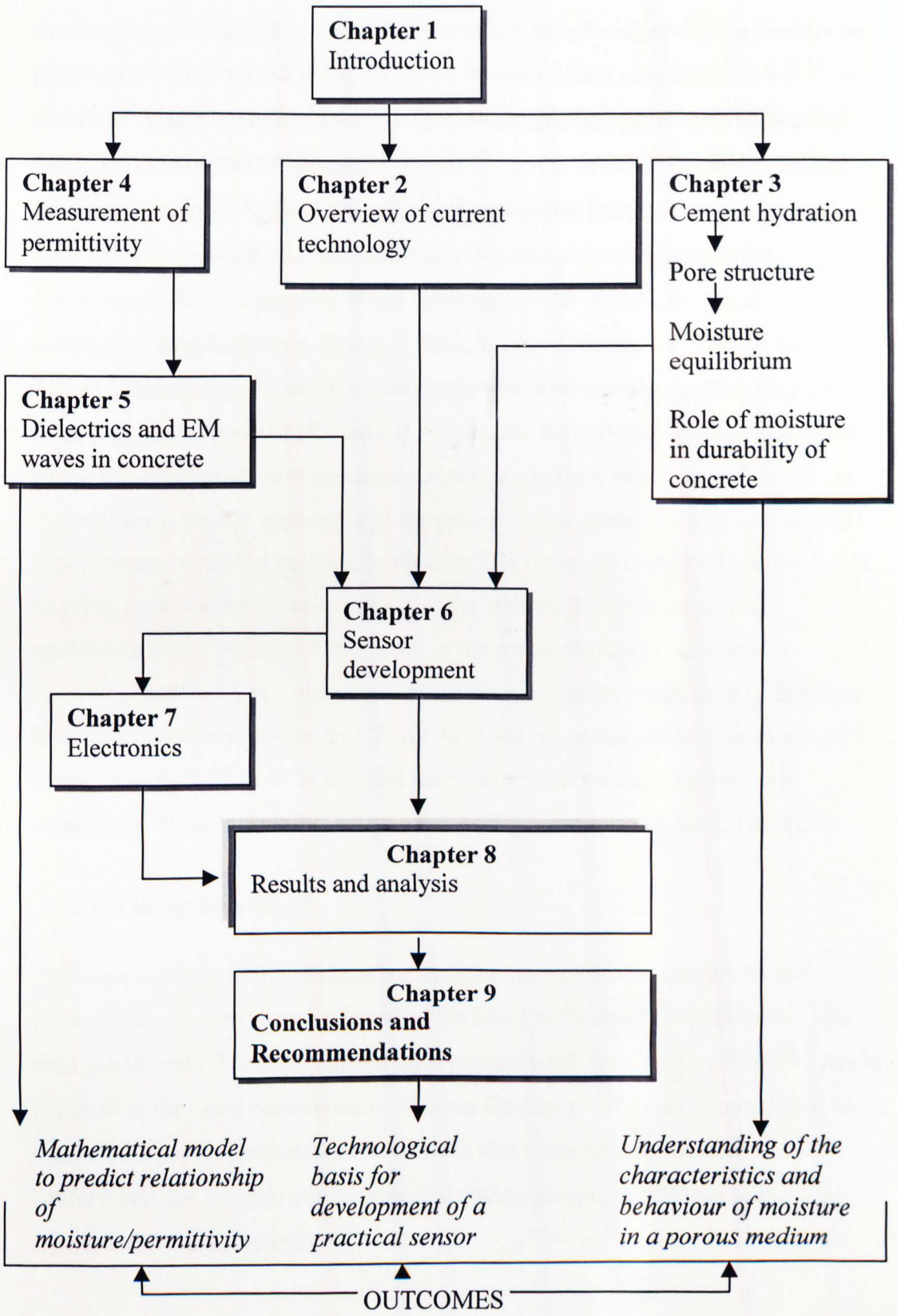

Chapter 2. Overview of current methods to measure moisture

In this chapter a brief review of the current methods of moisture measurement or aquametry, which has a bearing on the work done in this research, will be discussed. The *Fourth International Conference on Aquametry* held in Weimar Germany in May 2001 (hereinafter referred to as the Weimar Conference) is of great significance as it provided a convenient window into the latest work being done globally in this field. Useful information also came from the *Third Workshop on Electromagnetic Wave Interaction with Water and Moist Substances*, held in Athens, Georgia, USA in 1999 (hereinafter referred to as the Athens Conference). These conferences covered moisture detection with high frequency radio waves in all kinds of substances, notably in agricultural products where the determination of moisture content is of prime importance. Not all the methods are therefore applicable to the measurement of moisture in concrete but they provide extremely useful information. The literature review of section 2.1 is an effort to provide a broad overview of the state of the art in microwave aquametry with a potential application in the measurement of moisture in concrete. Section 2.2 is a discussion of methods to measure moisture in concrete including microwave aquametry. Some methods of general interest in moisture measurement, that had to be rejected immediately for this application, are mentioned. There is therefore some overlapping between sections 2.1 and 2.2.

2.1. Literature review.

The work reported in the Weimar and Athens international conferences on microwave aquametry covered most of the latest work that is being done in this field world-wide. The most current and relevant work is mentioned here. To avoid duplication the latest conference in Weimar Germany will be mentioned first as some of the papers presented covered work that were reported at both conferences, the Weimar conference often being an update of some of the work reported at Athens, Georgia.

2.1.1. Fourth Conference on Microwave Aquametry and reference to papers at Weimar, Germany, May 2001.

Völgyi (2001) described microstrip sensors that could be adapted for use as a transmission line in concrete. This paper gave an overview of some of the techniques described in the literature. Of interest and with possible use in the transmission line and oscillator investigated here, is the idea to use the same oscillator circuit with a switching element alternatively connecting the transmission line and a reference transmission line or tank circuit. The measured frequency shift will then be used as a measure of the moisture.

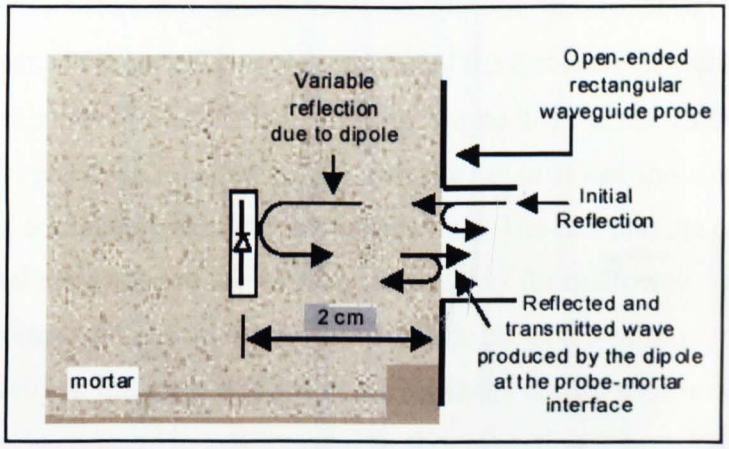

Figure 2-1 Embedded dipole with open-ended waveguide.
Extracted from Völgyi, 2001.

In the same paper mention is made of a technique where a switching dipole is embedded in the material like plaster or cement. The dipole is switched at low frequency with a switching diode. An open-ended waveguide probe is placed against the surface as shown in Figure 2-1. The amplitude of the change in the reflected wave is an indication of the transmission loss (indicating ε'', the imaginary component of the complex permittivity) in the material due to moisture. In the author's view it is only really useful if the time delay can also be measured (ε', the real part of the complex permittivity). The time delay, therefore the velocity of propagation, can be determined by measuring the phase shift between the modulating and modulated signal, taking the distance to the dipole into account.

The use of stripline technology for the measurement of permittivity was discussed in some detail in the same paper. The striplines described were used both as a microwave antenna and as a transmission line for measuring the change in relative permittivity and therefore the moisture content of the material under test.

Joshi and Pollard (2001) reported on a microstrip resonator technique to measure permittivity. The paper describes a method in which the material under test (MUT) is placed on top of a stripline transmission line as mentioned by Völgyi (2001). Because the MUT were all thin layers, the calculation of permittivity was done as an extrapolation to a thick layer assuming that there is a linear relationship between thickness and effective permittivity, or at least that this relationship is known. The paper compared the test and calculation results with a typical mixture formula. It is interesting to note that the results of the mixture formula agreed with the test results over the range of low moisture content, but deviated completely at higher moisture levels. The fact that the calculation uses a fractional mass content for moisture is incorrect for microwave aquametry and will be discussed in detail in section 3.1. The method is strongly influenced by the permittivity in the surface layer, which limits its use for the measurement of moisture in concrete to be discussed further in section 2.2.

Glay *et al.* (2001) gave an idea of the advantages and disadvantages of free space microwave aquametric measurements. The paper described a method where a simple horn antenna is used to scan a surface in one dimension to give a profile of the moisture distribution. Presumably this technique can be expanded to two dimensions. However, no depth information is gained, something which is important in moisture measurements in concrete. This provides a method that could be of value to study damp in walls (rising damp). Even in this case an indication of the depth of the moisture would be better as it then could make a distinction between say rising damp and condensation on the surface. The other problem is that it requires a reflector in the form of a metal plate on the opposite side of the material, making it totally unsuitable for studying damp in concrete structures such as bridges. This is discussed further in section 2.2.6.

Woodhead *et al.* (2001) described another method using Time Domain Reflectometry (TDR) on the surface of a material with what they call Time Domain Reflectometry Imaging (TDRI) to map the distribution of permittivity. The method involves considerable data processing using an iterative process starting from an assumed moisture profile. The paper did not describe the hardware involved and assumed data received from a TDR probe that was not described. Third dimension information must be obtained by means of orthogonal measurements from the side. Figure 2-2 shows the results as reported in the reference.

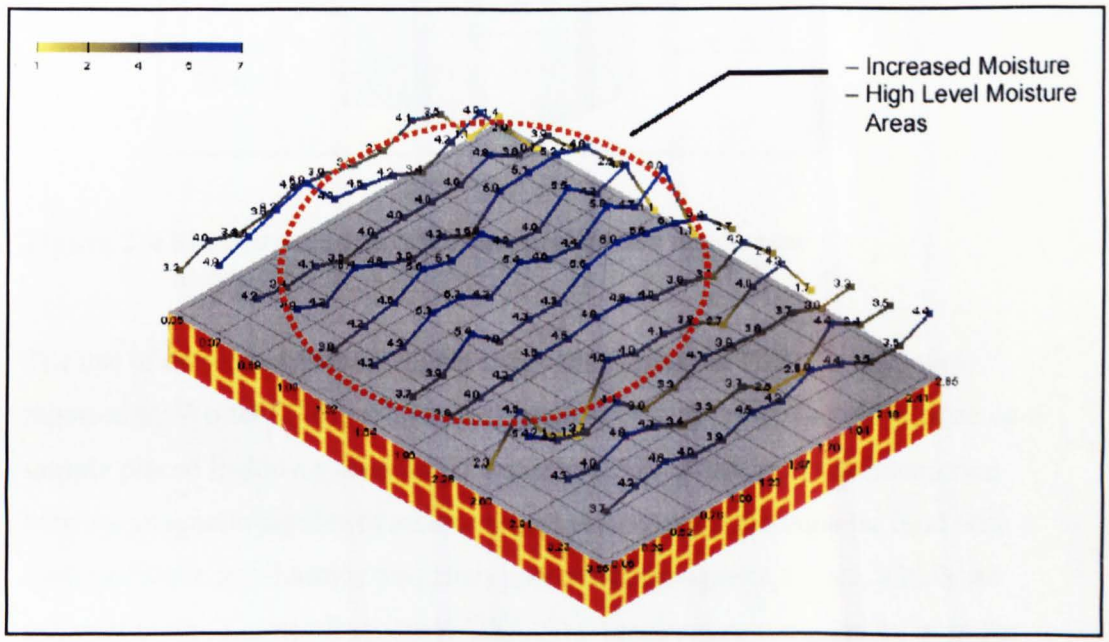

Figure 2-2 Moisture distribution using TDRI

(extracted from Woodhead *et al.*, 2001)

Mathematical modelling of 'One Sided Microwave Moisture Sensors' was described by Tsentsiper (2001). The model used is a quarter wave coaxial resonator that is shown in Figure 2-3.

resonator, interaction volumes of about 20 cm^3 and penetration depths of about 3 cm can be reached. The shape of one of these heads is shown in Figure 2-4.

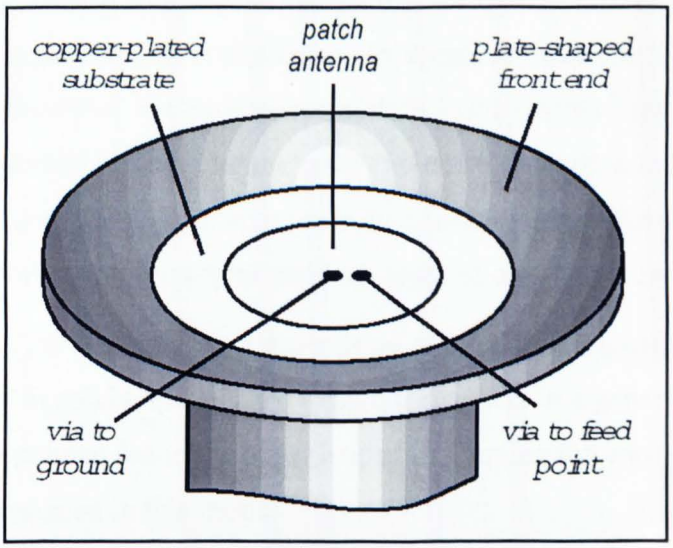

Figure 2-4 Shaped antenna head for microwave applicator
as described by Göller (2001)

The use of one-sided access nuclear magnetic resonance (OSA-NMR) was reported by Wolter (2001) where NMR measurements are customarily done on a sample placed inside a cylindrical container. NMR is based on the interaction between magnetic dipoles of atomic nuclei precessing in a magnetic field with a specific frequency (Larmor frequency) and electromagnetic waves, which are resonant to this Larmor frequency. OSA-NMR instrumentation can be used for depth profiling of the NMR signal in the specimen. With present equipment, the resolvable depth increment is about 1 mm and the maximum measuring depth is approximately 30 mm. A method to distinguish between the hydrogen atoms in the wood and the hydrogen in the liquid (water) was shown. The density of the material, which is an important parameter in the manufacture of chipboard, can be determined and from that, plus the volumetric moisture content, the gravimetric moisture content can be calculated. A point of interest in this paper is the distinction made between the relaxation times of hydrogen in different types of water depending on the degree to which the water molecules and thus the atoms are bound. Bounding of water molecules due to the adhesive force with solid and the effect on permittivity is discussed in 5.2.3.

2.1.2. Discussion of some papers delivered at the Athens Conference that have a bearing on this study.

Methods of density independent measurements were described by Kupfer (1999). This is an important aspect of microwave aquametry that has the potential to overcome the errors due to density variation in the material under test. It is of greater importance in agriculture when the moisture in grain is to be determined, sometimes on a moving conveyor belt. In a solid material like concrete it could still be useful especially where different types of concrete are measured.

Jachowicz (1999) gave a good description of the limitations of the measurement of moisture in solid materials and treated the subject in a general manner. The limitations pointed out in the paper helped in pointing the way to proceed in the research presented in this thesis.

Schmugge and Jackson (1999), also referred to in section 2.2.7, looked at remote microwave sensing of soil moisture. The radiation of soils with different moisture contents can be sensed at a wavelength of around 21 cm from remote platforms like aircraft or satellites. Radiation responds to moisture to depths of 5 cm and through moderate vegetation cover.

Zhang and Okamura (1999) described a method to measure the moisture content in wood independent of density using the phase shift of two microwave frequencies. The sample was placed between a transmitting and receiving antenna and the signal transmitted and received on a RF Vector Network Analyzer.

Wisniewski (1999) used an insulated dipole as antenna inside a material under test to measure the moisture content. This is an interesting method that could probably be applied with some success to the measurement of moisture in concrete by inserting the dipole into a drilled cavity in the concrete.

Völgyi (1999) described a system for the assessment of plasterboard quality during manufacture. The microwave transmitting and receiving antenna were on one side of the board and reflectors were placed on the other side. Delay and transmission loss could be measured with this arrangement to determine board quality and moisture content.

Jazayeri and Ahmet (1999) introduced a multi-electrode capacitance method to measure moisture gradient in timber. This method deviates from the conventional two-electrode capacitance method to give some measure of moisture gradient.

Vaz and Hermann (1999) used Time Domain Reflectometry on a two-wire transmission line probe attached to a penetrometer to measure the moisture content of soil. This is a close equivalent to the transmission line method used in this study for concrete. The transmission line for the soil moisture measurement could have been used as a tuning element (as was done in this study) instead of the TDR measurement. The only problem with the use of such an arrangement in a solid like concrete is the less intimate contact with the surrounding material due to small variations in the diameter of the drilled hole. Even a very small air gap between the transmission line and the surrounding material introduces considerable errors.

The free space method described by Lasri *et al.* (1999) is discussed further in section 2.2.7.

The paper by Leschnik and Schlemm (1999) described in general terms a system where the transmitting and receiving antenna functioning at around 2.45 GHz were inserted into two separate holes in the concrete. This method promises to measure the complex permittivity of the material between the antennas, which was claimed to give an indication of the salt content apart from the moisture content. The salt content affects conductivity, which in turn will affect the imaginary part of the complex permittivity. By determining both the real and imaginary parts of the complex permittivity, it was claimed to obtain some indication of the salt content of the material under test.

Finally in this brief review Venkatesh and Raghavan (1999) discussed the use of cavity perturbation techniques to determine the complex permittivity of a sample material placed inside a resonant cavity.

The list is just an example of the range of areas presented at the conference that have some relevance to the present study.

2.2. Overview of different methods to measure moisture in concrete

A number of different methods are currently used to measure the moisture content in concrete. It will be seen that not one of the methods used met the requirements of a system for ongoing long term moisture content monitoring in concrete.

2.2.1. Gravimetric method

The gravimetric method to determine moisture can be carried out by taking a drilled sample of the concrete and then determining the moisture contained in the sample by oven drying and comparing the mass before and after drying. This is the most basic and reliable method as the measurements are direct and are often used for the calibration of other, non-destructive methods. The destructive and time-consuming nature of the gravimetric method makes it impractical for ongoing monitoring on a structure. Although the drilled holes can be 'plugged', the process is time consuming and not suitable for continuous monitoring. The labour intensive nature of this method means that the monitoring will not be as frequent as required and there may be an upper limit to the number of holes that can be drilled. Although accuracy is good, it must be accepted that some loss of moisture due to heating and evaporation during the drilling process will affect the result. Care must also be taken to ensure that no other volatile compounds are driven off during the heating process. Also, some moisture will be retained in the form of non-evaporable water (see section 3.2.5). This is water trapped in the cement gel after oven drying. Presumably this non-evaporable water cannot take part in any transport of chemicals and is therefore not important in the consideration of moisture content. It will however have an effect on the relative permittivity of the dried cement paste. By disturbing the solid matrix with drilling, some of the closed pores may be opened and some previously non-evaporable water released.

2.2.2. Chemical analysis of drilled sample

A traditional method of measuring moisture is to analyse a drilled sample chemically instead of gravimetrically. A measured quantity of the drilled sample is placed in a pressure vessel where it is mixed with carbide. The vessel, which

has a pressure-measuring gauge, is sealed and shaken to enable the carbide to completely react with the water, forming acetylene. The amount of gas formed in the reaction is directly proportional to the amount of water present. The increase in pressure is read off the pressure gauge dial, calibrated directly in percentage moisture content. Again there is likely to be some loss of moisture during the drilling process as in the case of the gravimetric method. A convenient portable test set is available for carrying out the test in the field, which makes it less time consuming than the direct gravimetric method. Once again this method is not suitable for the continuous monitoring of moisture.

2.2.3. Measurement of Resistance to determine the Conductance as a function of Moisture Content

Methods to measure the resistivity of concrete were explained in the paper by Weydert and Gehlen (1999):

1. Two-electrode method
2. Multi-ring electrode
3. Wenner probe

The two-electrode method is a direct measurement of resistivity on a sample block of the material. A sample block is placed between two electrodes covering opposite sides of the block and the resistance measured. The resistivity ρ can then be calculated directly from the formula:

$$\rho = \frac{RA}{l} \qquad \textbf{Equation 2-1}$$

Where

ρ = Resistivity (Ω m)

R = Resistance measured (Ω)

A = Area of the block face (m^2)

l = length of the block (m).

The Multi-Ring-Electrode is a special embedded sensor composed of several 2.5 mm thick stainless steel rings which are kept separated at a distance from one

another by 2.5 mm thick insulating plastic rings. Cable connections in the sensor enable the resistivity of the concrete to be determined between each pair of neighbouring stainless steel rings by means of AC resistance measurement. The measuring process with this sensor offers an advantage over other resistivity measuring processes in that the depth-dependent resistivity can be determined at intervals of 5 mm.

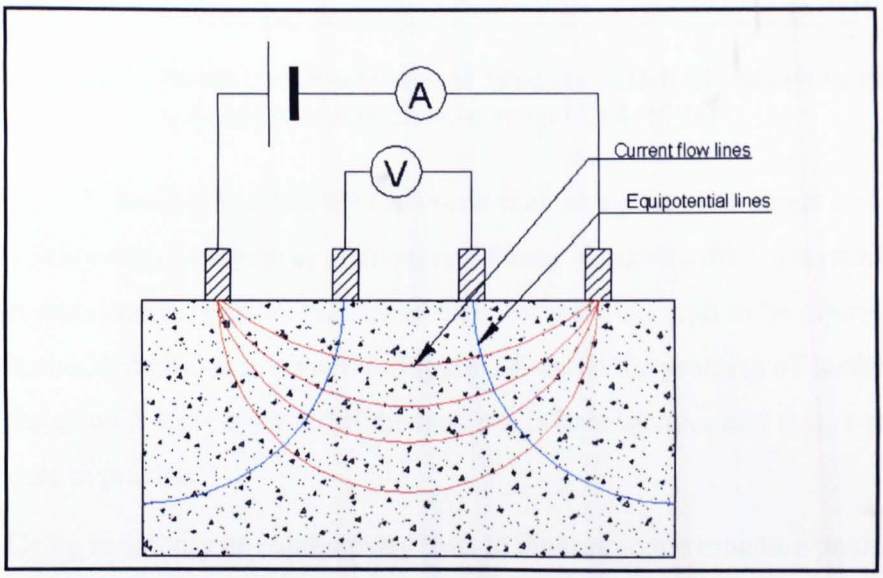

Figure 2-5 The Wenner probe principle of operation

The Wenner method works from the concrete surface by using a special arrangement of four evenly spaced electrodes to inject a constant alternating current between the outer pair of electrodes as shown in Figure 2-5. The voltage measured between the inner probes leads to the resistance of the concrete. The cell constant for the Wenner probe is found using Equation 2-2, derived for a semi-infinite homogeneous material. Commercially available devices give the resistivity as output directly with an internal conversion of the determined resistance, assuming the requirement of a homogeneous material has been met.

$$\rho = R \times k_{cell} \qquad \textbf{Equation 2-2}$$

Where

ρ = resistivity (Ω.m)

R = Electrolytic resistance (Ω)

k_{cell} = cell constant given for the specific configuration.

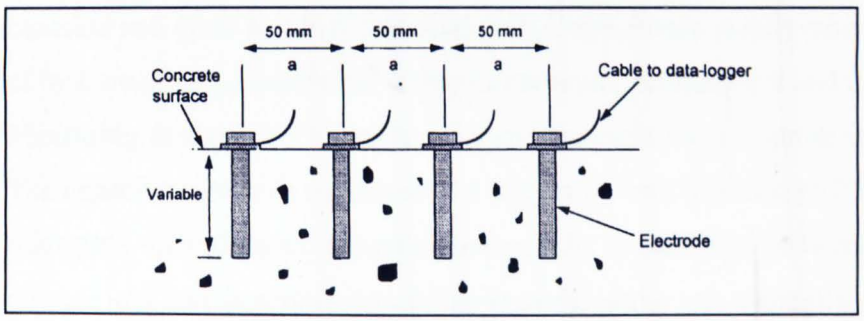

Figure 2-6 Embedded electrodes of Wenner resistivity measurement
(extracted from Hammersley and Dill, 1998)

The Wenner method has the drawback that the surface resistance can change quickly with a change in ambient conditions. Concrete dries out rapidly on the surface and the contact resistance then becomes too high to be of practical use. Embedded probes as shown in Figure 2-6 avoid the problem of surface drying. Equation 2-2 is only valid if the material is homogenous and that is seldom the case in practice.

Using resistivity or conductivity tests to determine the moisture content in concrete is fraught with difficulties. Conductivity is a measure of the free ions available to conduct the current. Although water is needed for this, the concentration of dissolved substances in the concrete can vary greatly especially close to the surface. Concrete structures are invariably exposed to the environment where conditions can change all the time. The high moisture gradient close to the surface means that surface moisture is seldom an indication of the moisture content of the concrete a few millimetres below the surface. Steel reinforcement can seriously affect the resistance reading, something that is bound to happen if a probe like the one in the multi-ring method is inserted into a drilled hole which happens to be close to steel reinforcement bars in the concrete. The conductivity is also strongly affected by temperature (Hammersley and Dill, 1998).

2.2.4. Capacitance measurements

If the problem associated with surface measurement of moisture (condensation, surface wetting by rain and mist etc.) can be dealt with or is acceptable, the capacitance method is an excellent way to determine the moisture content close to

the surface. A number of instruments are available to measure the moisture in concrete and other building materials using capacitance measurement. This type of instrument is calibrated for different materials, temperature and thickness. Measuring moisture with the capacitance type instrument is quick and convenient. The capacitance can be measured at a frequency with a period well above the relaxation time of the ions from dissolved salts in the structure to reduce the effect of such ions on the permittivity of the material under test, typically above 400 MHz. Provided the calibration has been carefully carried out, it is a very good indication of moisture. No drilling is required. The instrument is simply pressed against the material under test and the reading taken. The fact that it can measure moisture on or near the surface makes this type of instrument suitable for measurement of effects like rising damp in buildings. Jazayeri and Ahmet (1999) describe a system with multiple electrodes to obtain some depth information of the moisture content in timber. The system can conceivably be adapted for use on concrete, but the depth (10 to 20 mm) is still too little to meet the requirements of a monitoring system and conversely can be affected by steel reinforcement close to the surface. Again the strong surface effect will render the method useless on exposed structures.

The usefulness of the capacitance method for measurement of moisture in concrete is limited by the fact that it cannot detect the type of moisture that is potentially harmful to concrete (see section 3.3). It has to be assumed that exposed concrete structures will always be as wet on or close to the surface as ambient conditions dictate and the method should only be used on internal/indoor surfaces. As mentioned in section 2.2.3 there would always be a high moisture gradient close to the surface of exposed structures due to rain or condensation formed on the surface. Under dry conditions there could be a high moisture level close to the surface due to previous ingress of moisture, but the dry surface layer would reduce the permittivity measured thus indicating a low moisture level.

From the above argument it can be seen that the surface capacitance moisture meter is not suitable for exposed structures. It can detect moisture just below the surface even if the surface is completely dry and is a good indication of potential

problems like rising damp in buildings. Comparative readings over an entire surface help to map out the damp areas.

2.2.5. Relative Humidity (RH) as an indication of moisture content.

The moisture in concrete can be measured by mounting an RH probe in a drilled hole to form an enclosed cavity in the concrete. This is an excellent method to measure the "dryness" of the concrete and is used by the Building Research Establishment (BRE) as one of the standard methods to detect moisture (Dunster A, personal communication, BRE, 15/10/1999). The measurement of relative humidity is discussed in more detail in section 3.4.2 where it will be shown that the relationship between RH and moisture content is dictated by the pore structure of the material as well as the temperature. The air in the drilled cavity could reach a relative humidity of close to 100% even before the concrete is fully saturated with water. The method can therefore only detect moisture up to a certain level. It will be shown in section 3.4.2 that RH measurement can be translated to moisture content only when the total volume of pores smaller than a specific size and the adhesive force between water and the dry material in the pore system are known. Although RH is therefore an excellent qualitative indication of the "dryness" of the concrete, measurement of relative permittivity (ε_r) is a better indication of moisture content. Relative permittivity is less dependent on the pore characteristics (only affected by boundary effects as discussed in section 5.2.3) and can measure moisture content over the full range of completely dry to saturation.

An example of a simple relative humidity test to check the state of dryness of flooring or a wall, is by measuring the relative humidity in the air above the surface under a plastic covering or container that is sealed from the outside atmosphere. In fact the presence of droplets from condensation inside a transparent container with the open side pressed and sealed against the concrete surface is a clear indication of evaporation from the surface, indicating that the RH is 100% and the material (concrete or plaster) is still drying out.

2.2.6. Microwave resonators and sensors

Advances in microwave aquametry have been boosted by the availability of cheaper high frequency electronic components. The development in communication technology with the advent of cellular phones brought about a rapid development in components that can handle frequencies above 1 GHz. Part of this development is the availability of very small surface mount components. The small components make it possible to use normal printed circuit boards for circuits that could handle high frequencies due to the reduction in the length of transmission paths and stray capacitance between components. Generally microwave resonators would be used on samples of the material under test placed inside the resonator (Rouleau *et al.*, 1999). It will be seen that the method proposed in this study is closely related to this method (Chapter 6).

A fringe field resonator microwave moisture meter is described by Daschner *et al.* (2001), which does not need to have the resonant cavity filled with the material under test. The multivariate approach of multiple linear regression described seems to be too complicated for the simple moisture sensor planned. There may be some merit in considering a fringe field resonator described in the paper as a probe for surface moisture measurements that could reduce the density dependence of a simple tuned resonator type probe. Surface measurement and the complexity of the data processing system appears to have ruled it out for the purpose of this study.

A microstrip resonator described by Joshi and Pollard (2001) is another type of resonator used to measure permittivity and thus moisture content. The material under test is placed against the microstrip that forms the resonator. The change in resonator frequency and quality factor (affected by the loss in the resonator) give an indication of the real and imaginary parts respectively of the complex permittivity. A general discussion of microstrip sensors in microwave aquametry is discussed by Völgyi (2001).

The method used by Göller (2001) (see section 2.1.1) has great potential for measuring moisture in concrete near the surface as a surveying tool. Due to the bulk and cost of the equipment the method is not suitable for long term

monitoring where the sensor is required to remain in situ for extended periods. This is a comment that applies to most of the microwave resonator and antenna sensors.

2.2.7. Remote microwave sensing and Radar detection of moisture

A method that could possibly be applied to the measurement of moisture in concrete is described by Schmugge and Jackson (1999). The thermal emission from the surface is observed at frequencies in the 21cm wavelength region. The advantage is that at this longer wavelength, as compared to infrared, the moisture is observed in a surface layer a few tenths of a wavelength thick. At 21cm wavelength moisture can be detected between depths of 0 to 5cm with a microwave radiometer. No indication could be found in the literature that this method has been tried on concrete but as mentioned in section 2.2.6 it has the potential to be used as a surveying tool.

Lasri *et al.* (1999) describes a free space moisture measurement of cellular concrete at 2.54 GHz using a transmit/receive horn antenna coupled to an S-parameter measuring system to measure transmitted and reflected signal levels from a metal reflector through the specimen under test (Figure 2-7). His method is a mixture of the technology used as described in section 2.2.6, and remote sensing. Excellent results were obtained but from a practical point of view there is the problem of using a reflector on the other side of a known thickness material under test when measuring an existing structure. The bulky and expensive equipment involved makes it impractical as a method for continuous monitoring of moisture conditions in a structure.

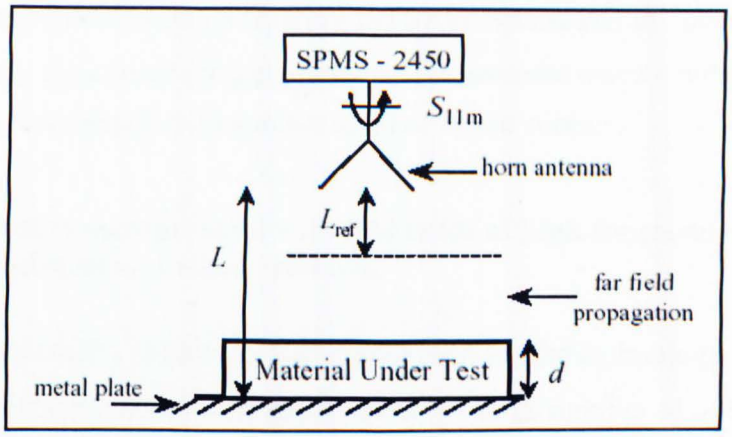

Figure 2-7 Free space measurement of reflected signal with transmitting and receiving microwave horn antenna.
Extracted from Lasri *et al.* (1999).

The method described above is similar to the use of radar. When considering radar as a possible means of detecting moisture, the author came to the conclusion that the reflected signal from a moisture gradient will not be detectable. The diffused moisture front will tend to dissipate the signal rather than reflect it back to the receiver as reflections from different points over a distance of the same order of magnitude as the wavelength of the signal tend to cancel out (due to the phase difference between them). A metal reflector will have to be placed on the opposite side of the structure as described above and the apparent distance through the concrete measured, the change in permittivity due to moisture can be measured (using Equation 4-16 in section 4.3). Again however, the other side may not be accessible in many structures. The measurement could only give an indication of the average moisture content in the signal path. The method is not suitable for continuous, long term monitoring.

2.2.8. Surface Acoustic Wave Moisture Sensors

A method to measure the permittivity of a medium and therefore the moisture content by means of the effect on surface acoustic wave (SAW) devices is described by Zaghloul *et al.* (1999). This method cannot be considered for the measurement of moisture in concrete as the effect of the material under test on the acoustic wave in the substrate used is limited to a very thin layer of the material close to the SAW device. It is interesting to note however that this method does

not assume an intimate contact between the SAW device and the material under test, but allows for a small air gap otherwise the acoustic wave would be dampened by the contact with another solid or liquid surface.

2.3. Moisture measurement with EM fields at high frequency – agricultural and other products.

Microwave aquametry is now the recognised term for the technology of measuring moisture content with microwaves[2]. A large number of publications were produced on the topic of microwave aquametry for cereal grains (Nelson *et al.*, 1999). To determine the moisture content of cereal grains in bulk, the variation in density becomes an important factor to be taken into account. Methods used are multi-frequency measurements to eliminate the effect of density variations and are referred to in the above paper. Although it would be useful to use this technology in developing a density independent system for the measurement of moisture in concrete, it is not essential, as there are other simpler methods to compensate for density of different concrete types (this is a theme discussed in Chapter 6).

In this chapter the different methods available were discussed. The conclusion drawn that is that there is not a method available to measure moisture content in concrete to suit the requirements of long term cost effective monitoring.

2.4. Summary of aims of study

The search for a suitable method to monitor moisture in concrete will be done as follows (see also section 1.5): Chapter 3 will look at the pore system of concrete and the nature of chemical attack being the main reason why moisture content in concrete should be monitored. To determine the parameters that should be used to measure moisture content, Chapter 4 will briefly investigate dielectrics (section 4.1) and the permittivity of water (section 4.2). The results of the investigation in Chapter 4 on the permittivity of bulk water (section 4.2.2) indicated that for moisture measurement, permittivity should be determined at a frequency high

enough to eliminate ionic conduction effects, but low enough not to be affected by the relaxation time of the water molecule. Section 4.4 develops the transmission line idea to measure relative permittivity. The cage-coaxial line is introduced in section 4.4.2. This leads to the use of TDR to measure relative permittivity with the cage-coaxial transmission line (section 4.5.3) and the measurement of the permittivity of concrete in section 4.6. Chapter 5 investigates the effect of temperature on bulk water as this may have a bearing on the influence of temperature on the moisture measurement and in section 5.2 the effect of moisture content on the relative permittivity in concrete is discussed. Chapter 6 describes how the specific design of transmission line evolved. Chapter 7 then shows that the transmission line can be used as a tuning element in practical oscillator capable of measuring the moisture content of concrete instead of using TDR measurements (section 7.2). Note that TDR was used in this study to measure the average relative permittivity of the material under test over a broad frequency spectrum while the method employed by the moisture probe in Chapter 7 uses the effect of change in relative permittivity and therefore moisture content on the input impedance of the transmission line at discrete frequencies. Although the measurement of relative permittivity using TDR gave an insight into the influence of moisture on the relative permittivity of concrete, it was found to be an unsuitable method to monitor the moisture content of concrete. A much more cost effective and practical method is to use the transmission line as a tuning element in an oscillator and then to calibrate the oscillator frequency directly against moisture content (section 8.9.1).

---

[2] Discussions at Weimar (2001) on the creation of an International Society of Microwave Aquametry.

Chapter 3. Investigating physical characteristics of moisture in concrete.

A good understanding of the nature of moisture in concrete is required to know what is actually being measured by a moisture sensor. It will become clear why this knowledge was of paramount importance for the design of the sensor when the sensor development is discussed in Chapter 6.

The moisture content in concrete is closely related to all the different types of chemical attack of concrete. Chemical attack of concrete will be considered in section 3.3.2 in order to help understanding the parameters that are important e.g. accuracy, level of moisture and where in the concrete the measurement should be taken.

Concrete is a mixture of different materials and it would not be possible here to investigate the behaviour of moisture in all the different types of concrete. In this discussion, concrete will mean that produced by Portland cement mixed with natural coarse and fine aggregates of varying particle sizes and reinforced with steel, except where specified otherwise. As concrete has high compressive strength but low tensile strength, steel reinforcement ensures high tensile strength where required. The compressive strength would be high enough in the majority of applications but as concrete members are often subjected to bending moments, a good tensile strength is of paramount importance. Any corrosion of the steel reinforcement will thus affect the strength of the concrete structure.

3.1. Definition of moisture content per unit volume

In the building and agricultural industry, percentage moisture content (MC_g) is generally defined as the ratio in percentage of the difference in mass before and after drying to the dry mass (Equation 3-1).

$$MC_g = \frac{\text{Mass of sample before drying} - \text{Mass of sample after drying}}{\text{Mass of sample after drying}} \times 100\%$$

Equation 3-1

The definition comes from the gravimetric determination of moisture content. With the gravimetric method, samples are weighed before and after drying and the moisture content calculated from the results. The gravimetric method is probably still the most reliable method of measuring moisture in spite of the fact that some moisture may be left in the sample if the temperature was not high enough or if the moisture is trapped in closed pores. Further, if the sample contained other volatile materials they could be driven off during the heating process, resulting in a false measurement of moisture content.

The disadvantages of using the gravimetric definition are:

1. Moisture content is a function of the relative density (specific gravity, SG) of the material under test and it is not possible to compare the moisture content of two different materials without taking the SG of the materials into account.
2. When materials of different densities are in close contact, comparison of moisture content between them has to be on the basis of moisture per unit volume in order to have a common denominator.
3. The increase in relative permittivity of a substance due to the presence of water molecules depends directly on the number of water molecules per unit volume (volume density). If moisture is to be measured in terms of relative permittivity, as is the case in microwave aquametry, it is more logical to measure the moisture content in terms of volume rather than in terms of mass ratios. It will be shown later (see section 5.3.1) that the calculation of the permittivity of a mixture of different dielectric materials is based on the volume of the materials, including the volume of water in the material.

The volumetric moisture content (MC_v), also referred to as absolute moisture content, is defined as:

$$MC_v = \frac{\text{Volume (or mass in gram if volume is in cm}^3\text{) of water in sample}}{\text{Volume of the sample}} \times 100\%$$

Equation 3-2

Note that, because the volume and mass of water are numerically the same when measured in cm^3 and gram respectively, the numerators in Equations 3-1 and 3-2 are the same if the mass is in gram. The mass of the sample is obtained by multiplying the volume in cm^3 by the density in $g \times cm^{-3}$. Therefore dividing MC_v by the density in $g \times cm^{-3}$ gives MC_g. In a material with a higher density (dry) than water the percentage of moisture in MC_v will be higher than in MC_g. As MC_v will be used throughout this study, it will be abbreviated to MC.

3.2. The Microstructure of Cement Paste and Concrete

Some understanding of the microstructure of concrete is deemed essential if the behaviour of moisture in concrete is to be understood sufficiently to enable the right sensor to be developed. The pore structure of the cement has a direct bearing on the strength of the cement paste and has been studied extensively (Neville, 1995).

The microstructure of concrete is a complex combination of the different materials in the mix. Of the three main components namely cement, aggregate and steel, the only relatively constant component is the cement paste which is the binding agent of the mix. Therefore the pore structure of cement paste will first be investigated. To see how these pores are formed the physical and chemical changes in the cement from the dry powder to the final hard material after setting and hardening is next discussed.

3.2.1. Hydration of cement.

While this study is not a detailed investigation into concrete technology, it was clear that some knowledge of the basic reactions and physical changes is required to understand the pore system of concrete and cement in particular. Hydration is the chemical process that turns the fine cement powder in a reaction with water into a dense solid binding material.

The reactions of cement are described in greater detail in Taylor (1997). Garboszi and Bentz (1992) who in turn referred to Gartner and Gaidis (1989), describe the process in broad terms as follows:

"Cement paste is formed from a disordered aqueous suspension of irregularly shaped cement particles, which undergo random growth due to hydration reactions. Since the original cement particles have a wide size distribution and an average size of 15-20 μm, the complex microstructure of cement paste extends over many length scales from small fractions of a micrometer to tens of micrometers. Neglecting chemical details, the reactive growth process that cement particles undergo to produce cement paste can be thought of in the following simple way. The solid cement particles supply calcium ions to the surrounding water via dissolution of surface layers. These ions then react with silica-rich surfaces of cement particles to form solid reaction products called surface products covering the cement particles. Some ions spontaneously nucleate in the pore space to form crystals called pore products, which can then grow further by accretion. In cement paste, the main surface product, calcium silicate hydrate, is denoted C-S-H. The main pore product, calcium hydroxide, is denoted CH, where the usual cement chemistry shorthand notation is C=CaO, S=SiO_2, H=H_2O, A=Al_2O_3, and F= Fe_2O_3. The reason that cement hydration can produce a rigid solid from a viscous suspension of cement particles in water is that the hydration reaction products have a larger volume than the solid reactants. As the hydration process is nearly a constant total volume process, the reaction products can fill in the initially water-filled pore space, eventually forming a rigid solid backbone capable of bearing mechanical loads. It is convenient to define the following volume ratios. β_s is the ratio of the volume of surface products produced to the volume of cement reacted, and β_p is the analogous ratio for the pore products. The total volume expansion factor β_T is defined as $\beta_T = \beta_s + \beta_p$. Typical ranges for these parameters, for various types of Portland cements, are $1.6 < \beta_s < 1.9$, and $0.4 < \beta_p < 0.7$. These parameters include the reaction of tricalcium silicate (C_3S), dicalcium silicate (C_2S), and the less abundant aluminate phases. The very small amounts of ferrite phases present in cement are not included in the above description. Somewhat surprisingly, for a variety of cements the volume expansion β_T is fairly constant around 2.3 ± 0.1."

3.2.2. The pore system of cement paste

The hardened cement paste described in 3.2.1 is characterised by a porous microstructure with high surface area of around 200 m^2/g when fully hydrated, based on measurement by water adsorption (Consolati *et al.*, 2001). The interconnections between pore spaces (percolation) are important for moisture transfer, as closed pores would not contribute to the transfer of moisture. A description of the percolation properties of the pore space by Garboszi and Bentz (1992) is next summarised:

"As cement hydration progresses, the pore space is gradually filled, because the factor β_T is greater than one. The connectivity of the pore space as a function of hydration is a percolation problem. In this description, the term "pore space" refers to capillary pore space, the water-filled space between the cement particles and their reaction products that is left over from the original cement-water mixture. There are nanometre-scale pores in the C-S-H surface product (β_s) material, which form continuous pathways, called gel pores. The size of the gel pores have been determined by various methods. The measured sizes range from 2 nm (Taylor, 1997), 5 nm to 50 nm as measured by means of NMR by Halse and Strange (1999), and 10 nm to 100 nm across according to Consolati *et al.* (2001). However, the much larger capillary pores dominate transport properties as long as they percolate, i.e., form a continuous pathway. If the capillary pores close off however, then transport must be dominated by the much smaller gel micropores. There is no sharp size cut-off between capillary and gel pores. The capillary pores are considered to have a size ranging from hundreds of micrometres down to tens of nanometres, with the upper end of the gel pore size distribution overlapping the lower end of the capillary pore size range. The volume of the capillary system is reduced with the progress of hydration since the products of hydration occupy more than twice the volume than the original solid phase of the cement. In fully hydrated cement the capillary pores represent that part of the gross volume that has not been filled by the products of hydration. The initial pore space is filled with water so that the initial pore volume is determined by the water/cement (w/c) ratio. Thus the capillary porosity of the paste depends on both the w/c ratio of the mix and the degree of hydration."

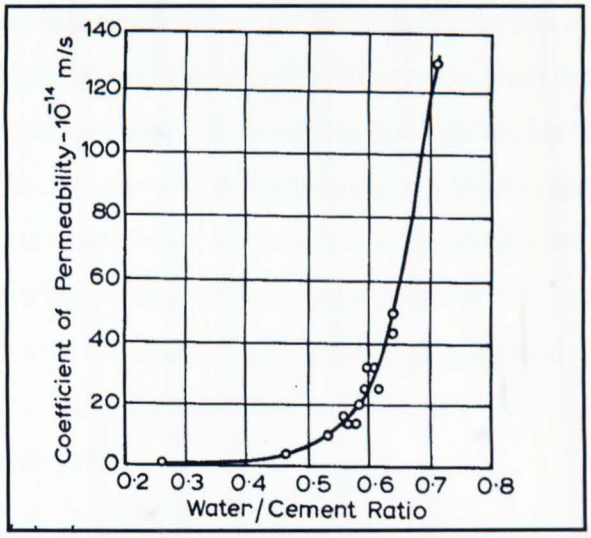

Figure 3-1 Relation between w/c ratio and permeability for cement paste with 93% of cement hydrated (extracted from Neville, 1995)

Figure 3-1 shows the relationship between permeability (and thus porosity) and w/c ratio. The degree of hydration is a function of time and available water.

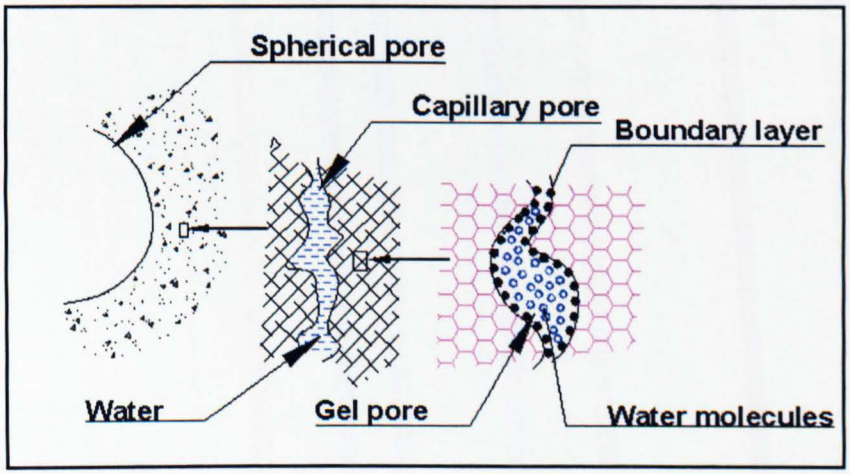

Figure 3-2 Diagrammatic representation of the pore system in cement.
The drawing is based on the description of Garboszi and Bentz (1992)

At a w/c ratio of more than 0.38 the volume of the gel is not sufficient to fill all the pore space available to it (initially filled with water) so that there will be some volume of capillary pores left even after the process of hydration has been completed (Neville, 1995). Too low a w/c ratio will result in incomplete hydration of the cement particles, leaving larger capillary pores. Presumably incomplete hydration will result in effective desiccation of the capillary space and any

subsequent influx of moisture will be used up in the formation of more hydration product. Therefore the pores in the microstructure range from nanometre size pores in the gel to capillary spaces between the gel regions. Larger pores are formed by micro-cracks caused by thermal stress or uneven expansion or contraction and fissures and voids where either air or water was trapped during setting and the hydration product of the cement particles in the immediate surroundings did not fill the space. Figure 3-2 is a diagrammatic representation of the pore system in cement paste produced by the author based on the description by Gartner and Gaidis (1989).

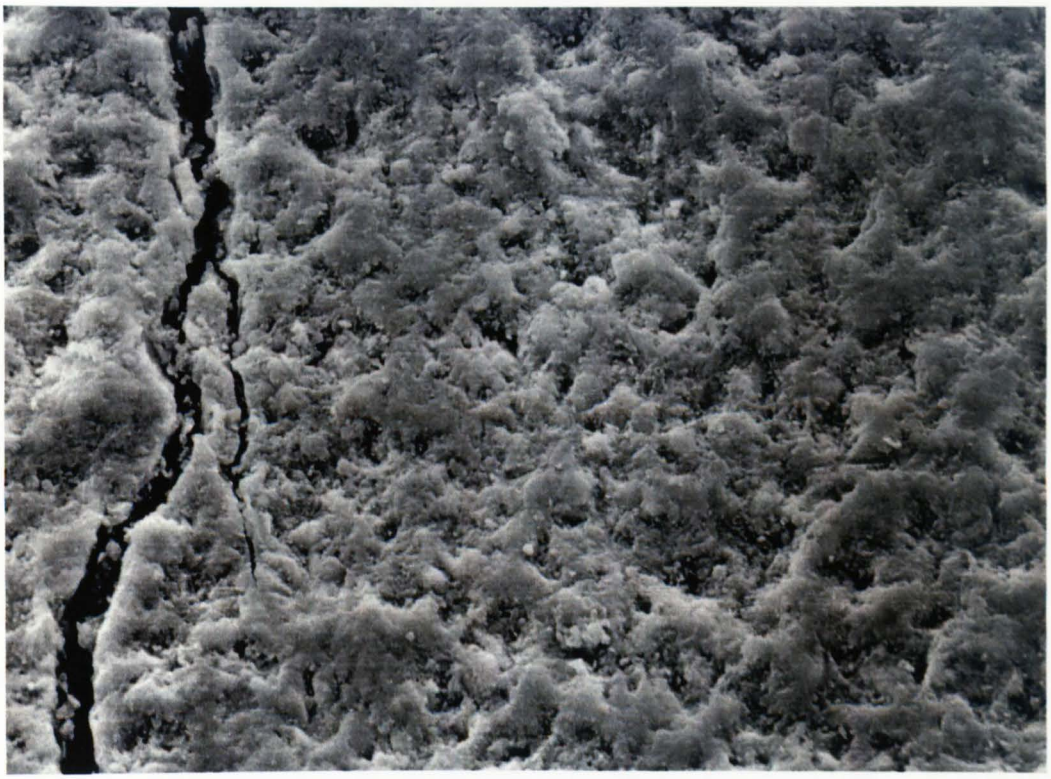

Figure 3-3 Scanning electron microscope (SEM) photograph of a crack about 6 μm wide in cement paste (w/c ratio 0.5).
Magnification 600 times. (SEM taken at Luton University of a polished surface)

Scanning electron microscope (SEM) photos were taken of the polished surfaces of the test block samples referred to in section 3.4.1. Figure 3-3 clearly shows the interconnected regions where the hydration product formed an apparent near solid

mass with larger pores between these regions. An impression of the scale is given by the relatively large crack shown, which is only about 6 μm wide.

Figure 3-4 Micro-crack width about 500 nm at the widest point in cement paste.
Magnified 5000 times (SEM taken at Luton University of a polished surface)

At a magnification of 5000 times an even smaller micro-crack (about 0.5 μm at the widest point) is shown in Figure 3-4, where the crack appears to be in the gel region of the cement paste. At greater magnification of 15000 times, Figure 3-5 shows a part on the same polished surface to give an indication of the large variation in sizes of the pores visible under the microscope. Closer inspection indicates that the view in Figure 3-5 is close to a crack that appears as some straight edges on the left in the photograph. The magnification of the SEM was insufficient to detect the nanometre pores in the cement paste referred to above. The range of pore sizes is therefore much wider than those visible in the SEM photograph of Figure 3-5. The small cracks in Figure 3-3 are of the same order of

magnitude as the large "cavity" seen in Figure 3-5 and are probably formed by stresses that developed in the cement paste during setting.

In summary the SEM pictures reveal the wide range of sizes of pores and cracks in the cement matrix and show that it is far from homogenous when viewed at a large enough magnification.

Figure 3-5 SEM of cement paste near a crack.
The w/c ratio was 0.5, cured under water for 28 days. Magnification 15000 times (SEM taken at Luton University of a polished surface)

3.2.3. Aggregate porosity

The aggregate has an important effect on the density and porosity of the concrete. There is a wide variation in the porosity of different aggregates. The sand used by the author in a mortar mix for tests on permittivity appeared to be non-permeable for all practical purposes as the total porosity of the mortar as measured was reduced by the volume of sand added to the cement paste. The porosity measured was reduced from 28% to 14% when 50% sand was used in the mortar. Table 3-1

from Neville (1995) compares the porosity and the pore sizes of different types of aggregate with that of cement paste with different water/cement ratios.

Table 3-1 Comparison of permeability of aggregate types with cement paste

Type of Rock	Coefficient of permeability m s^{-1} (See section 3.3.1)	Water/cement ratio of mature paste of the same permeability
Dense trap	6.27×10^{-16}	0.38
Quartz diorite	2.1×10^{-15}	0.42
Marble	6.07×10^{-15}	0.48
Marble	1.46×10^{-13}	0.66
Granite	1.36×10^{-12}	0.70
Sandstone	3.12×10^{-12}	0.71
Granite	3.96×10^{-12}	0.71

For example the granite and sandstone have the same order of magnitude of permeability (3×10^{-12} < permeability/m s^{-1} < 4×10^{-12}) as cement paste formed with a w/c ratio of 0.71 (see definition of permeability Darcy's equation 3.3.1). A cement paste with w/c ratio of 0.71 will have a relatively high porosity compared to the ideal w/c ratio of 0.38 as explained in section 3.2.2. Where concrete is used as heat insulation for example a very different type of aggregate is used to increase the pore volume and size. It will be shown in section 3.4.1 that the distribution of moisture in concrete depends on the relative size of the pores in the different materials in the concrete mix. The exception is where an aggregate has low percolation as a result of a closed pore system that would not absorb moisture even though it has a large pore volume with pore sizes small enough to draw moisture from the cement paste.

3.2.4. Pores in the concrete mix

In section 3.2.2 the wide range of pore sizes in the cement paste was discussed. Section 3.2.3 discussed the porosity of the aggregate material. The range of pore

types and sizes is increased even more when the complete concrete mix is considered. In practice the aggregate is never completely pure. Fine material such as clay particles or even organic matter can adhere to individual aggregate pieces (Neville, 1995) and can form a porous buffer layer around the pieces of aggregate[3]. The nature of such pores is unpredictable. Further, incomplete compaction could result in air being trapped in the concrete mix.

Figure 3-6 Core drill sample of a typical concrete showing the range of aggregate sizes used.

A core drill sample taken from a concrete block cast to exact mixture standards is shown in Figure 3-6. The apparently solid appearance of the concrete is misleading. Although thorough mixing and compaction minimises the volume of trapped air or water that create voids, some trapped water or air cannot be avoided totally.

[3] In this investigation only washed sand was used as fine aggregate in a mortar mix.

3.2.5. Non-evaporable water and bound water

Recall that the aim of this study is to produce the basis of a sensor to enable monitoring of the moisture content of fully hydrated mature concrete in order to monitor the conditions that could lead to chemical attack. There is a considerable amount of non-evaporable water in the cement paste after complete hydration (about 28% of the cement paste pore volume, Taylor, 1997). As this water cannot be driven off by oven drying, it is for the purpose of this study regarded as part of the dry material. Some of the non-evaporable water could be trapped in closed pores where it would add to the total permittivity of the dry material. Water molecules are present in hardened cement paste in various forms. Taylor (1997) defines chemically bound water as that present in interlayer spaces, or more firmly bound, but not that present within pores larger than this. The problem with such a vague definition is that there is no sharp distinction between interlayer space and micropores. The latter can be as small as 2 nm across. The difficulty in determining the point at which cement can be regarded as "dry" or zero moisture content is illustrated by the method to determine the point where only non-evaporable water is present. This method, known as D-drying, is described by Taylor (1997) and summarised next: The sample is equilibrated with ice at a temperature of –79 °C by continuous evacuation with a rotary pump through a trap cooled in a mixture of solid CO_2 and ethanol. The sample is then heated to 105 °C, which reduces the water content. The water still retained in the paste is then called non-evaporable water. The ambient condition during the heating process must exclude any CO_2 that could react with the cement paste. For the purpose of this study some reference point in terms of moisture content was needed that could be defined as 0% moisture content. The method used was to maintain the sample in an oven at 100 °C for 24 hours and then determine the "dry" mass. From the forgoing it is clear that there would have been an unknown amount of water still present, which had to be ignored as it would have played no part in the normal wetting and drying of the concrete. The water trapped in pores would not play a part in the transportation of dissolved chemicals through the concrete.

In Appendix C, a quotation from Neville (1995), gives an insight into the complexity of the pore system and the way water is held in cement paste.

3.3. The role of Moisture in Concrete with regard to Durability of Concrete

Damaging chemical reactions in concrete can only take place in the presence of moisture. In this section it will be shown what role moisture plays in the durability of concrete.

3.3.1. Permeability of concrete

Penetration of concrete by materials in solution may adversely affect durability. This penetration by damaging chemicals depends on the permeability of the concrete. The vulnerability to frost is caused by the relative ease by which concrete can become saturated with water and therefore by its permeability (see section 3.3.2). Furthermore, in the case of reinforced concrete, the ingress of moisture and of air can result in the corrosion of steel (see carbonation, section 3.3.3). Since this leads to an increase in the volume of the steel, cracking and spalling of the concrete cover can occur. The photograph in Figure 3-7 of a structure that was deemed to be unsafe, is a good example of spalling caused by the corrosion of the steel.

Figure 3-7 Example of spalling due to the corrosion of steel reinforcement.
Photograph taken by the author of a building subsequently demolished.

Apart from the problem of chemical attack, the permeability (in hydraulic terms) of concrete is an important consideration where concrete is employed to retain bodies of water. Permeability is expressed as a coefficient of permeability, K, given by Darcy's equation (Neville, 1995).

$$\frac{dq}{dt} = K \times A \times \frac{\Delta h}{L} \qquad \textbf{Equation 3-3}$$

where

$\frac{dq}{dt}$ = the rate of flow of water ($m^3 s^{-1}$)

A = cross sectional area of the sample (m^2)

Δh = drop in hydraulic pressure through the sample (m)

L = thickness of the sample (m).

K = Coefficient of permeability (m s^{-1})

Note that the expression does not make provision for capillary pressure where according to Equation 3-3 there would be no flow if $\Delta h = 0$, while in fact the pressure could be negative and there would still be considerable flow due to the capillary pressure (see section 3.4.1). The author could not find any reference in the literature to this fact. However, the experimental arrangement as described in Neville (1995) to measure K, measures the rate at which moisture will penetrate cement paste as a function of hydraulic pressure. Powers *et al.* (1956) measured the reduction in permeability of cement paste as a function of time (progress of hydration) for cement paste with a high w/c ratio of 0.7. K was measured to be 1×10^{-12} m s^{-1} after 24 days and calculated to be 6×10^{-13} m s^{-1} when fully hydrated. The relatively high w/c ratio would have made this paste more permeable than would have been the case with an optimum w/c ratio of around 0.4 when the diffusion rate drops to around 7×10^{-16} m s^{-1} according to Neville (1995).

Care should be taken not to equate porosity with permeability. The permeability of concrete is not a simple function of its porosity, but depends also on the size, distribution, and continuity (percolation) of the pores. Thus, although the cement gel has a porosity of 28%, its coefficient of permeability is only about 7×10^{-16} m s^{-1}. This is due to the extremely fine texture of hardened cement paste: the pores and the solid particles are very small and numerous. Rock pores on the other hand, though fewer in number are much larger and lead to a higher permeability. For the same reason, water can flow more easily through the capillary pores than through the much smaller gel pores. The cement paste as a whole is 20 to 100 times more permeable than the gel itself. It follows that the permeability of cement paste is largely controlled by the capillary porosity of the paste. It was shown in 3.2.2 that the capillary porosity in turn is largely determined by the w/c ratio.

In conclusion this section has shown that concrete has, despite a low coefficient of permeability K, enough permeability to allow the ingress of moisture containing chemicals in solution that could cause damage as will be discussed in the next

section (3.3.2). On the other hand in a high quality concrete with w/c ratio in the order of 0.4 the diffusion rate would be extremely low, which means that any meaningful ingress of moisture containing harmful chemicals would mostly be through cracks and other imperfections in the concrete matrix.

3.3.2. Chemical attack of concrete

The chemical attack of concrete will be dealt with only as far as it serves to indicate the importance of moisture measurement in dealing with the durability of concrete.

Solid salts do not attack concrete, but when present in solution they can react with hardened cement paste. Moisture is thus a prerequisite for chemical damage and moisture content is a useful parameter to act as an early warning mechanism. In practice only a small proportion of concrete used is exposed to serious chemical attack. This is fortunate, since the resistance of concrete to attack by certain chemical agents is generally low. At low moisture levels the moisture will be concentrated in the gel pores and diffusion will be largely by means of the diffusion of water vapour. At such a moisture level there would be no movement of ions through the matrix as the empty capillary pores create gaps and no chemical damage can occur.

The more common forms of chemical attack are the leaching out of cement, and the action of sulphates, sea water and natural slightly acidic waters that would reduce the alkalinity of the concrete. The high pH of concrete (typically pH≈14) protects the steel reinforcement against corrosion (see 3.3.3). Any reduction in the alkalinity (pH) is therefore a potentially dangerous condition. Carbonation is a condition where CO_2 from the atmosphere forms dissolves in the pore solution of cement paste producing CO_3^{2-} ions, which react with the Ca^{2+} ions to produce $CaCO_3$ (Taylor, 1997). The OH^- and Ca^{2+} ions required for this reaction are obtained by the dissolution of CH and by lowering the Ca/Si ratio of the CSH, which in turn lowers the compressive strength of the concrete. Water is required for the free ions to exist. The action of CO_2 takes place even at small concentrations such as are present in rural air, where the partial pressure of CO_2 is about 3×10^{-4} atmospheres. The rate of carbonation increases with an increase in

the concentration of CO_2. The $Ca(OH)_2$ (the CH pore product, see section 3.2.1) in the cement carbonates to $CaCO_3$, but other cement compounds are also decomposed, hydrated silica, alumina, and ferric oxide being produced. Such a complete decomposition of calcium compounds in hydrated cement is chemically possible even at the low pressure of CO_2 in normal atmosphere. Fortunately carbonation penetrates extremely slowly beyond the exposed surface of concrete. The rate of carbonation depends also on the moisture content of the concrete and the relative humidity of the ambient medium. Although moisture is an essential ingredient for carbonation to take place, a high level of moisture would stop the ingress of CO_2 by effectively blocking the pores and therefore the resultant carbonation (Taylor, 1997).

When concrete is subjected to alternating wetting and drying in air containing CO_2, shrinkage due to carbonation (during the drying cycle) becomes progressively more apparent. The total shrinkage at any stage is greater than if drying took place in CO_2 free air, so that carbonation increases the magnitude of irreversible shrinkage and may contribute to crazing of exposed concrete.

According to Neville (1995) the damage caused by de-icing salts is more physical than chemical in nature because of the increase in the severity of the freezing and thawing cycles. The salts normally used are NaCl and $CaCl_2$, and their repeated application with intervening periods of freezing or drying results in surface scaling of the concrete (see section 3.3.4). An important effect of chloride contamination from de-icing salts on steel is discussed in 3.3.3.

3.3.3. Corrosion of Steel Reinforcement

The corrosion of steel is an electrochemical process and the moisture content of the concrete plays an important part as water is needed to form the positive and negative cells required for the electrolytic action. Taylor (1997) describes the corrosion action as follows:

The anodic reaction is given by the chemical equation:

$$3Fe + 8OH^- \rightarrow Fe_3O_4 + 4H_2O + 8e^- \qquad \textbf{Equation 3-4}$$

and the cathodic reaction is:

$$4e^- + 2H_2O + O_2 \rightarrow 4OH^- \qquad \textbf{Equation 3-5}$$

At the anodes iron is dissolved and an oxide deposited. Electrons travel from anode to cathode within the metal and OH^- ions travel from cathode to anode through the solution with which is in contact. For these processes to occur the surfaces must remain wet and a continuing source of oxygen is needed. If the pH remains above about 11.5 and Cl^- ions are absent, the oxide is deposited as a thin protective layer and the corrosion rate is negligible. At lower pH, an oxide or oxyhydroxide is deposited in an incoherent form and corrosion is rapid.

Chloride ions (Cl^-) cause local breakdown of the passive film even at high pH levels. The regions of iron exposed become anodes and the unaffected areas cathodes. Since the areas of breakdown are small, the current density at the anodes could be high, causing pitting and a localised decrease in pH.

Corrosion can be inhibited if the permeability of concrete to water or oxygen is low enough and may not occur even if the cement in contact with the steel is carbonated. It would appear that corrosion of steel would occur when there is sufficient moisture present, but not so much as to inhibit the ingress of CO_2 and O_2 . It is believed to occur when there is a wetting and drying cycle allowing moisture (on a wetting cycle) and the atmospheric gases (on a drying cycle) to reach the steel.

3.3.4. Effects of frost on hardened concrete

The effect of frost on hardened concrete will briefly be considered as it has a direct bearing on the durability of concrete coupled to the moisture content or more importantly, the degree of saturation. It will show the importance of measuring moisture content close to saturation. Although the effect of frost on freshly poured concrete is important in the building industry, the discussion here will be limited to the effect of frost on hardened concrete, described by Neville (1995) in the following manner:

As the temperature of hardened concrete is lowered, the water held in the capillary pores in the cement paste freezes in a manner similar to the freezing in the capillaries in rock, and expansion of the concrete takes place. On thawing the

expanded volume can absorb more water, so that on re-freezing, further expansion takes place so that repeated cycles of freezing and thawing have a cumulative effect. The larger pores in concrete, arising from incomplete compaction, are usually air-filled and therefore not appreciably subject to the action of frost (which is not the case under saturated conditions). Freezing is a gradual process, partly because of the rate of heat transfer through concrete, partly because of a progressive increase in the concentration of dissolved alkalis in the still unfrozen water, and partly because the freezing point varies with the size of the cavity. Since the capillary pressure of the bodies of ice in the capillaries puts them under pressure inversely proportional to the hydraulic radius (see section 3.4.1) of the pore, freezing starts in the largest cavities and gradually extends to smaller ones. Gel pores are too small to permit the formation of nuclei of ice above –78 °C, so that in practice no ice is formed in them (see section 5.2.4). However, with a fall in temperature, because of the difference in entropy of gel water and ice, the gel water acquires an energy potential enabling it to move into the capillary cavities containing ice. The diffusion of gel water that takes place leads to a growth of the ice body and to expansion.

There are thus two sources of dilating pressure. First, freezing of water results in an increase in volume to ice of approximately 9 per cent so that the excess water in the cavity is expelled. The rate of freezing will determine the velocity with which water displaced by the advancing ice front must flow out. The hydraulic pressure developed will depend on the resistance to flow, i.e. on the length of path and the permeability of the paste between the freezing cavity and an adjacent void that can accommodate the excess water.

The second dilating force in concrete is caused by diffusion of water leading to a growth of a relatively small number of bodies of ice. This latter mechanism appears to be particularly important in causing frost damage of concrete. Diffusion is caused by osmotic pressure brought about by local increases in solute concentration due to the separation of frozen pure water from the solution. For instance, a slab freezing from the top will be seriously damaged if water has access from the bottom and can travel through the thickness of the slab due to a combination of capillary and osmotic pressure. The total moisture content of the

concrete will then become greater than before freezing. This is what happens when de-icing salts are applied. The salts produce osmotic pressure and cause movement of water toward the top layer of the slab where freezing takes place. Since greatest damage occurs when concrete is exposed to relatively low concentrations of salts between 2% and 4% solution (see Figure 3-8) it is believed that the attack is primarily physical and not chemical in nature.

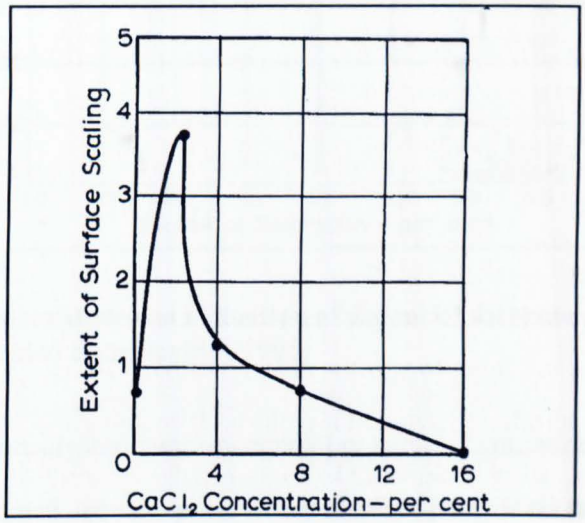

Figure 3-8 Graph of extent of surface scaling against salt concentration in concrete (Neville, 1995)

When the dilating pressure in the concrete exceeds its tensile strength, damage occurs. The extent of the damage varies from surface scaling to complete disintegration as layers of ice are formed, starting at the exposed surface of the concrete and progressing through its depth. According to Neville (1995) the road kerbs in England are particularly vulnerable to frost damage, as they remain wet for long periods. The second most vulnerable are concrete road slabs. When salts are used for de-icing roads, some of these salts become absorbed by the upper part of the concrete. This produces a high osmotic pressure with a consequent movement of water toward the coldest zone where freezing takes place.

While the resistance of concrete to frost depends on its various properties, the main factors are the degree of saturation and the pore structure of the cement paste. Figure 3-9 shows the influence of degree of saturation of concrete on its resistance to frost. The definition for coefficient of resistance to frost is not given

in the reference and it is assumed here that it is the percentage of samples undamaged by a fixed number of freeze/dry cycles. A sample is classified as damaged when it has more than 25% loss in mass due to flaking (Neville, 1995).

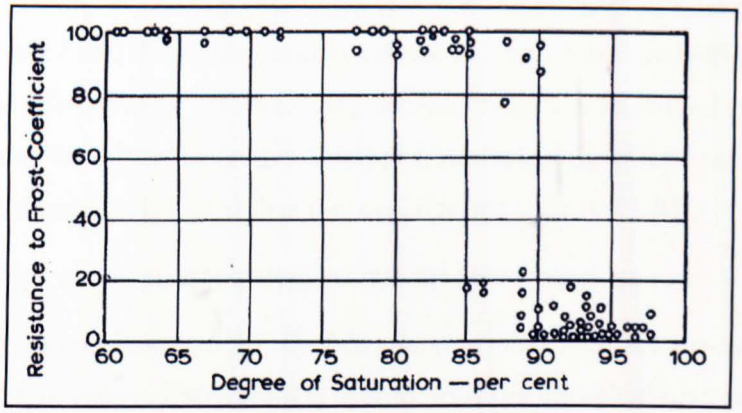

Figure 3-9 Frost resistance as a function of degree of saturation S (extracted from Neville , 1995)

3.3.5. Porosity and moisture content in terms of saturation level

Saturation is assumed to be the point where no more water is taken up by a volume of concrete that is completely immersed in water. When defining porosity of the material, it will be assumed that pores that are completely closed and therefore play no role in the movement of moisture can be ignored. Porosity, p, can then be defined as:

$$p = \frac{\text{volume of water absorbed at saturation}}{\text{total volume of sample}}$$

The degree of saturation or saturation level S can be defined as:

$$S = \frac{\text{volume of water absorbed}}{\text{volume of water absorbed at saturation}}$$

Volumetric moisture content MC as defined in equation 3.2 can be written as a ratio v_w (instead of a percentage) as:

$$v_w = \frac{\text{Volume of water absorbed}}{\text{Total volume of sample}}$$

So that:

$$S = \frac{v_w}{p}$$ **Equation 3-6**

Figure 3-9 shows the damage coefficient in terms of the degree of saturation *S*. It can be assumed that the critical saturation level will fall above the 100% RH range (also referred to as "above the hygroscopic range") as Fagerlund (1999) observed that the critical saturation level for frost damage S_{cr} will be at a level of moisture content that is higher than the level reached with 100% RH.

An interesting and important quotation from the above paper is:

"There are no good methods for the determination of the moisture content above the hygroscopic range. Therefore it is difficult to verify the calculation methods. Methods such as WR (weight ratio) *can be used, but they are limited to laboratory test and are very expensive. Weight measurements are fairly precise but they are destructive. One theoretical possibility is to use an osmotic cell by which it ought to be possible to measure the capillary under-pressure, and thereby indirectly the moisture content, but so far no cells have been developed. Electrical methods (resistive or capacitive) might be used, but they are very sensitive to salt migration in the material, or to other disturbances."*

In the sensor developed in this study, the moisture content can in fact be measured up to saturation level.

3.4. Characteristics of Moisture in Concrete

The intricate pore system of concrete described in section 3.2 shows that moisture can be present in relatively large cracks and voids down to nanometre size gel pores in the cement paste (see Appendix C). Provided that the pores are interconnected, moisture will move through the matrix due to capillary action (see sections 3.2.2 and 3.3.1) or diffuse as water vapour where there is a break in the liquid water. Under saturation conditions, especially where concrete is under water, water pressure will force some water through cracks and voids. Where the gravitational force exceeds capillary force, gravity plays a role in the movement of water through the concrete. If gravitational effects are seen in a porous material,

especially at relatively low moisture content, it can be assumed that the capillary force is relatively low and the pores therefore relatively large (see section 6.2.4). In a porous solid material like concrete with a wide range of pore sizes, gravitation will exceed the capillary force only in the larger pores. Such large pores will probably only become filled with water under conditions close to saturation.

Water molecules in concrete and specifically in the cement paste, appear in both bound and unbound form. Bound H_2O molecules will not change orientation under the influence of an electromagnetic field and thus will not contribute to the change in the permittivity of the concrete due to their presence. As the aim of the study is to measure moisture as an early warning system against chemical attack or physical damage (cracks) in the concrete, bound water is not of any interest in this study except where some interfacing molecules are bound through adhesion forces between water and solid molecules (see section 5.2.3).

Hygroscopic salts in the concrete absorb some of the water, but the bulk of the unbound water will appear in the pore system of the concrete. It will be shown that it is important to understand the characteristics of the capillary pressure in the pore system in order to understand the behaviour of moisture in concrete.

3.4.1. Capillary pressure and the transfer of moisture between different porous media

Richards (1928) gives a clear (and early) description of capillary forces in a porous medium. Early on in the investigation the author of this thesis postulated that the moisture equilibrium between two different porous media in contact would be such that the ratio of moisture content in the two media would be equal to the ratio of the respective porosity. This was shown to be completely erroneous. Some of the history of the sensor development as described more fully in section 6.1 is repeated here to explain why this was important.

In section 6.1 it will be explained how the idea was developed to use another porous medium that would absorb the moisture from the surrounding concrete until it reached moisture equilibrium with the concrete based on the postulated theory of porosity ratios. This porous medium could then be calibrated accurately

for change in permittivity with moisture content. The material selected was ceramic clay (hereinafter referred to as clay) baked at a temperature below the vitrification point where the porosity was still high, yet the clay was hard enough to be mechanically stable. To test the theory of moisture equilibrium, samples of the clay were cut into small blocks. Sample blocks consisting of cement paste with a w/c ratio of 0.5 and mortar blocks with equal cement to sand ratio and w/c ratio of 0.5 were prepared. The samples were cured under water for 28 days and then cut into small blocks (about 25×25×7 mm). One 25×25 mm face of the cement and mortar blocks was polished to ensure intimate contact with the clay that was also smoothed on one side. The diffusion rate of moisture through cement is extremely slow (1×10^{-14} to 1×10^{-16} m s^{-1}, Neville, 1995), and the blocks were made thin enough (7 mm) in order to reach equilibrium in a reasonable time. The cement and mortar blocks were soaked in water for 24 hours. The wet blocks were taken out individually, surface dried with blotting paper, and weighed. Each block was placed against a dry clay block with the polished and smoothed surfaces facing each other. Each pair of blocks was sealed together in a few layers of PVC film. Two clay blocks, one wet and one dry, were tied together in the same way as a control test. After one week the blocks were weighed, oven dried and weighed again to determine the moisture content. The porosity of each material type was determined by soaking sample blocks of cement paste, mortar and clay for 24 hours, then weighed after the surface water was removed and then weighed again after oven drying. The results are shown in Table 3-2.

Table 3-2 Results of moisture transfer test

Sample	Porosity %	MC %
Clay 4	32.0	11.0
Clay 5	32.0	10.0
Clay A1	32.0	0.6
Cement paste A1	21.4	14.0
Clay A2	32.0	0.4
Cement paste A2	21.4	12.5
Clay B1	32.0	0.3
Mortar B1	12.2	5.4
Clay B2	32.0	0.3
Mortar B2	12.1	5.1
Clay C1	32.0	0.3
Mortar C1	12.1	5.4

In Table 3-2 the pairs of samples that were clamped together are as shown together. The control sample of one wet and one dry clay block moisture content of 11% and 10% respectively. Clay block A1 and cement paste block A1 had moisture contents of 0.6% and 14% respectively. Clay block B1 and mortar block B1 had moisture contents of 0.3% and 5.4% respectively. The other pairs showed similar results. These results showed conclusively that there was little or no transfer of moisture from the cement and mortar blocks to the clay blocks, whilst the two clay blocks (clay 4 and 5) ended up with similar moisture contents. The initial moisture level in the wet blocks was considerably lower than the porosity (14% against 20% for sample A1 as an example). It indicates that a considerable percentage of the water was removed with the surface drying action on such thin blocks (7 mm). A wet clay block and a dry cement paste block were tied together in the same manner to test the moisture flow in the other direction.

Table 3-3 Moisture transfer test with wet ceramic clay under dry cement or mortar blocks

Sample	Porosity/%	MC/%
Clay A1	32	2.13
Cement paste A1	21	20.9
Clay A2	32	1.17
Cement paste A2	21	20.63
Clay B1	32	9.54
Mortar B1	12	12.29
Clay B2	32	11.58
Mortar B2	12	9.12
Clay C1	32	7.01
Mortar C1	12	11.45

The result shown in Table 3-3 was similar to that in Table 3-2 with the clay block at 2.1% and the cement paste block at 20.9% moisture content (close to the porosity of 21%) after a week. The total initial amount of water in the clay was more (porosity 32%) than the cement paste block could absorb. That is why the moisture content of the clay block (2.1% in the case of A1 for example in Table 3-3) was higher than was the case for the test of moisture transfer from the cement to the clay (0.6% in Table 3-2). When the moisture level in the cement or mortar was close to saturation, no further transfer of water took place. In the case of B1 in Table 3-3 the moisture content is higher than the porosity, probably due to some additional cracks in the specific sample

The results showed conclusively that the transfer of moisture had nothing to do with the relative porosity of the two samples in contact. The highly permeable clay would soak up water very rapidly, an indication that the pore structure is relatively large, which allows a more rapid flow through the pore system of the material than if the pores were smaller. The mechanism of the moisture equilibrium conditions could be explained by looking at the capillary pressures.

The capillary pressure (P, measured in Pa) in a capillary tube (adapted from Richards, 1928) is given by:

$$P = \frac{2\gamma}{r}$$ **Equation 3-7**

where: γ is the water/cement adhesion force per unit length (N m^{-1})

r is the capillary radius or hydraulic radius (m)

Equation 3-7 can be derived from first principles (see Appendix A), which shows that r is not dependent on the shape of the capillary and can be the distance between the two sides of a crack of any width. That is why the term 'hydraulic radius' is more accurate than the term 'capillary radius'.

In section 3.2.2 it was shown that the gel pores in the cement paste are extremely small. P in Equation 3-7 is inversely proportional to r and would therefore be very large in the case of the nanometre size gel pores in the cement. It is clear that if the pores in the clay were bigger there would be little or no flow from the cement to the clay as we have seen. If the cement or mortar was saturated and contained some larger pores, some moisture would have been transferred to the clay.

Concrete or even cement paste structures are not completely homogenous and there would be some areas with larger pores as can be seen in the SEM photograph of Figures 3-3, 3-4 and 3-5. Such pores would be the last to fill up with water and conversely the first to dry out on reduction of moisture content. As the junctions between the gel regions form the capillary pores, there would be some discontinuities in the gel pore system. The capillary pressure would thus be less than if it were continuous, but still very high compared to the clay.

Although the effect of pore pressure is well known, it is of great importance in understanding the flow of moisture through different porous mediums in close contact. This knowledge has significant implications in building technology and specifically in old buildings where rising damp is a problem.

Note also the common confusion between adhesion force and surface tension. Surface tension is due to the cohesive force between the molecules of the same liquid, whilst adhesion force between a liquid and a solid and the resultant capillary pressure is not due to surface tension as it is commonly referred to. In fact if the surface tension or cohesive force were greater than the adhesion force

between the liquid and solid there would be no capillary pressure and the solid would repel water.

3.4.2. Relative humidity and its relation to moisture in concrete

It is common practice to measure moisture in concrete by means of relative humidity (RH) probes (private communication Dunster, BRE, 2001). The relationship between RH and moisture content will be investigated and the limitations of the measurement method shown.

Relative humidity RH is a measure of the water vapour pressure[4] at a certain temperature. The two most common direct methods to measure it are determination of the dew point temperature and the wet and dry bulb hygrometer test. Of the two, the dew point measurement is the most direct, while the wet and dry thermometer test is the most convenient. The common method to determine RH by determining the dew point is to fill a polished metal container with water, then add ice while stirring and measuring the temperature. As soon as the outer surface turns dull with condensation, the temperature is taken and the relative moisture read off a table of RH versus dew point temperature. The same principle is used in the cooled mirror test. This method is used for example by research at BRE to measure the relative humidity in a closed cavity in concrete.

If free water is available in an enclosed space RH rises to 100%. It would appear that with any unbound water in a porous material and therefore with any moisture present, the RH would be 100%. The reason that this is not the case is due to the intermolecular force between the water molecules and the solid (adhesion force as discussed in section 3.4.1) preventing evaporation of some water molecules that are closely bound to the surfaces of the pores. The relationship between the relative humidity and the largest pore size filled with water is given by the Kelvin-Laplace formula (Bentz *et al.*, 1999) which has been adapted here:

$$\ln\frac{RH}{100} = \frac{-2V_m\gamma}{rRT} \qquad \textbf{Equation 3-8}$$

where

[4] $RH = \dfrac{\text{water vapour pressure}}{\text{saturated water vapour pressure at the same temperature}} \times 100\%$

RH = relative humidity (%)

V_m = molar volume of water ($m^3\,mol^{-1}$)

γ = adhesion force between water and solid ($N\,m^{-1}$)

r = capillary radius, or hydraulic radius (m)

R = Universal gas constant ($J\,K^{-1}$)

T = Absolute temperature (K)

In a homogenous porous solid, this can be rewritten as:

$$RH = 100\,e^{-\frac{C}{r}} \qquad \textbf{Equation 3-9}$$

where $C = \frac{2V_m\gamma}{RT}$ is constant for given values of γ and T.

It can be shown[5] that RH will drop below 100% only when the largest capillaries containing water are in the nanometre region. Equation 3-5 shows that RH is a measure of the size of gel pores still filled with water. RH measurement can only be translated to moisture content when the total volume of pores smaller than this particular size is known. The size of pores filled with water increase rapidly above 98% relative humidity. That is why RH is a good qualitative indication of the "dryness" of the concrete. On the other hand RH can be used together with a method like oven drying to determine the volume distribution of different pore sizes in the matrix (provided we know the magnitude of the adhesion force γ).

Under normal environmental conditions, concrete structures are regularly subjected to running or standing water. Sometimes the moisture content in concrete could be as high as full saturation with all capillaries and other voids filled. The relative humidity in an enclosed cavity would then reach 100% well before all the pores are filled. Frost damage in concrete occur at moisture levels above 91% saturation (see Figure 3-9), which is well above the hygroscopic range (up to 100% relative humidity) and makes measurement of relative humidity unsuitable as an early warning system of potential frost damage.

---

[5]Inserting values: $V_m = 1.8 \times 10^{-5}\ m^3\,mol^{-1}$, $R = 8.3\ J\,K^{-1}$, $T = 300$ K, $\gamma = 0.07\ N\,m^{-1}$ for water-air (may be higher adhesion force for water- solid)
Which gives: $C = 10^{-9}$
$RH/100 = \exp\text{-}[10^{-9}/r]$.
It means that the RH will be 98% when the largest capillary filled with water, has a hydraulic radius of 52 nm.

The poor relationship between relative humidity and moisture content is illustrated by Hedenblad (1996) as shown in Figure 3-10 for aerated concrete. The problem is aggravated in aerated concrete by the fact that the pores are larger than ordinary concrete, but it is a good example to emphasise the problem experienced with using relative humidity as a measure of moisture content.

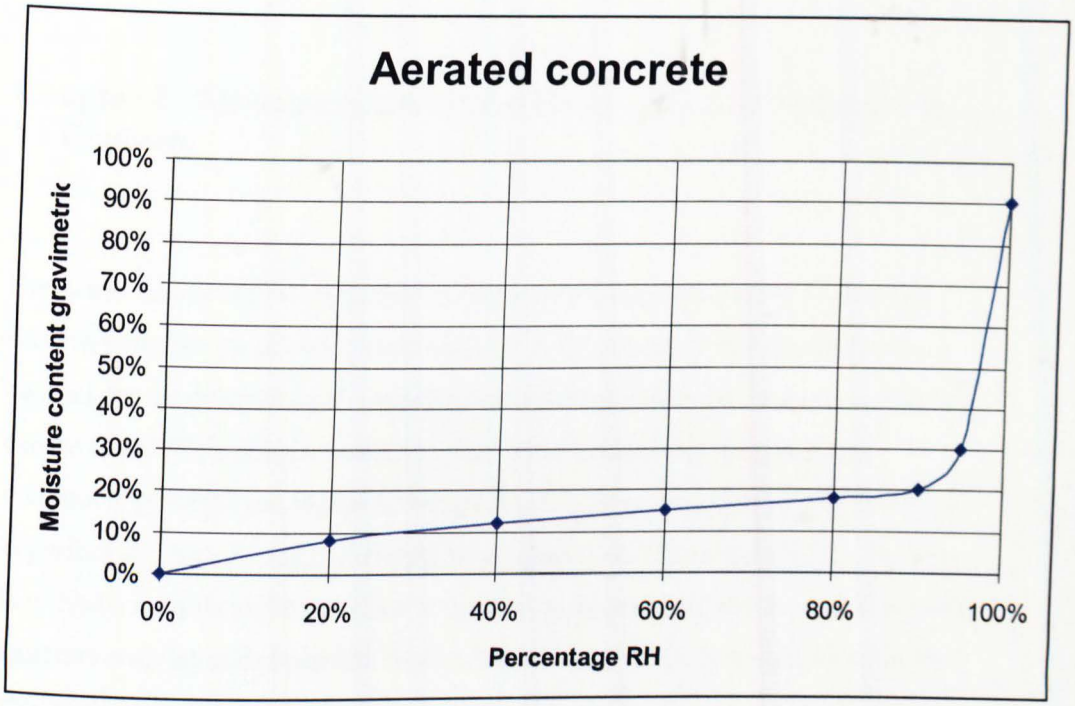

Figure 3-10 Moisture content per volume as a function of relative humidity in aerated concrete.

From Hedenblad (1996). Moisture content is given as a percentage of the dry mass.

Chapter 4. Measurement of Permittivity Effects of Moisture in Concrete

Dielectric theory will be discussed in section 4.1 with a discussion of the high relative permittivity of water in section 4.2. It became clear that the moisture content can be determined if a reliable method to measure the relative permittivity can be found. This chapter looks at some methods used and discusses the methodology employed in this investigation. It is fair to say that no single method is perfect and that the method should be adapted to suit the requirement. The aim is to find a reliable and cost effective method to monitor the moisture in a concrete structure over extended periods. Such a method may differ from one suitable for spot measurements of the moisture content. This aspect will be discussed again in Chapter 6.

4.1. Dielectrics, a general discussion

The study of dielectrics is a broad field and Anderson (1964) covers the theory of dielectrics extensively. Only the relevant aspects of dielectric theory and application are considered here.

Pure dielectric materials do not conduct electricity and are used as insulators in various applications. Although electrically a non-conductor, a dielectric material is affected by an applied electric field and in turn affects the field. The reaction to the electromagnetic field depends on the type of dielectric. The deviation in a dielectric from the permittivity of free space is due to the additional charge needed to polarise atoms or molecules. For non-polar dielectrics, which include all pure

elements or single atoms, polarisation is entirely electronic, which means that the polarisation is caused by the displacement of the electrons in the atoms. Some polar materials exhibit principally electronic polarisation when they are of a highly symmetrical nature (Anderson, 1964).

Dipolar materials have molecules with a specific charge orientation. Water is a typical dipolar material (see section 4.2.1). A molecule in a liquid such as water is free to rotate in the presence of an electric field and the dipole aligns itself in the direction of the applied field.

In a liquid the molecules are randomly orientated in the absence of an electric field. Anderson (1964) describes the situation as follows: If one of the molecules should change its angular position the other molecules will rearrange themselves to preserve equilibrium charge. Their average motion can be described by treating them as a continuous medium, exerting a viscous frictional damping force on the original dipole molecule. If the dipole has an effective radius a and the viscosity of the fluid is η, the frictional constant ξ is given by Stokes law as:

$$\xi = 8\pi\eta a^3 \qquad \textbf{Equation 4-1}$$

When an electric field is applied at an angle θ to the axis of the dipole a torque of magnitude Γ will act such that:

$$\Gamma = \xi \frac{d\theta}{dt} \qquad \textbf{Equation 4-2}$$

The dipole will align itself (turn) at a rate depending on the factor ξ and the change will not be instantaneous. The time taken for the change to take place is known as the relaxation time τ of the dielectric (water in this case). The dipole is also subjected to thermal movements known as Brownian movement, affecting the rate of change of the angle when a field is applied. Debye was able to take this into account and derived the following expression for the relaxation time τ:

$$\tau = \frac{\xi}{2kT} \qquad \textbf{Equation 4-3}$$

where

k = Boltzmann constant = 1.38×10^{-23} (J K^{-1})

T = temperature (K)

Substituting for ξ from equation 4-1,

$$\tau = \frac{4\pi\eta\alpha^3}{kT} \qquad \textbf{Equation 4-4}$$

or

$$\tau = \frac{3\eta}{kT}V \qquad \textbf{Equation 4-5}$$

Where

V = the volume of the molecule (m^3)

a = effective radius of the molecule (m)

If the relaxation time is calculated with the molecular volume of water taken as 3.5×10^{-23} cm^3 (Anderson 1964) and the viscosity η of water at room temperature of 0.001 N s m^{-2}, $\tau \approx 21\times10^{-12}$ s. This is about 2.3 times longer than the 9.2×10^{-12} s used in the calculation in Appendix B taken from Nelson (1991) based on experimental data. The author could not find an explanation for this difference, which may be due to the difference in the bulk viscosity of water compared to the viscosity at molecular level.

4.2. Permittivity of water

The fact that water has a much higher relative permittivity (ε_r) than the dry material in concrete makes it possible to detect small quantities of water by measuring the relative permittivity of the concrete containing moisture. This section discusses the reason for this, the factors influencing the relative permittivity and how experimental data compares with the theory described.

4.2.1. The Dipolar Character of Water

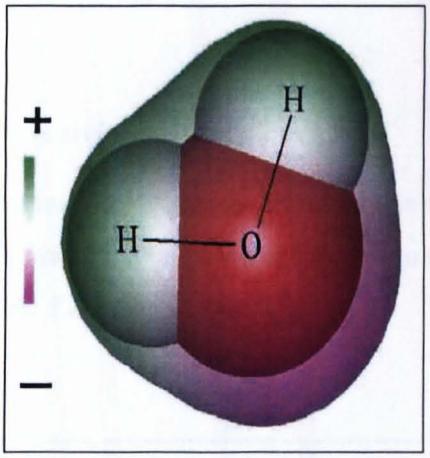

Figure 4-1 Pictorial representation of a water molecule.
The angle between the hydrogen atoms is 104°. The representation shows the electric dipole characteristic of the molecule.

Water is a dipolar molecule. In the water molecule the two hydrogen atoms are not situated symmetrically around the oxygen atom, but at an angle of 104° between the hydrogen atoms as shown in Figure 4-1, resulting in a negative charge on the side of the oxygen atom. The dipolar molecule of water makes it a good example of a dipolar type dielectric with orientational polarisation. When an electric field is applied the molecule will align itself with the field, provided it is free to turn. It therefore shows orientational polarisation and the relative permittivity is high due to the electric charge (energy) stored.

4.2.2. Factors influencing the permittivity of water

The Debye equation of complex permittivity (see Appendix B) is given by

$$\varepsilon_r = \varepsilon' - j\varepsilon'' \qquad \textbf{Equation 4-6}$$

where

$$\varepsilon' = \varepsilon_\infty + \frac{(\varepsilon_s - \varepsilon_\infty)}{1 + \omega^2\tau^2} \qquad \textbf{Equation 4-7}$$

and

$$\varepsilon'' = \frac{(\varepsilon_s - \varepsilon_\infty)\omega\tau}{1+\omega^2\tau^2} \qquad \textbf{Equation 4-8}$$

(a) ε_s the steady state permittivity or dielectric constant,

(b) ε_∞ the permittivity at infinite frequency, which is also the permittivity when the molecules have a random orientation and unable to move under the influence of an electric field and

(c) the relaxation time τ.

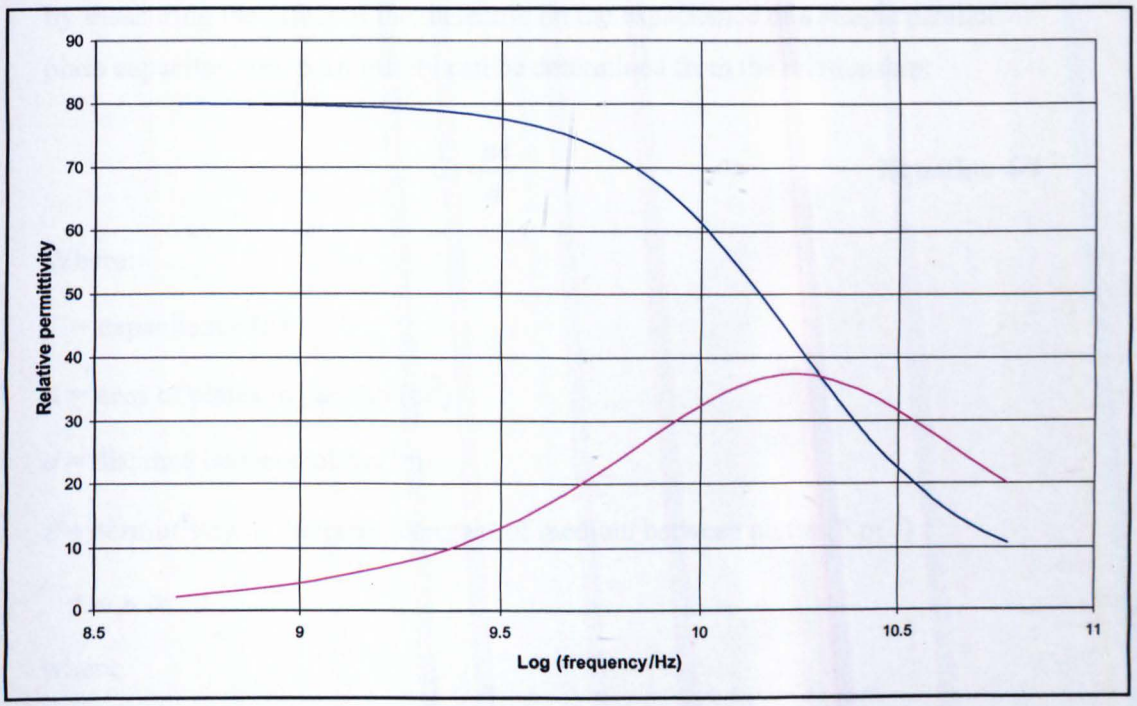

Figure 4-2 Real and imaginary relative permittivity of water.

Debye equations (Equations 4-7 and 4-8) with $\varepsilon_s = 80$, $\varepsilon_\infty = 5$ and $\tau = 9.25 \times 10^{-12}$ s from Nelson (1991) indicate real (—), and imaginary (—) graphs of relative permittivity of water. It shows the range of constant permittivity below 1 GHz (log frequency = 9).

Note that in Figure 4-2 there is a maximum point in the value of the imaginary permittivity where the real permittivity graph has a maximum slope and the permittivity is nearly half the value compared to that at low frequencies. This point is at log frequency (in Hz) of 10.25 or 17.8 GHz. Provided measurements

are done at a frequency well below this point, the real relative permittivity of water will be high enough to facilitate detection. Water bound in a chemical bond is unable to re-orientate itself to the electric field and thus has a permittivity of ε_∞ making only a small contribution to the overall permittivity. Factors (a), (b) and (c) apply to free or unbound water. The case where free water molecules are bound by adhesion force to a solid is discussed in section 5.2.3.

4.3. Measuring Permittivity

The most basic method to measure relative permittivity ε_r or dielectric constant is by measuring the effect of the dielectric on the capacitance of a simple parallel plate capacitor. The permittivity can be determined from the relationship:

$$C = \frac{\varepsilon A}{d} \qquad \textbf{Equation 4-9}$$

Where:

C = capacitance (F)

A = area of plates in parallel (m^2)

d = distance between plates (m)

ε = permittivity or dielectric constant of medium between plates (F m^{-1})

$= \varepsilon_r \times \varepsilon_0$

where

ε_r = relative permittivity (dimensionless)

ε_0 = permittivity of a vacuum (or air) = 8.854×10^{-12} F m^{-1}

An alternative to determining the relative permittivity ε_r by means of capacitance measurement, is to measure the propagation velocity of an electromagnetic (EM) wave through the concrete. Propagation velocity v is given by;

$$v = \frac{1}{\sqrt{\varepsilon\mu}} \qquad \textbf{Equation-4-10}$$

where,

v = propagation velocity (m s^{-1})

ε = permittivity of the medium (F m^{-1})

μ = magnetic permeability of the medium (H m^{-1})

The velocity in free space c_0 is then

$$c_0 = \frac{1}{\sqrt{\varepsilon_0\mu_0}} \qquad \textbf{Equation 4-11}$$

where,

c_0 = propagation velocity in free space (m s^{-1})

ε_0 = permittivity of free space (F m^{-1})

μ_0 = magnetic permeability of free space = $4\pi \times 10^{-7}$ H m^{-1}

If the relative velocity v_r is the ratio of the velocity in the medium to the velocity in free space,

$$v_r = \frac{v}{c_0} \qquad \textbf{Equation 4-12}$$

and similarly

$$\varepsilon_r = \frac{\varepsilon}{\varepsilon_0} \qquad \textbf{Equation 4-13}$$

$$\mu_r = \frac{\mu}{\mu_0} \qquad \textbf{Equation 4-14}$$

then from Equations 4-10 and 4-11 and given that in a non-magnetic medium μ_r = 1, Equation 4-12 can be written as

$$v_r = \frac{1}{\sqrt{\varepsilon_r}} \qquad \textbf{Equation 4-15}$$

or

$$\varepsilon_r = v_r^{-2} \qquad \textbf{Equation 4-16}$$

This simple relationship has the advantage over capacitive measurements (Equation 4-9), which is a function of A and d as well as ε. The physical dimensions must be known for the relative permittivity to be calculated. In contrast, Equation 4-16 is a function of velocity in terms of ε_r only. Note that no mention has been made of the complex permittivity here (see section 4.2.2). The permittivity ε_r referred to above is therefore in fact ε'_r, the real component of the complex permittivity.

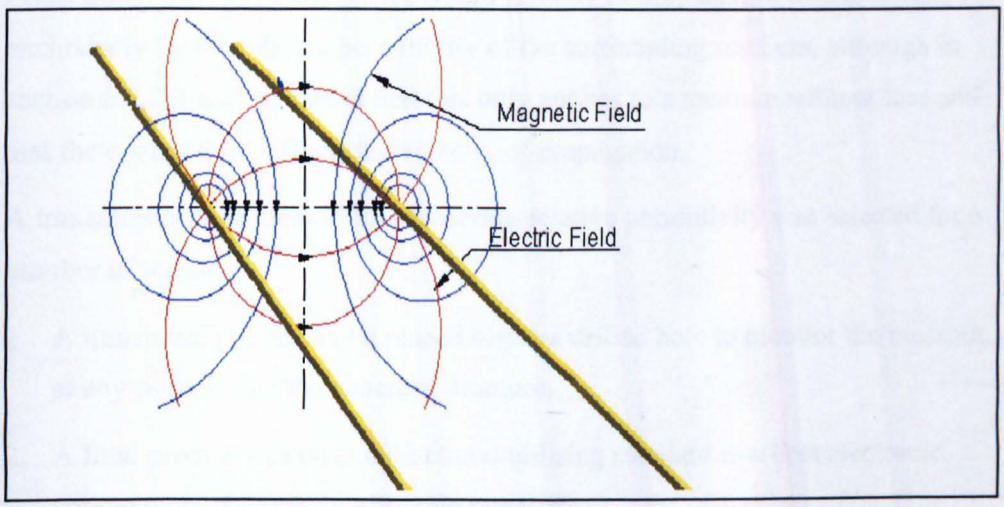

Figure 4-3 EM field lines around a 2-wire transmission line of infinite length.

The relative velocity can be measured by means of a transmitting and receiving antenna on opposite sides, or by means of reflection from the opposite side of the specimen under test. Problems with this technique for measuring moisture in concrete are that the far side may not even be accessible in a typical concrete structure and that the equipment is too bulky and vulnerable to physical damage for effective field use.

The measurement of moisture content by means of microwaves, is the basis for the increasingly popular field of "Microwave Aquametry" (see section 2.1.1). As the component cost of microwave technology is reduced, the employment of microwave aquametry will increase. An example of this development is the use of microstrip antennas and arrays to measure moisture in different substances (Völgyi, 2001). Microstrips can be manufactured with high repeatability and low cost, making it an attractive technology.

4.4. Transmission Line for Measuring Permittivity

Figure 4-3 is a simplified representation of a two-wire transmission line of infinite length, showing the shape of the electromagnetic (EM) field around the conductors. The EM field in the dielectric medium around the conductors determines the propagation characteristics of a signal along this transmission line. From Equation 4-15 it was seen that the velocity of propagation is determined exclusively by the relative permittivity of the surrounding medium, although in section 5.2.2 it will be shown that this only applies to a medium without loss and that the conductivity affects the velocity of propagation.

A transmission line method for measuring relative permittivity was selected for a number of reasons.

1. A transmission line can be placed inside a drilled hole to monitor the moisture at any point inside the concrete structure.
2. A final product can be manufactured utilising standard low cost electronic components and readily available materials.
3. The conductors in a transmission line can be insulated to provide protection from chemical attack over long periods of time and is therefore suitable as an *in situ* sensor for decades if necessary.

Because the propagation velocity in a transmission line is determined by the characteristics of the dielectric medium surrounding the conductors, Equation 4-16 shows that a measurement of the relative transmission velocity enables ε_r, the relative permittivity to be determined. Figure 4-3 shows the electromagnetic (EM)

field around an infinite length transmission line in the surrounding medium (concrete). The relative permittivity ε_r is the square of the ratio of the propagation velocity or phase velocity along the transmission line with air as dielectric and the propagation velocity with the material under test as dielectric. The phase velocity is not measured directly, instead in the case of a finite length, the electrical length of the transmission line is determined. The electrical length of the transmission line is the apparent length of the transmission line if the velocity is assumed to be constant at the free space value (or air for all practical purposes). If the velocity is assumed to be constant, a longer reflection time appears like an increase in transmission line length. The relative permittivity is then the square of the ratio of the apparent length and the physical length as shown in Equation 4-17.

$$\varepsilon_r = \left(\frac{l}{l_0}\right)^2 \qquad \textbf{Equation 4-17}$$

where

l is the apparent length (m)

l_0 is the physical length of the transmission line (m).

4.4.1. The two-wire Transmission Line

As the name indicates, the two-wire transmission line is the most basic form. An example is shown in Figure 4-4.

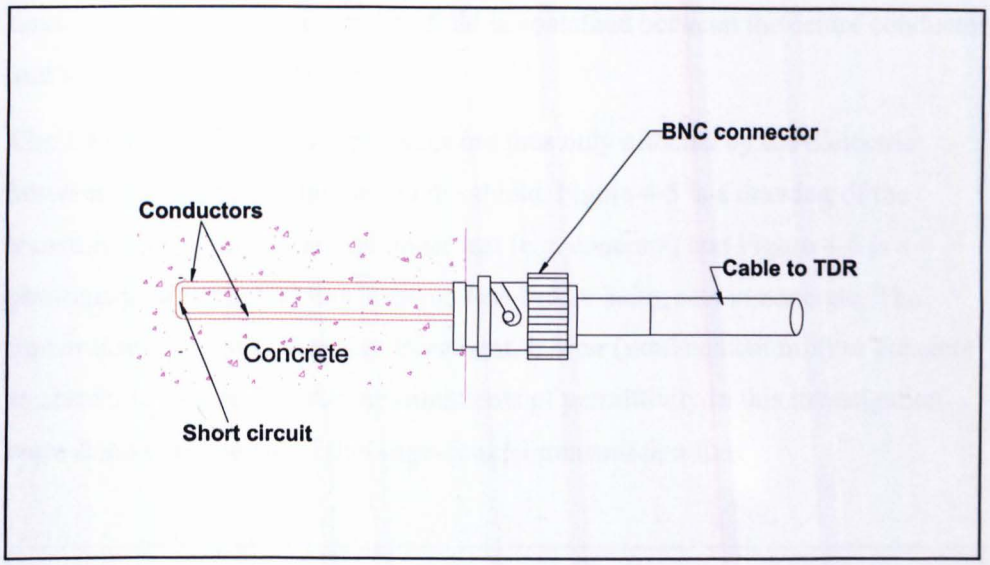

Figure 4-4 Two-wire transmission line in concrete

Tests revealed that the main disadvantage of the 2-wire transmission line was the sensitivity to changes in the relative permittivity in the surrounding dielectric some distance away from the transmission line. Such effects are due to the EM field lines that tend to spread far enough from the transmission line to enter areas that are not of interest or are completely different to the material under test. This is an important consideration in concrete with steel reinforcement or close to the surface of the concrete. The short circuit end (termination) also appeared to be less than ideal. It was affected when a hand was brought closer to the end of the transmission line, an indication that the field lines extend beyond the end of the transmission line. The length of the transmission line in air determined with TDR invariably appeared to be substantially longer than the physical length. An increase of 1 or 2 mm in apparent length due to the non-ideal nature of the conductors and the short-circuit must be expected, but a large increase is not acceptable.

4.4.2. The "Cage-coaxial" Transmission line

The history of the cage-coaxial transmission line will be discussed in more detail in section 6.2.1. In the cage-coaxial transmission line, as in the case of a normal

coaxial transmission line, the EM field is contained between the centre conductor and shield or outer conductors.

The transmission line characteristics are thus only affected by the dielectric between the centre conductor and the shield. Figure 4-5 is a drawing of the transmission line in a material under test (e.g. concrete) and Figure 4-6 is a photograph of an actual transmission line before being cast in concrete. The transmission line was then cast in cement, mortar (sand/cement mix) or concrete as shown in Figure 4-7. All measurements of permittivity in this investigation were done with the aid of this cage-coaxial transmission line.

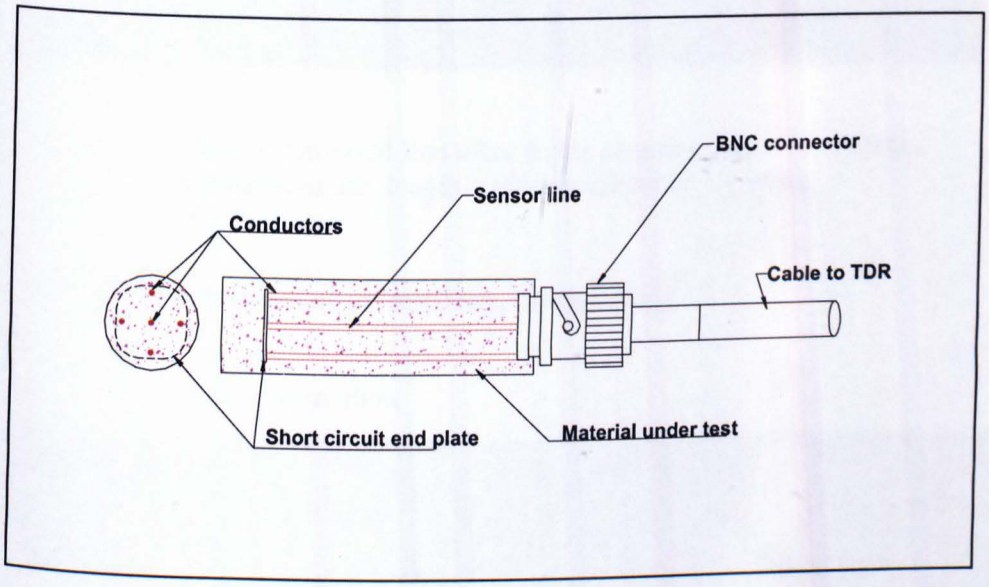

Figure 4-5 The "cage-coaxial" transmission line encapsulated by the material under test (for example cement paste)

Figure 4-6 The cage-coaxial transmission line before being cast into cement.

Length of transmission line 50 mm.

Figure 4-7 The transmission line after being cast in cement or mortar.
Dimensions are: length = 60 mm, diameter = 15 mm

4.5. Measurement of permittivity, methodology

4.5.1. Instrumentation

Figure 4-8 The HP 8752C Network Analyzer.
The display shows a polar diagram for phase measurements.

The Hewlett Packard 8752C RF Network Analyser (Figure 4-8) was used almost exclusively for the investigation of the transmission characteristics of the

transmission lines tested. The HP 8752C is, as the name indicates, primarily a network analyser to measure electronic networks (circuits) in either the transmission or the reflection mode. It can measure the impedance of a transmission line at any frequency within the frequency band 300 kHz to 6 GHz. A useful feature is the fact that the measurement point can be adjusted to any point along the transmission line, but specifically can measure from the start of the transmission line after the connecting cable between the transmission line and the instrument output point. A test short-circuit was made up to provide a reference point at exactly the same distance as the start of the transmission line under test.

The Time Domain Reflectometry or TDR capability is an optional extra facility on this instrument and proved to be of great value for this research. TDR will be discussed in more detail in section 4.5.2.

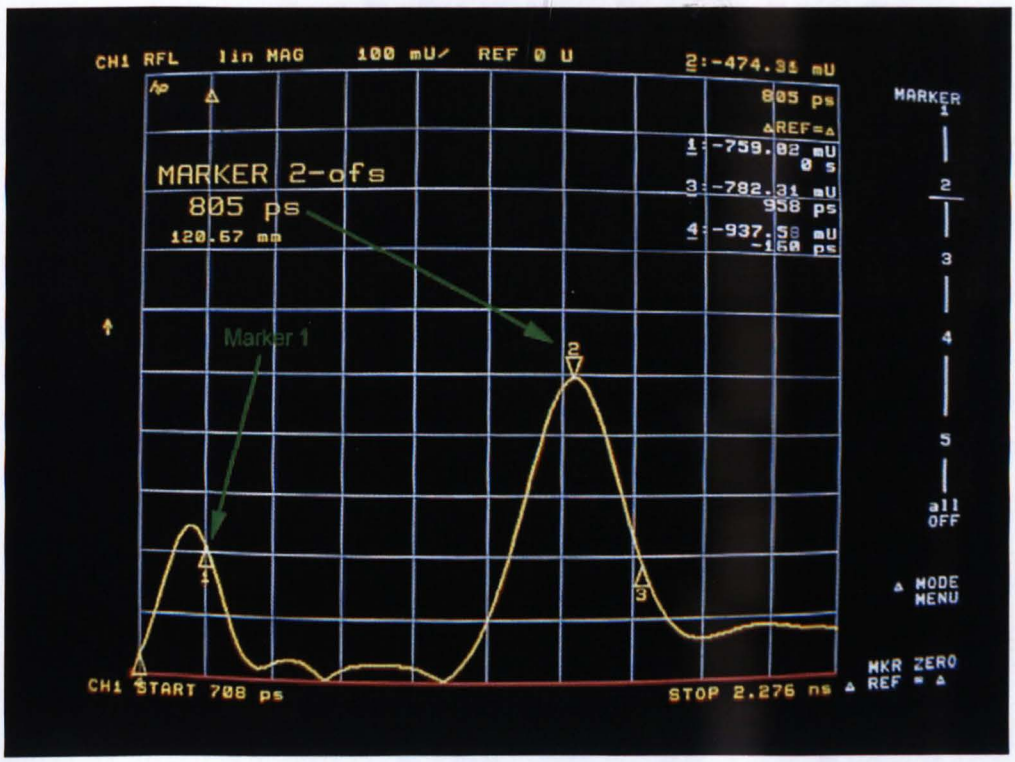

Figure 4-9 A typical TDR trace on the HP 8752C Network Analyser.

The marker 2 is at the reflection point from the termination and shows a reflection time of 805 ps, equivalent to a transmission line length of 120.67 mm in air. Marker 1 is at the start of the transmission line. The

reflection just before the marker is from the adapter between the transmission line and the lead cable.

When used in the TDR mode the HP 8752C does not actually send out a pulse as is the case with dedicated TDR instruments (see section 4.5.2) but converts the reflected signal from a swept frequency (frequency domain) to the time domain by means of a Fast Fourier Transform (FFT) algorithm. The only possible disadvantage of this method compared to pure TDR pulse analysis, is the time required to do the conversion. The instrument cannot react to rapid changes in the reflected signal. This delay (about one second) can be seen as equivalent to changes happening during the interval between two pulses in the pulse system (low pulse repetition frequency) and is not important in the case of a static situation. The TDR pulse is displayed on the screen as shown in an example in Figure 4-9 for a transmission line terminated in a short circuit. A marker can be placed on the crest of the pulse (marker 2 in Figure 4-9) and the reflection time read off the screen (805 ps in the example). Note that a length of 120.67 mm is also indicated below the time, denoting the length of an equivalent transmission line with air dielectric for a reflection time of 805 ps. The instrument can be adjusted for a known relative transmission speed along the transmission line under test and the distance the pulse has travelled to and from the reflection point can be read off directly. In this case the relative velocity was set to 0.5 (half the speed of light in vacuum), which gives the distance to the reflection point in vacuum (or air) instead of the total path length which would be double that. This indicated length is the length used in Equation 4-17 and the indicated time used in Equation 4-18 to calculate the relative permittivity. The start is at marker 1, which is set by connecting a good short circuit at the start of the transmission line under test.

The HP 8752C also measures impedance when employed in the reflection mode. Due to the fact that only reflections are of interest in this work, the transmission mode was not used on the instrument. The reflection is displayed on either a Smith Chart (see section 7.2.1 and Appendix D) or as a vector chart with amplitude and phase angle information as shown in Figure 4-8 and Figure E-1.

4.5.2. Time Domain Reflectometry or TDR

Time Domain Reflectometry or TDR is the measurement of the time taken for a reflection of a pulsed input to be returned back to the source. The technology was developed principally as a means to detect fault conditions along a transmission line. TDR is used mostly for telecommunication test purposes and is a convenient method to find the exact location of faults in transmission lines like underground cables, or to test the impedance match at a connection between transmission lines. A mismatch will result in a reflection and thus power loss. There are numerous dedicated TDR instruments available for this purpose.

The shortest distance that can be measured is determined by the resolution of a TDR instrument, which in turn is determined by the length (duration) of the transmitted pulse. If the pulse width or duration should be longer than the reflection time, no reflection could be detected. The resolution of the HP 8752C is such that it can easily measure the reflection time from the end of a transmission line only a few centimetres long. The pulse peak can be measured to within one picosecond, but the resolution is determined by the maximum frequency of 6GHz, which has a period of 167 ps. Therefore the minimum theoretical transmission line length, l, that can be measured is the transmission velocity × minimum time, or: $l = 3 \times 10^8 \times 167 \times 10^{-12}$ m = 50 mm total path length, or a short circuit terminated transmission line of 25 mm in air.

This physical length of 25 mm is assumed to be the minimum line length in air that could be measured with the HP 8752C RF Network Analyser using TDR.

4.5.3. Use of TDR to measure relative permittivity

TDR was found to be a convenient method to measure the relative permittivity of materials. It should be noted that a pulse method is broad band in nature as illustrated by the fact that it is a conversion (FFT) of a broad frequency band swept signal. The relative permittivity measured is thus the combined permittivity averaged over the frequency spectrum used.

Instead of using the line lengths in Equation 4-17 for measuring the relative permittivity, the reflection t_r time can be used in the formula. The relative

permittivity will therefore be the square of the ratio of the reflection time and the reflection time with air dielectric.

$$\varepsilon_r = \left(\frac{t_r}{t_0}\right)^2 \qquad \textbf{Equation 4-18}$$

where

t_r = reflection time measured (s)

t_0 = reflection time with air as dielectric (s)

Considering again the short-circuited transmission line, the phase angle between the transmitted and received signal is a direct measure of the path length of the signal. The phase angle is a function of frequency f and line length l or:

$$\phi = G(f,l)$$

It can be shown[6] that the phase change will be:

$$\phi = 2.4fl \qquad \textbf{Equation 4-19}$$

where

ϕ = phase angle (degrees)

f = frequency (GHz)

l = length of short-circuited transmission line (mm)

In a loss free medium the transmission velocity is given by Equation 4-11.

---

[6] $\phi = 360 \times 2l/\lambda$ degrees
where
$2l$ = total path length for a short-circuited line of length l (m)
λ = wavelength of the signal (m)
Therefore
$\phi = 720l \times f/c_0$
where
f = frequency of the signal of wavelength λ (Hz)
c_0 = velocity of EM wave in free space (m s^{-1})
with f in GHz, l in mm and $c_0 = 3 \times 10^8$ m s^{-1}, the phase will be:
$\phi = 2.4fl$ degrees.

Equation 4-17 shows that the relative permittivity is the square of the ratio of the apparent transmission line lengths. From Equation 4-19, if ϕ_0 is the phase in free space with l_0 the physical transmission line length, then:

$$\phi_0 = 2.4fl_0 \qquad \textbf{Equation 4-20}$$

For a transmission line in a medium with relative permittivity ε_r the phase angle ϕ_1 will be:

$$\phi_1 = 2.4fl_1 \qquad \textbf{Equation 4-21}$$

where,

l_1 = apparent transmission line length (m)

and

$$\frac{\phi_1}{\phi_0} = \frac{l_1}{l_0} \qquad \textbf{Equation 4-22}$$

Combining with Equation 4-17

$$\varepsilon_r = \left(\frac{\phi_1}{\phi_0}\right)^2 \qquad \textbf{Equation 4-23}$$

Differentiating Equation 4-20 and Equation 4-21 in terms of f, $(\frac{d\phi}{df})$ shows that the slopes will be $2.4l_0$ and $2.4l_1$ respectively.

The ratio of the slopes of two functions with different transmission line lengths l_1 and l_0 will be the ratio of the transmission line lengths. If one of the lines is the transmission line in free space (air), the relative permittivity can be found from the square of this ratio.

$$\varepsilon_r = [\frac{\text{slope of line measured}}{\text{slope of the line in free space}}]^2 \qquad \textbf{Equation 4-24}$$

4.5.4. Phase Velocity – Permittivity Spectrum

The relative permittivity or dielectric constant of a dielectric material is not the same for all frequencies. This is the basis of dielectric spectroscopy where the material characteristic is investigated by measuring the dielectric constant or relative permittivity at various discrete frequencies.

In a plot of phase angle versus frequency for a transmission line in a dielectric medium, the phase of the transmission line at any one frequency can be used from Equation 4-23 to determine the permittivity at that frequency. If a transmission line is used to measure the permittivity at one frequency, the relative permittivity at that frequency will be measured rather than the wide band permittivity as seen by the TDR measurement. For the purpose of calibration the permittivity over the frequency band to be used is thus the important parameter to measure. It will also be shown in section 4.6 that the permittivity at discrete frequencies, measured by using the phase relationship with an ideal theoretical transmission line with air dielectric, could be affected by unique transmission line characteristics.

4.6. Permittivity of Concrete as measured with the Transmission Line

Figure 4-10 is a plot of permittivity versus frequency for a 30 mm transmission line embedded in a mortar of 50:50 ratio of fine aggregate (sand) to cement at three values of moisture content. Permittivity was determined at discrete frequencies by measuring the phase change and applying Equation 4-23. The moisture level was determined gravimetrically with the oven dry mass taken as 0% MC. Note the considerable variation in the apparent permittivity over the frequency spectrum and notably towards the lower end of the spectrum.

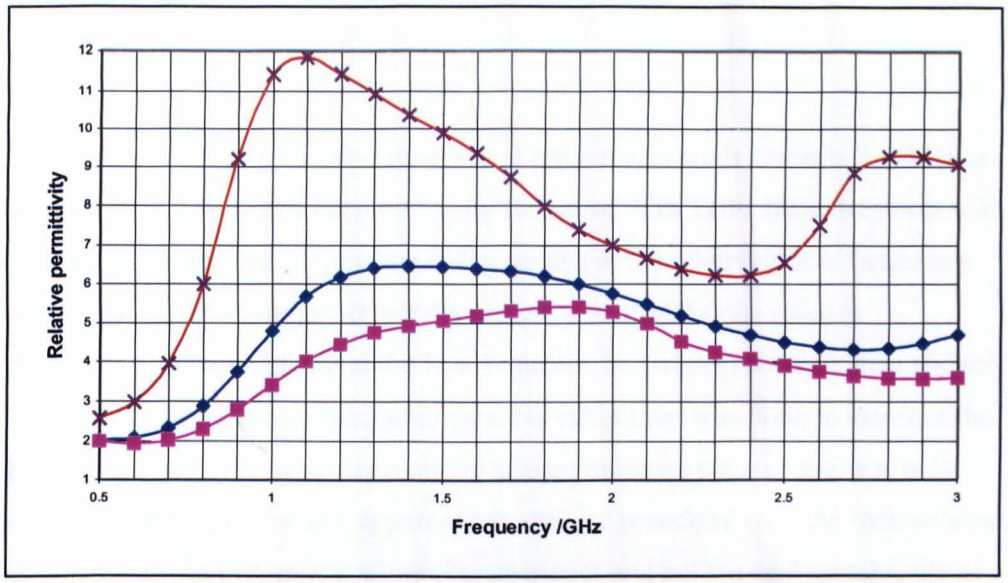

Figure 4-10 Calculated permittivity at discrete frequencies for the 30mm mortar filled transmission line exposed to different moisture contents.

Mortar composed of sand and cement in 50:50 ratio (by mass).

Moisture content, MC/%: (—■—) 0; (—♦—) 3.9; (—×—) 11.5.

The moisture content was calculated from Equation 3-2. The volume in the denominator of Equation 3-2 was determined by subtracting the volume of the transmission line conductors from the total volume of mortar and the volume of moisture in the numerator of Equation 3-2 was the difference in the oven dry mass and the mass of the sample with moisture added. The relative permittivities ε_r were calculated as in Equation 4-23 from the square of the ratios of the phase shift measured and the phase shift of the transmission line with air dielectric (before being encased in mortar).

The apparent relative permittivity at lower frequencies tends towards 2, which is considerably lower than the permittivity measured with TDR. Measurements with a capacitance type moisture meter indicates that at the relatively low frequency used by such an instrument (typically around 4 to 40MHz) the relative permittivity is much higher at the low frequency end of the spectrum than shown by the discrete frequency measurements. No calibration was done to measure the permittivity with the capacitance meter against moisture content and was only used to confirm that the low apparent permittivity measured with the transmission line is due to the transmission line characteristics and not the real permittivity at that frequency. If the transmission line is used to measure the permittivity at a discrete frequency, the frequency must be high enough not to be affected by the transmission line effect at lower frequencies. It cannot therefore be assumed that the permittivity would be the same as that measured over a wide bandwidth using TDR.

To illustrate the variation in relative permittivity measured with the transmission line, another set of graphs, shown in Figure 4-11, was produced from the results of relative permittivity against moisture content at different frequencies.

In conclusion this chapter has shown how the effects of moisture on the permittivity of concrete can be measured by means of a transmission line. The change in the apparent length of a transmission line embedded in the concrete can be used as the parameter to measure moisture content. If the permittivity is measured at discrete frequencies, the frequency must be high enough to avoid the cut-off effect as seen in Figure 4-10. The method to determine the apparent transmission line length will be discussed in the following chapters.

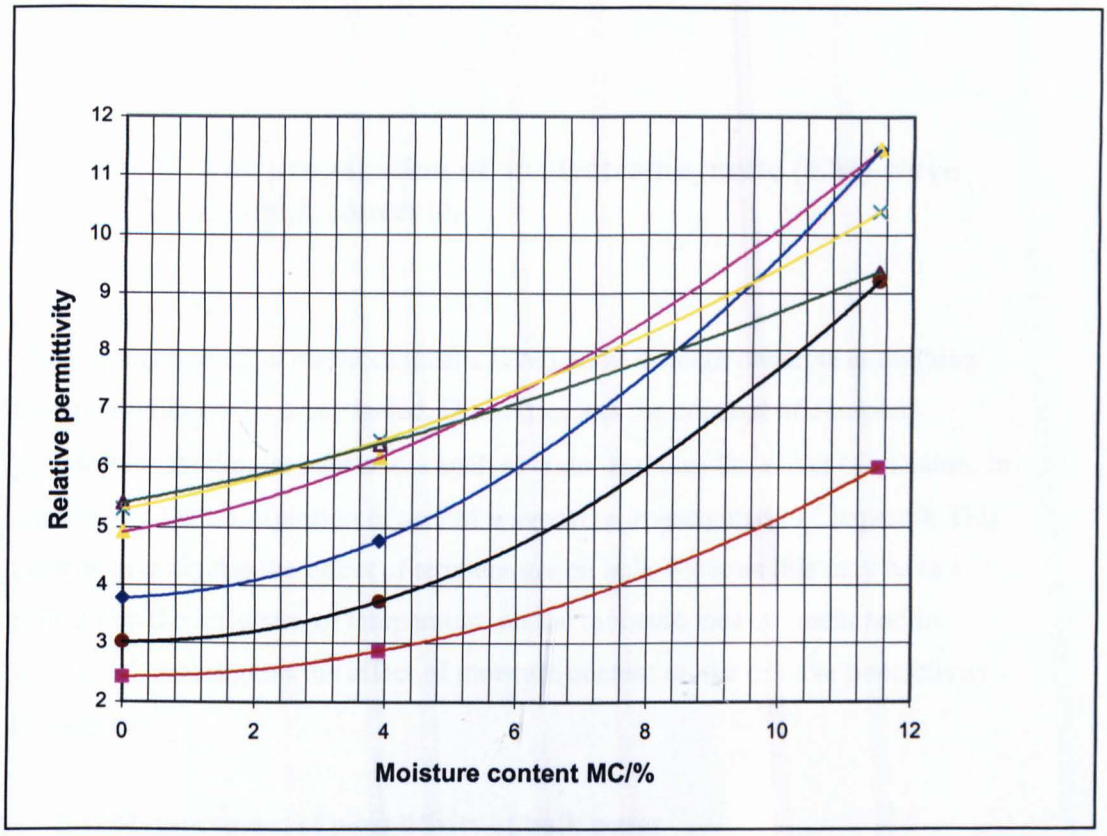

Figure 4-11 Relative permittivity versus moisture content at discrete frequencies on the 30mm mortar filled transmission line.

Frequency/MHz: (—■—) 800; (—●—) 900; (—◆—) 1000; (—▲—) 1200; (—×—) 1400; (—△—) 1600.

As in Figure 4-10 the moisture content was calculated from Equation 3-2. The volume in the denominator of Equation 3-2 was determined by subtracting the volume of the transmission line conductors from the total volume of mortar and the volume of moisture in the numerator of Equation 3-2 was the difference in the oven dry mass and the mass of the sample with moisture added. The relative permittivities ε_r were calculated as in Equation 4-23 from the square of the ratios of the phase shift measured and the phase shift of the transmission line with air dielectric (before being encased in mortar). Moisture content versus relative permittivity was then drawn for the various discrete frequencies.

Chapter 5. The propagation of an electromagnetic (EM) wave through concrete.

The propagation of an electromagnetic (EM) wave through concrete containing moisture will now be investigated. Dielectrics and the concept of complex permittivity for dipolar substances such as water and thus the effect of moisture in concrete on the transmission of an EM wave were investigated in Chapter 4. This chapter investigates the effect of temperature on bulk water as this may have a bearing on the influence of temperature on the moisture measurement and in section 5.2 investigates the effect of moisture content on the relative permittivity in concrete.

5.1. Measurement of permittivity of bulk water

The relaxation time τ is a function of temperature with a resultant effect on permittivity. The permittivity of bulk water as a function of temperature (T) is given by Scott and Or (2001) quoting Weast (1986) to be:

$$\varepsilon_{fw}(T) = 78.54[1 - 4.579\times10^{-3}(T-298) + 1.19\times10^{-5}(T-298)^2 - 2.8\times10^{-8}(T-298)^3]$$

Equation 5-1

where

ε_{fw} = relative permittivity of bulk water

T = temperature (K).

TDR measurements were carried out to determine the relationship between the relative permittivity of bulk water and the temperature of the water using a 50 mm bare copper conductor cage-coaxial line, Figure 5-1. The Scott-Or-Weast equation (Equation 5-1) needed to be modified slightly so as to fit the measured data:

$$\varepsilon_{fw}(T) = 77.23[1-4.79\times10^{-3}(T-298)+0.48\times10^{-5}(T-298)^2-2.8\times10^{-8}(T-298)^3]$$

Equation 5-2

The results show that the relative permittivity of water at a temperature of 298 K should be modified slightly from 78.54 to 77.23 in order to fit the experimental results. The other factors were also changed slightly as shown when Equation 5-1 is compared with Equation 5-2.

The result shown in Figure 5-1 shows a good agreement with experimental results for the bare copper conductor with a small difference in slope.

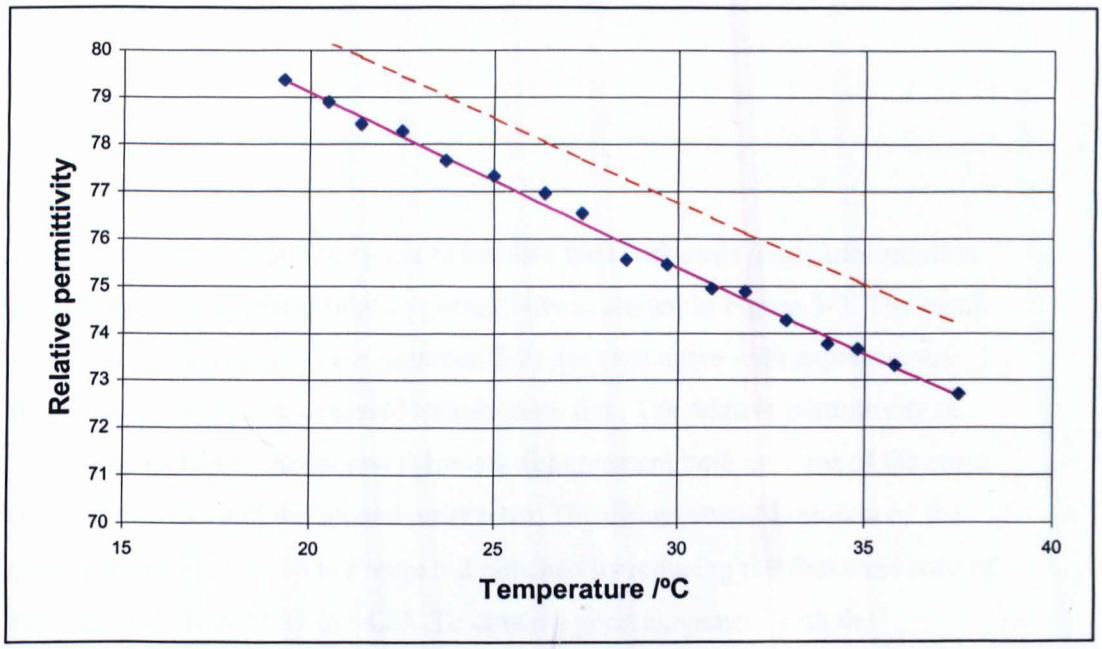

Figure 5-1 Temperature dependence of the relative permittivity of bulk water with bare copper conductors in a 50 mm cage-coaxial transmission line.

(♦) Relative permittivity determined from TDR delay time in water t_r and air t_0 = 338 ps and calculated with Equation 4-18.

(– – –) Relative permittivity of water calculated with the Scott-Or-Weast relationship of Equation 5-1.

(—) Line of best fit calculated using Equation 5-1 but allowing Solver in Microsoft Excel to 'optimise' the factors of Equation 5-1 leading to Equation 5-2. The relative permittivity was found to be 77.23 rather than 78.54 at 25°C (298 K). The first order term was changed slightly from -4.579×10^{-3} to -4.79×10^{-3} to adjust the slope and the second order term from 1.19×10^{-5} to 0.48×10^{-5}. The very small second order term had a negligible effect over the temperature range investigated.

Using a thin layer of lacquer paint to insulate the conductors in the transmission line changes the apparent relative permittivity as shown in Figure 5-2. The result predicted by Equation 5-1 (or Equation 5-2) does not agree with experimental results obtained for the insulated transmission line. The relative permittivity at 25°C is considerably lower and there is a disagreement both in terms of the slope (first order term) and the second order term. The disagreement is shown by the graph dotted line (– – –) in Figure 5-2 obtained by reducing the first term only of Equation 5-2 from 77.23 to 54.83. To obtain a good agreement with the experimental results the least-mean-square technique with Solver in Microsoft Excel was used to determine all the factors for the best fit to the measured data. The results are shown in Equation 5-3.

$$\varepsilon_{fw}(T) = 54.88[1-2.99\times10^{-3}(T-298)-2.67\times10^{-5}(T-298)^2+138.32\times10^{-8}(T-298)^3]$$

Equation 5-3

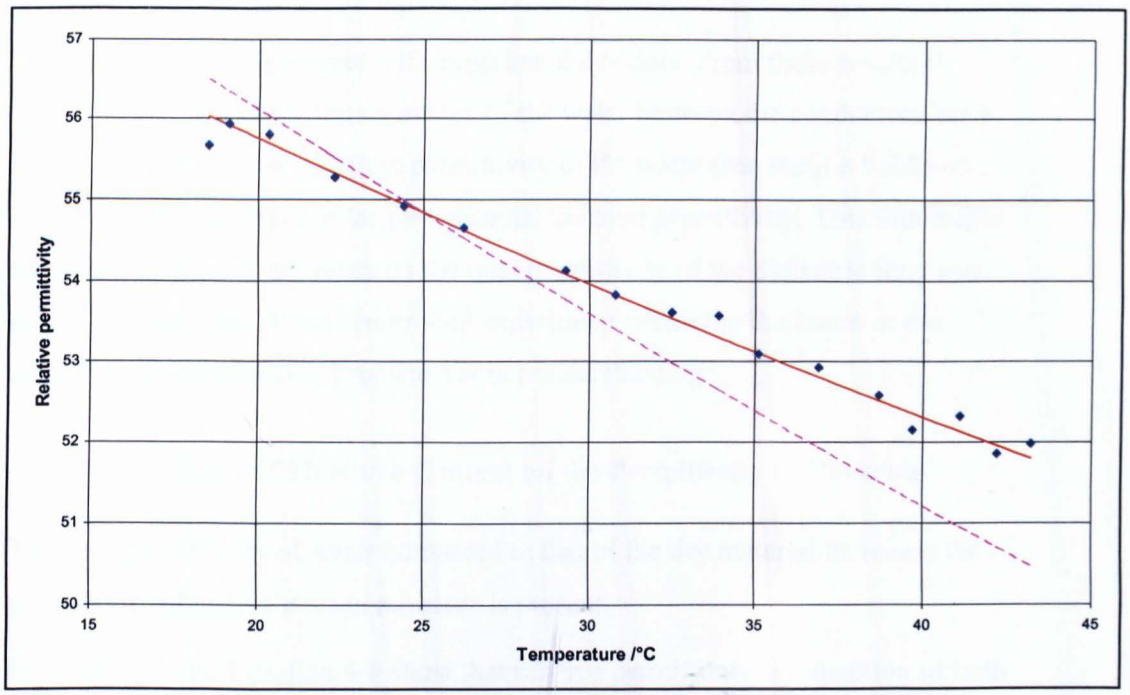

Figure 5-2 Effect of insulated copper conductors of a 50 mm cage-coaxial transmission line on the temperature dependence of the apparent relative permittivity of bulk water.

(♦) Relative permittivity determined from TDR delay time in water (t_r) and air (t_0 = 338 ps), calculated with Equation 4-18.

(– – –) Resultant graph when only the first term (multiplication factor or zeroth order factor) in Equation 5-2 is adjusted for a relative permittivity of water at 25°C from 77.23 to 54.83.

(—) Line of best fit calculated using Equation 5-2 but allowing Solver in Microsoft Excel to 'optimise' the factors of Equation 5-2 leading to Equation 5-3. The relative permittivity was found to be 54.83 rather than 77.23 at 25°C (298 K). The first order term was changed from -4.79×10^{-3} to -2.99×10^{-3} to adjust the slope and the second order term from 0.48×10^{-5} to -2.67×10^{-5}. Again the small second order term had a negligible effect over the temperature range investigated.

Note the excellent agreement with experimental results. From these results it would appear that either the resistance of the water between the conductors has a strong influence on the apparent permittivity of the water (see section 5.2.2) or that the added thin layer of lacquer changed the total permittivity. This thin buffer may have a stronger influence on the total permittivity of the dielectric than was originally expected. A well-controlled experiment where the thickness of the insulation is varied would produce a better understanding.

5.2. The Effect of Moisture Content on the Permittivity of Concrete

The high permittivity of water compared to that of the dry material increases the permittivity of concrete when moisture is present.

Equation 4-7 and Equation 4-8 show that relative permittivity is a function of both frequency f (where $f = \frac{\omega}{2\pi}$) and the relaxation time τ. The relaxation time τ is in turn a function of temperature (Equation 4-3).

In a single dielectric substance the change of permittivity with frequency can be calculated from Equation 4-7 and Equation 4-8 if τ and T are known. Where there is a mixture of different dielectric materials however, the total permittivity is affected by different factors and the relationship is in general not linear (see section 5.3.1). Thus far it has been assumed that there is no conduction current in the medium, which is not the case with concrete and other moist substances.

The various models proposed by different authors to calculate the permittivity of mixed dielectrics (section 5.3.1) are all formulae applicable to a specific dielectric mix. The mathematical model of moisture in concrete will be investigated further in section 5.3.

5.2.1. Bound and free water

Only the water molecules that are free to turn in the electric field increase the overall permittivity enough to be detected. The moisture content measured by this technique thus excludes bound water. Chemically bound water molecules include those present in interlayer spaces, but not those present in pores larger than this

(Taylor, 1997) (see also Appendix C). The boundary effect discussed in section 5.2.3 produces another form of bound water.

5.2.2. Apparent permittivity as measured with propagation velocity and the effect of conductivity in a lossy medium

The electromagnetic field equations for a non-conducting medium (Collin, 1966) lead to a differential equation with a solution representing a wave with velocity of propagation equal to $\frac{1}{\sqrt{\varepsilon\mu}}$. This solution assumes that there is only displacement current[7] and no conduction current in the medium of propagation. That would be the case if the conductivity σ of the medium was zero. However, in the case of concrete with moisture $\sigma \neq 0$, so both conduction current and displacement current must be considered. It will be shown that conduction current tends to reduce the propagation velocity and as the relative permittivity is calculated from the propagation velocity there is an apparent increase in the permittivity due to the conduction current. Note that the complex permittivity in Equation 4-7 and Equation 4-8 do not contain the conductivity factor σ. To obtain the equations for complex permittivity using the Debye model, only the phase lag due to the relaxation time was taken into account (see Appendix B).

Now considering the propagation of an electromagnetic wave in a conducting medium, Jordan (1962) shows how the intrinsic propagation constant γ is derived from the EM field equations when there is also a conduction current present.

$$\gamma = \sqrt{j\omega\mu(\sigma + j\omega\varepsilon)} \qquad \textbf{Equation 5-4}$$

The real part of Equation 5-4 is the attenuation as the wave moves through the medium and the imaginary part is the phase shift for the wave per unit length.

Where

ω = the angular velocity (rad s^{-1})

μ = magnetic permeability of the medium (H m^{-1})

ε = permittivity of the medium (F m^{-1})

σ = conductivity (mho m^{-1})

The propagation constant γ can be split up into the real and imaginary parts:

$$\gamma = \alpha + j\beta \qquad \textbf{Equation 5-5}$$

where

α = attenuation constant (nepers m^{-1})

β = phase constant (rad m^{-1})

In a medium with no conduction $\sigma = 0$, therefore

$$\gamma = j\omega\sqrt{\mu\varepsilon} \qquad \textbf{Equation 5-6}$$

As the real part is 0,

$$\beta = \omega\sqrt{\mu\varepsilon} \text{ rad } m^{-1} \qquad \textbf{Equation 5-7}$$

The phase velocity v is given by

$$v = \frac{\omega}{\beta} \text{ m } s^{-1} \qquad \textbf{Equation 5-8}$$

In a medium with no conduction:

$$v = \frac{1}{\sqrt{\mu\varepsilon}} \text{ m } s^{-1} \qquad \textbf{Equation 5-9}$$

This is the propagation velocity of an EM wave derived from the field equations for a non-conducting medium (Jordan 1962).

To find the expression for α and β when $\sigma \neq 0$, consider Equation 5-4 and Equation 5-5 again:

$$\sqrt{j\omega\mu(\sigma + j\omega\varepsilon)} = \alpha + j\beta$$

---

[7] Current flowing in a time varying magnetic field without a conductor introduced into the EM field equations that led to the differential equation with a solution predicting the existence and speed of the EM wave by Clark Maxwell.

Squaring both sides give

$$(\alpha + j\beta)^2 = j\omega\mu(\sigma + j\omega\varepsilon)$$

Now equating real and imaginary parts:

$$\alpha^2 - \beta^2 = -\omega^2\mu\varepsilon \qquad \textbf{Equation 5-10}$$

and

$$2\alpha\beta = \omega\mu\sigma \qquad \textbf{Equation 5-11}$$

Eliminating α from Equation 5-10 and Equation 5-11, results in a fourth order equation for β

$$4\beta^4 - 4\beta^2\omega^2\mu\varepsilon - \omega^2\mu^2\sigma^2 = 0$$

Solving for β yields four possible values. Put $\sigma = 0$ in the four solutions and it shows that only one solution gives a positive non-zero result, namely:

$$\beta = \omega\sqrt{\frac{\mu\varepsilon + \mu\sqrt{\varepsilon^2 + \sigma^2\omega^{-2}}}{2}}$$

Again dividing ω by β to find the phase velocity v:

$$v = \frac{1}{\sqrt{\frac{\mu\varepsilon + \mu\sqrt{\varepsilon^2 + \sigma^2\omega^{-2}}}{2}}}$$

$$= \frac{1}{\sqrt{\mu\varepsilon}} \times \sqrt{\frac{2}{1 + \sqrt{1 + \sigma^2\omega^{-2}\varepsilon^{-2}}}} \qquad \textbf{Equation 5-12}$$

The term $\sigma^2\omega^{-2}\varepsilon^{-2} << 1$ when $\sigma \to 0$, or $\omega >> \sigma/\varepsilon$. Under these conditions

Equation 5-12 reduces to:

$$v = \frac{1}{\sqrt{\mu\varepsilon}} \text{ m s}^{-1}$$

Which is the same as Equation 5-9 for the phase velocity in a non-conducting medium.

Similarly eliminating β from Equation 5-10 and Equation 5-11:

$$4\alpha^4 + 4\alpha^2\omega^2\mu\varepsilon - \omega^2\mu^2\sigma^2 = 0$$

The solution for α is found in the same way as for β:

$$\alpha = \omega \times \sqrt{\frac{\mu\varepsilon}{2}} \times \sqrt{\left(1+\frac{\sigma^2}{\omega^2\varepsilon^2}\right)^{\frac{1}{2}} - 1} \qquad \textbf{Equation 5-13}$$

Although Equation 5-13 shows that α is a function of ω (and therefore f), it is found to be the case only for low frequencies by the binomial expansion of the term $\left[1+\frac{\sigma^2}{\omega^2\varepsilon^2}\right]^{\frac{1}{2}}$:

$$(1+\frac{\sigma^2}{\omega^2\varepsilon^2})^{1/2} = 1+\frac{1}{2}\frac{\sigma^2}{\omega^2\varepsilon^2} + \ldots..$$

$$\approx 1+\frac{1}{2}\frac{\sigma^2}{\omega^2\varepsilon^2} \text{ when } \frac{\sigma}{\omega\varepsilon} << 1$$

Replacing the term in Equation 5-13 yields:

$$\alpha = \frac{\sigma}{2}\sqrt{\frac{\mu}{\varepsilon}} \text{ nepers m}^{-1} \qquad \textbf{Equation 5-14}$$

Inspection of Equation 5-12 shows that the velocity of propagation v decreases with increase in conductivity σ, which largely explains the reduction in the apparent relative permittivity of bulk water with insulation on the conductors (see section 4.2.2) when there is an absence of, or at least reduction in conduction current. In the absence of conduction current, only displacement current plays a role and ε_r is reduced. What is still not completely clear is how this difference affects the permittivity of a porous medium where there could be breaks in the conduction path between the conductors.

This section has shown that not only is the apparent relative permittivity of water a function of temperature as expected but also is affected by the presence of conduction current. The importance of the variation in relative permittivity of water will be clearer when the formula for the dielectric mix of moisture and concrete is discussed in section 5.3.2.

5.2.3. Boundary effect in a pore system of a solid matrix

Scott and Or (2001) state that the large disparity between dielectric permittivity of bound and free water results in erroneous moisture content estimates based on electromagnetic measurements of permittivity, especially in high surface area porous materials. Concrete and specifically the cement paste considered in this thesis are high surface area porous materials (see section 3.2.2). Water that is "bound" to solid surfaces due to the adhesion force between the liquid and solid molecules, is subject to surface forces that hinder its response to an imposed electromagnetic field. The first mono-layer of molecules in the boundary may not re-orientate at all and those close enough to the solid to be affected may be subjected to an increase in the frictional constant ξ of Equation 4-2. The result is both a lower relaxation frequency and in lower bulk relative permittivity (ε_b) relative to free liquid water. The bulk permittivity of successive molecular water layers increases with distance from the solid surface up to that of free water at around 3 molecular layers (Scott and Or, 2001). The size of the gel pores in cement paste is of the order of 5 nm to 100 nm (see section 3.2.2). Taking the size of a water molecule to be around 0.3 nm or 3 Å, small gel pores in cement paste would contain a high percentage of water molecules in the boundary layer.

There are thus two unrelated factors contributing to the apparent reduction in permittivity of the water, namely pore size and water/solid adhesion force.

5.2.4. The effect of ice formation on permittivity

Ice has a higher dielectric constant or static relative permittivity than bulk water. The relaxation time for ice is however much lower than liquid water so that whilst the static permittivity of ice is in the region of 100 at 0°C it decreases to around 3.2 to 3.3 at frequencies above 100 MHz (Hobbs, 1974). Although there should be

a sudden decrease in the permittivity on formation of ice, the probability of ice forming in the gel pores or even the capillary pores is very small. The reason is that the size of the water droplet and thus the size of the pore affect nucleation needed for ice formation. Water droplets of 2 to 3 μm in diameter could be supercooled to –35°C without the formation of ice. Figure 5-3 shows the relationship between the droplet size and the temperature at which nucleation (ice formation) occurs.

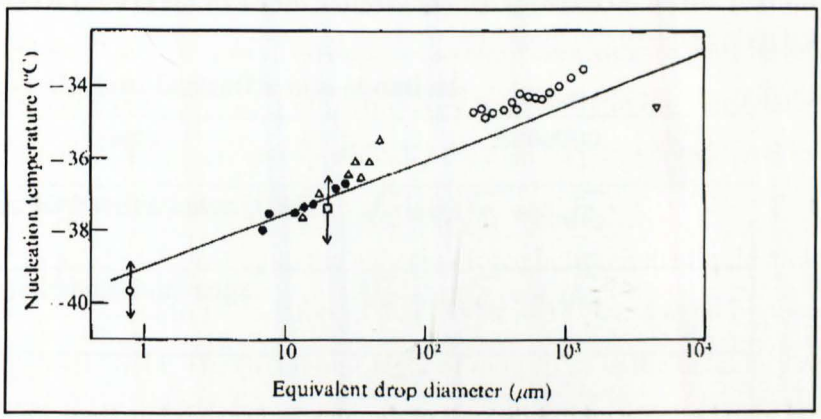

Figure 5-3 Nucleation temperature vs. droplet size from 3 sets of experiments.
(extracted from Hobbs, 1974)

From the above it can be deduced that under the normal conditions encountered the initial formation of ice will only occur in the larger cracks and fissures in the concrete. Water will be found in the larger pores, cracks and fissures only when the moisture content is very high, probably close to saturation. It explains why frost damage only occurs at moisture levels above the hygroscopic range as mentioned in section 3.3.5.

5.3. Mathematical modelling

In this section the total effective permittivity of material consisting of a mixture of different permittivities will be investigated. A mixture formula specific to concrete will be derived from a combination of experimental data and existing formulae. Concrete that contains some moisture is a mixture of at least three substances with different relative permittivity, namely solid material, air and

water. Even the solid material is a mixture of different substances, but as a first approximation these can be regarded as having the same relative permittivity.

5.3.1. Existing models or formulas for mixed dielectrics

Nelson (1991) mentions several mixture formulae. These are all two-component mixtures with fractional volumes of the two materials v_1 and v_2 (so that $v_1 + v_2 = 1$) and with relative complex permittivity of the materials ε_1 and ε_2 respectively. The formulae are listed in Table 5-1 for easy comparison.

Table 5-1 Various Dielectric mix equations

Name	Equation
Complex Refractive Index (CRI)	$\sqrt{\varepsilon} = v_1\sqrt{\varepsilon_1} + v_2\sqrt{\varepsilon_2}$
Landau, Lifshitz, Looyenga	$\sqrt[3]{\varepsilon} = v_1\sqrt[3]{\varepsilon_1} + v_2\sqrt[3]{\varepsilon_2}$
Böttcher	$\frac{\varepsilon_1 - \varepsilon_2}{3\varepsilon} = v_2\frac{\varepsilon_2 - \varepsilon_1}{\varepsilon_2 + 2\varepsilon}$
Bruggeman-Hanai	$\frac{\varepsilon - \varepsilon_2}{\varepsilon_1 - \varepsilon_2} \times \sqrt[3]{\frac{\varepsilon_1}{\varepsilon}} = 1 - v_2$
Rayleigh	$\frac{\varepsilon - \varepsilon_1}{\varepsilon - 2\varepsilon_1} = v_2\frac{\varepsilon_2 - \varepsilon_1}{2\varepsilon_1 + 2\varepsilon_2}$
Lichtenecker	$\ln\varepsilon = v_1\ln\varepsilon_1 + v_2\ln\varepsilon_2$

Each of these mixtures can be used to estimate the complex permittivity of the solid material from the complex permittivities of the air-particle mixtures by substituting 1–j0 (i.e. no loss situations) for ε_1, the complex permittivity of air and solving for ε_2.

A general observation is that the formulae differ to such an extent that the appropriate formula can only be found by testing it against experimental results to find the best fit.

5.3.2. Dielectric mix model for the dielectric constant of concrete with moisture

The Complex Refractive Index (CRI) formula used by Leschnik and Schlemm (2001) provides a good fit for the permittivity of concrete containing moisture and can be used as a starting point. Note that volumetric moisture measurement was used in the reference to enable a comparison to be made of the permittivity of different building materials with changes in moisture content. The results from the paper are shown in Figure 5-4.

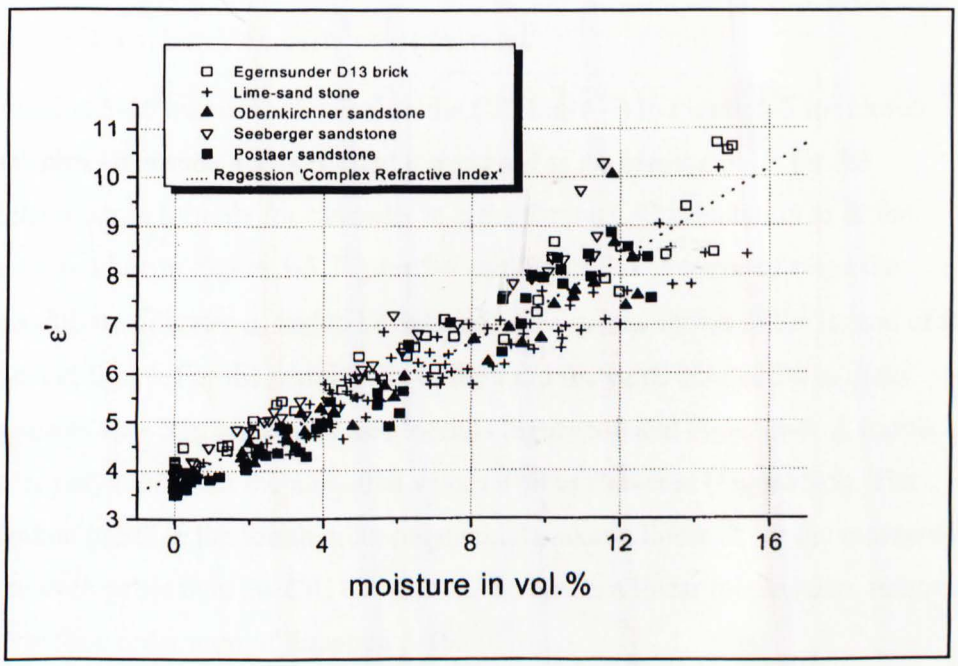

Figure 5-4 Comparison of permittivity of different building materials (from Leschnik and Schlemm, 2001)

The Complex Refractive Index (CRI) dielectric mix formula (Table 5-1) can be written as:

$$\sqrt{\varepsilon} = v_w\sqrt{\varepsilon_w} + (1 - v_w)\sqrt{\varepsilon_m}$$

rearranging it gives

$$v_w = \frac{\sqrt{\varepsilon} - \sqrt{\varepsilon_m}}{\sqrt{\varepsilon_w} - \sqrt{\varepsilon_m}} \qquad \textbf{Equation 5-15}$$

Where

v_w = Moisture content as a fraction of total volume

ε = relative permittivity of the mix

ε_w = relative permittivity of water

ε_m = relative permittivity of the dry material

Write ε in terms of v_w:

$$\varepsilon = v_w^2\left(\sqrt{\varepsilon_w} - \sqrt{\varepsilon_m}\right)^2 + 2v_w\left(\sqrt{\varepsilon_w} - \sqrt{\varepsilon_m}\right)\sqrt{\varepsilon_m} + \varepsilon_m \qquad \textbf{Equation 5-16}$$

Equation 5-16 was used to calculate the CRI line (—) in Figure 5-5 for mortar dielectric. It is such a good fit that it was used as the starting point for the dielectric mix formula for concrete. In order for the CRI calculation to fit the measured line in Figure 5-5, Figure 5-6 and Figure 5-7 in terms of slope the permittivity of water ε_w had to be reduced to the values shown in the legend of the relevant figure. For the permittivity of the solid the value obtained was in the region of $\varepsilon_m = 5$ in both cases (see legends Figure 5-6 and Figure 5-7. A fourth order polynomial fits the measured values well as shown in (Figure 5-5). The "double twist" in the fourth order polynomial makes a linear fit for the measured data even better than the CRI calculation. To obtain a linear relationship, remove the second order term of Equation 5-16:

$$\varepsilon = 2v_w\left(\sqrt{\varepsilon_w\varepsilon_m} - \varepsilon_m\right) + \varepsilon_m \qquad \textbf{Equation 5-17}$$

Adjust the ε_w term to 57.49 for cement paste (Figure 5-6) and ε_w = 68.5 for mortar (Figure 5-7) to fit the data.

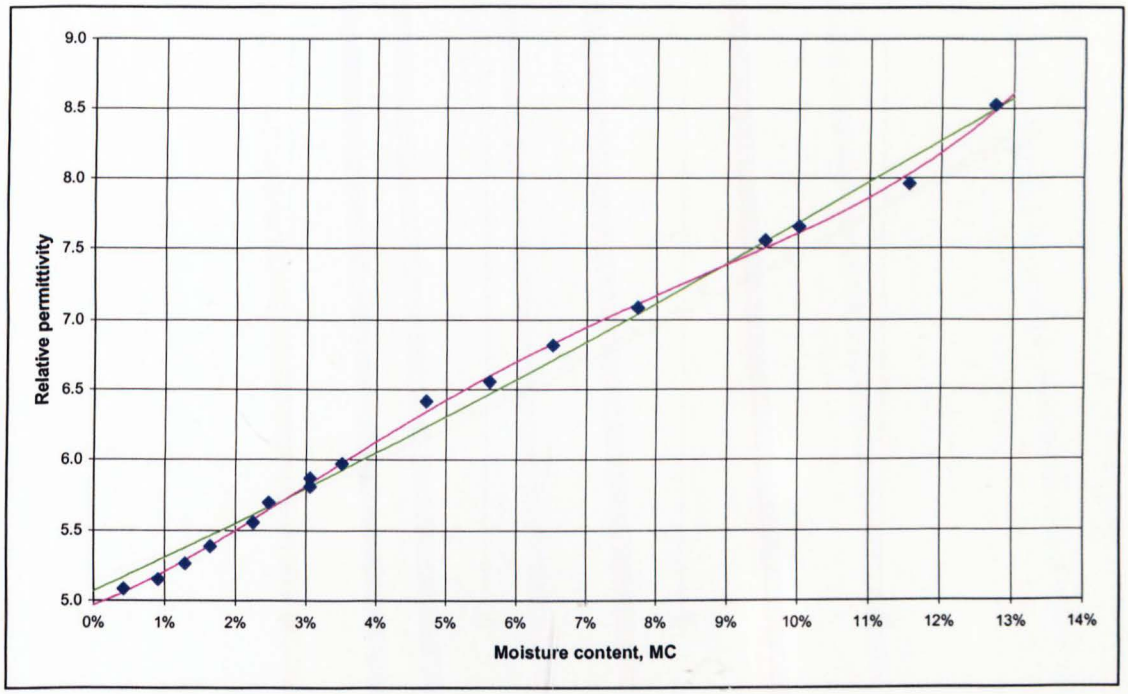

Figure 5-5 Characteristic of the relative permittivity of mortar (50% sand).

(♦) Measured with TDR on a 50 mm line (see section 4.5.3) and Equation 4-18 where t_r = 334 ps and t_m is the measured TDR time.
(—) Fourth order polynomial fitted to the data using least-mean-square (LMS) procedure with Solver in Microsoft Excel. The sum of the square of the differences (LMS total) was 0.025.
(—) Complex refraction index (CRI) line fitted to the measured data using the LMS procedure and calculated with Equation 5-16. LMS total was 0.125 with ε_w = 55.6 and ε_m = 4.95.

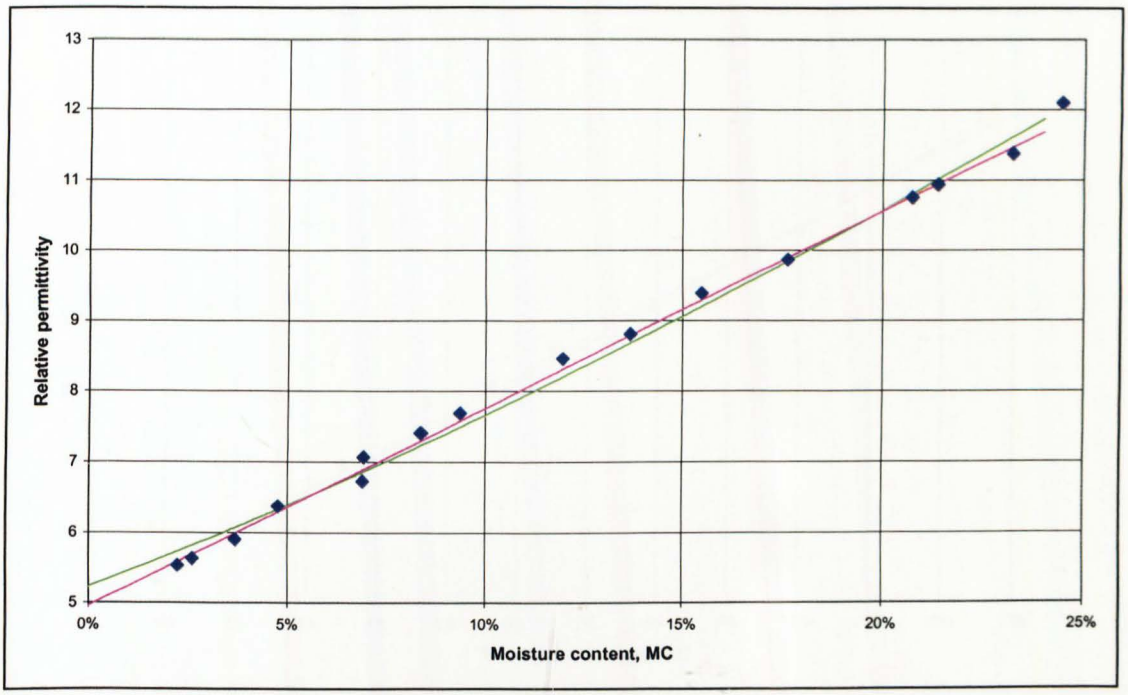

Figure 5-6 Relative permittivity of cement paste.

(♦) Relative permittivity measurement of the 50 mm cage-coaxial line with cement paste mix filler material. Relative permittivity calculated from the TDR results as in Equation 4-18.
(—) LMS procedure using Solver in Microsoft Excel was used to fit the CRI calculation of Equation 5-16 to the measured data. Best fit was obtained with relative permittivity of water $\varepsilon_w = 50.57$ and $\varepsilon_m = 5.22$ relative permittivity of the solid. LMS total of 0.376.
(—) The formula of Equation 5-17 with a LMS procedure was used to fit this curve to the data. Best fit was obtained with $\varepsilon_w = 57.49$ and $\varepsilon_m = 4.95$. LMS total of 0.114, indicating a closer agreement than the CRI calculation with the data. The relative permittivity of the water is slightly higher than the CRI calculation.

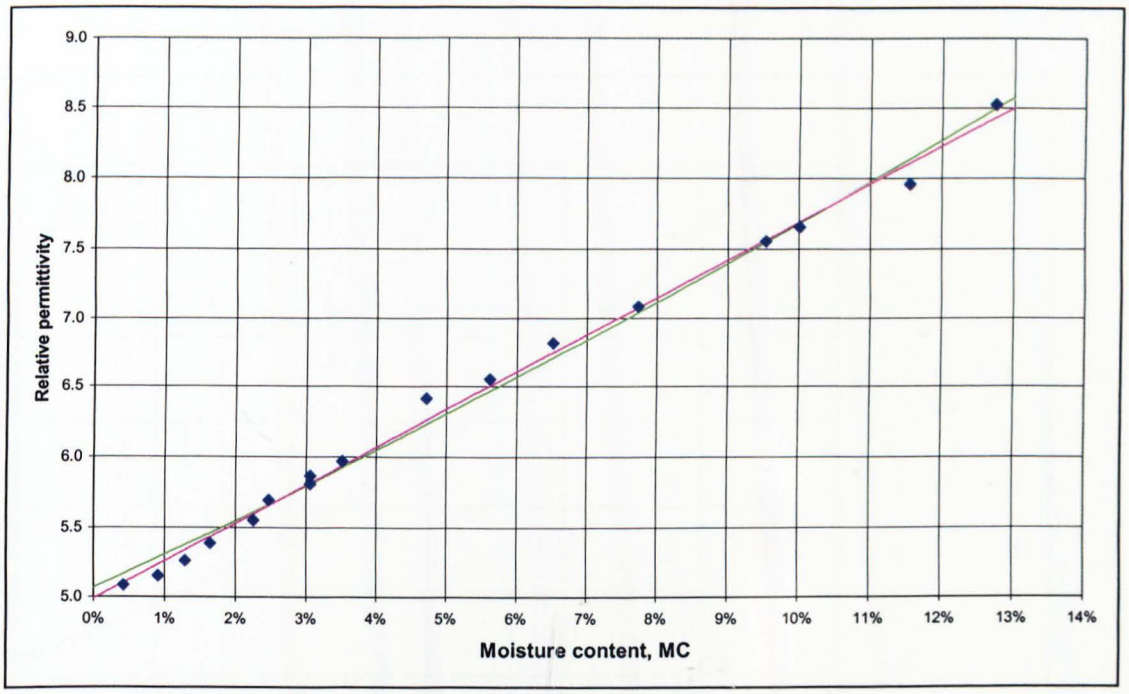

Figure 5-7 Relative permittivity of mortar with 50% sand.

(♦) Relative permittivity measurement of the 50mm cage-coaxial line with a 50% sand mortar mix filler material. Relative permittivity calculated from the TDR results with Equation 4-18. See Appendix F.
(—) LMS procedure with Solver was used to fit the CRI calculation of Equation 5-16 to the measured data. Best fit was obtained with relative permittivity of water $\varepsilon_w = 55.55$ and $\varepsilon_m = 4.95$ for the relative permittivity of the solid (LMS total of 0.125).
(—) The formula of Equation 5-17 with Microsoft Excel Solver was used to fit this curve to the data. Best fit was obtained with $\varepsilon_w = 68.54$ and $\varepsilon_m = 4.99$. LMS total of 0.081 indicates a closer agreement than the CRI calculation to the data. The value of relative permittivity of the water is also more realistic and closer to that of bulk water.

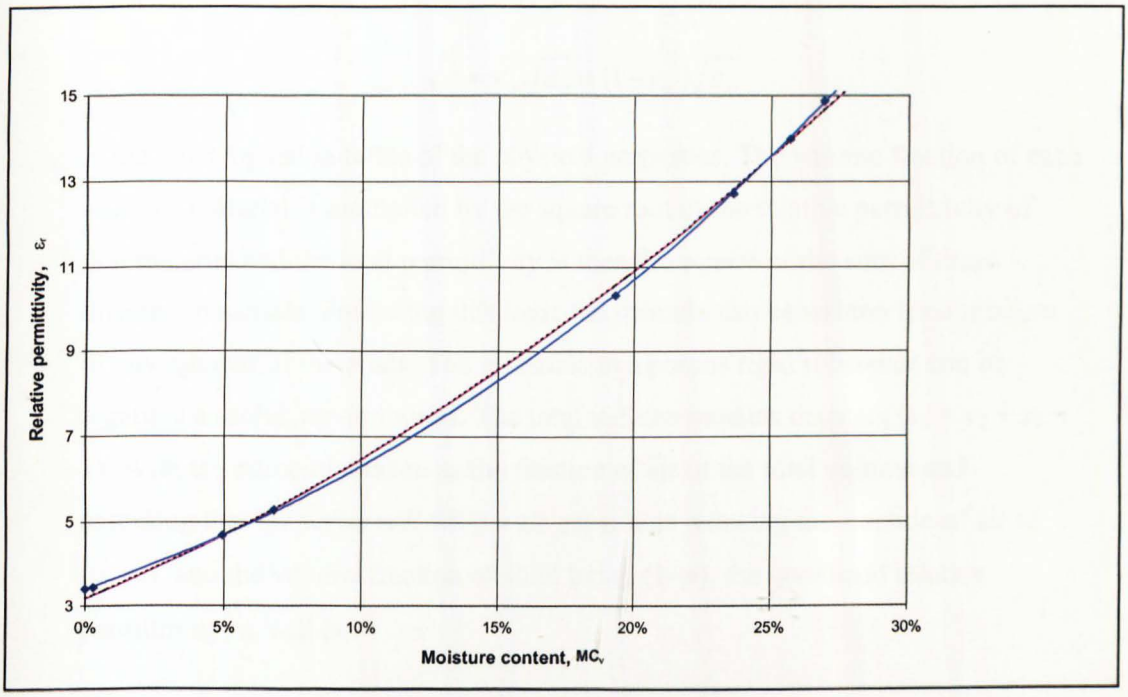

Figure 5-8 Relative permittivity of gypsum + 50% sand mix.

(♦) Relative permittivity measurement of the 50 mm cage-coaxial line with a 50% gypsum/sand ratio dielectric (filler material) using TDR. Relative permittivity calculated as in Equation 4-18.
(—) LMS procedure with Solver was used to fit the CRI calculation using Equation 5-16. The values for best fit were, $\varepsilon_w = 87.9$, which is higher than the relative permittivity for bulk water, and $\varepsilon_m = 3.2$.
(---) Data calculated using Equation 5-18, the CRI calculation that includes solid, air and water. With porosity set at $p = 0.3$, shows a best fit using Solver procedure with $\varepsilon_s = 4.5$ and $\varepsilon_w = 73.82$ thus a more realistic value for ε_w. Note that the graphs of the two CRI calculations are identical with LMS total of 0.144.
(—) Data calculated using the boundary effect formula of Equation 5-19. The best fit calculated as above, with porosity at $p = 0.3$, the boundary effect factor was found to be b=75.84, $\varepsilon_w = 73.73$ and $\varepsilon_s = 4.87$. Notice the close agreement with measured data. The LMS total was only 0.0092 indicating a near perfect fit.

Note that the Complex Refraction Index equation of Equation 5-15 written in the form

$$\sqrt{\varepsilon} = v_w\sqrt{\varepsilon_w} + (1 - v_w)\sqrt{\varepsilon_m}$$

is the most logical in terms of the physical properties. The volume fraction of each separate material is multiplied by the square root of the relative permittivity of that material and the total permittivity is then the square of the sum of these different materials. Following this logic the formula can be written for a mixture of any number of materials. The materials in a porous rigid substance can be regarded as solid, air and water. The total volume remains constant ($v_1 + v_2 + v_3 = 1$). With the porosity p taken as the fraction of air of the total volume and assuming that the water will fill the air gaps, thus reducing the fraction of air to $(p–v_w)$, and the volume fraction of solid being $(1–p)$, the combined relative permittivity, ε, will be:

$$\sqrt{\varepsilon} = (1 - p)\times\sqrt{\varepsilon_s} + v_w \times\sqrt{\varepsilon_w} + (p - v_w) \qquad \textbf{Equation 5-18}$$

where

ε_s = relative permittivity of the solid material.

To test the validity of Equation 5-18, it is tested against the results from a test sample of gypsum and 50% sand mix. For this mix (Figure 5-8) there is no decrease in the slope at low moisture content as seen with mortar and is therefore closer to an ideal porous material, probably due to a simpler pore system. When Equation 5-18 is applied to this material, the result (see Figure 5-8) is the same as the CRI (from Equation 5-16) calculation for the material. The significant difference is that Equation 5-18 provides an agreement with experimental results using a realistic value for the relative permittivity of water (ε_w). The value for ε_w should be less than that of bulk water (about 80) due to the boundary effect. The value found with Equation 5-18 is a realistic 73.8, against 87.9 using the CRI calculation with only two materials, which is too high in order to agree with experimental data. Equation 5-18 therefore gives a better agreement with experimental results.

The simpler gypsum/sand matrix allows for a correction factor to be brought in for the change in the relative permittivity due to the boundary effect by adjusting the permittivity of water in the expression by a boundary factor b, as shown in Equation 5-19 from:

$\sqrt{}$(total permittivity) = (volume solid)$\sqrt{}$(ε_s) + (volume water)$\sqrt{}$($\varepsilon_w - b \times$volume air) + (volume air)$\times 1$

$$\sqrt{\varepsilon} = (1-p)\sqrt{\varepsilon_s} + v_w\sqrt{\varepsilon_w - b(p - v_w)} + (p - v_w) \qquad \textbf{Equation 5-19}$$

where

p = Porosity

b = boundary effect factor

The line blue line (—) in Figure 5-8 shows how close the results of Equation 5-19 are to experimental results when the following values are inserted:

$\varepsilon_s = 4.87$

$\varepsilon_w = 73.73$

$p = 0.3$

$b = 75.84$

The close agreement supports the boundary effect theory. The author could find no other references in the literature that managed to support the theory so convincingly.

If the graph for mortar (Figure 5-7) is plotted for the moisture content below 2% as in Figure 5-9, the slope does in fact increase initially as expected. A possible explanation for the decrease in the slope of the permittivity/moisture content graph in the region between 2% MC and 9% MC for mortar (4% to 18% for cement paste) is given in Chapter 8 section 8.4. It is hoped that the explanation may be used to find the third order polynomial that fits the experimental results so well ($R^2 = 0.9984$ for cement paste and $R^2 = 0.9985$ for mortar).

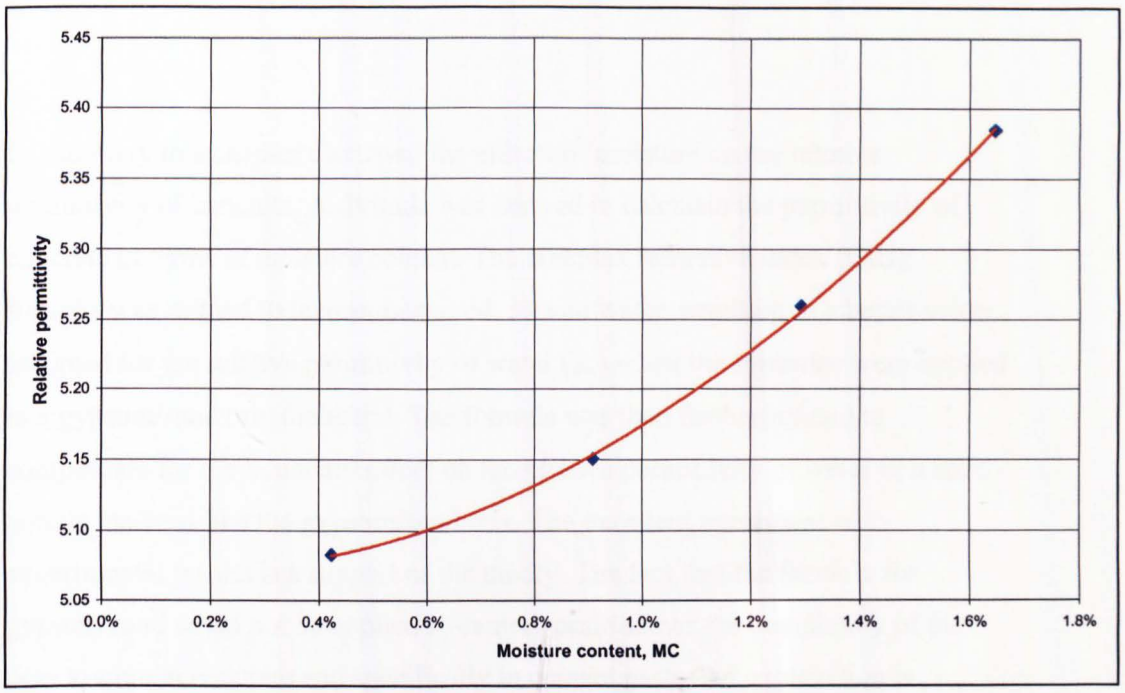

Figure 5-9 Relative permittivity of mortar at low moisture content.

(♦) Relative permittivity as in Figure 5-7.
(—) Second order polynomial trend line from Microsoft Excel applied to the first 4 points of the relative permittivity graph in Figure 5-7.
The relative permittivity at low moisture content for mortar shows the increase in slope due to boundary effect.

In summary this chapter discussed the effects of moisture on the relative permittivity of concrete. A formula was derived to calculate the permittivity of concrete in terms of moisture content. The complex refractive index (CRI) formula was refined to incorporate solid, air and water, resulting in a better value assigned for the relative permittivity of water (ε_w) when the formulae were applied to a gypsum/sand mix dielectric. The formula was then further refined to compensate for the boundary effect on the relative permittivity of water in a solid porous material like the gypsum/sand mix. The excellent agreement with experimental results is a support of the theory. The fact that the formula for gypsum/sand could not be applied to cement paste shows the complexity of the pore system in concrete and specifically in cement paste. An explanation is suggested in Chapter 8. For cement paste (and mortar) the fourth order polynomial of the trend line could be approximated with a linear curve that gave a closer fit than the classic CRI formula.

Chapter 6. Sensor Development

In this chapter the history and development of the sensor will be discussed in order to show why this particular configuration was chosen to measure the moisture in concrete. In high frequency moisture measurement (microwave aquametry) the tendency has been to employ more and more sophisticated data processing that made it possible to distinguish between the permittivity of the solid material where the density may change, and the moisture in the material. This is of particular importance with 'non-solid' or loose materials such as grain. The experience in this research with sand (see section 6.2.2) showed that the moisture in such materials could be difficult to measure accurately if there is a variation in the density of the air/solid mix (level of compaction). However, in the case of concrete, the density of the solid material is well defined and stable. Variations between different concrete structures occur due to differences in aggregate materials and mix ratios including differences in water to cement ratio, but this would change very little over the lifetime of the structure. The absolute moisture content can only be measured at the point where the sensor is mounted, which means that there could be a variation due to intrinsic differences in the concrete matrix only a short distance away. It is more important to ensure that the measured variation was indeed due to moisture content changes and not due to some other factor like temperature. In any case, one of the objectives of this research was to find a cost-effective method. Going for the simplest solution, as will be explained in the following chapters, seemed to be the best way to achieve this goal.

The reliability of an electronic device is a function of the number of active components (transistors) used. If the sensor is to be placed and sealed in a fixed position for many years, reliability is crucial. The ideal would be to have only a

single active electronic component. It will be shown that the single transistor radio frequency oscillator with a transmission line as the tuning element has the potential to achieve that goal.

6.1. Sensor Development, history to final form.

In the quest for the optimum configuration of transmission line a number of design iterations were tested. A description of these will provide a better understanding of why the final configuration was selected.

6.1.1. Background

It was clear from the outset that a fresh approach was required to measure moisture in concrete. As previously discussed, no existing system could fulfil the requirements of low cost, long life and ability to measure at any chosen depth in the concrete, which meant that no existing technology could simply be adapted for the measurement of moisture in concrete.

Concrete structures are as a general rule open to the environment and it is expected that there would be a corrosive effect caused by impurities or contaminants entering the concrete matrix. The presence of such contaminants in the moisture is the cause of concrete deterioration (section 3.3.2). As the moisture is the common factor in all the reactions, monitoring the moisture level provides a good basis for monitoring the general condition of the concrete. A probe measuring moisture content must be capable of measuring the moisture level without being adversely affected by the impurities present in the water. It should be immune from chemical attack. The presence of dissolved substances should not affect the reading of moisture level. Any ions of dissolved substances would have a relaxation time that is many orders of magnitude more (about 1×10^{-5} s) than the relaxation time of the water molecule (about 1×10^{-11} s) (Hobbs, 1974). All this indicated that the aim should be to work at as high a frequency as possible within the limitations of the technology and availability of low cost electronic components.

The choice of a frequency just below 1 GHz was dictated by the availability of inexpensive and readily available electronic components that can function at this frequency. There appeared to be no need to go to higher frequencies, as the length of a transmission line around 1 GHz is short enough for practical purposes.

Capacitive methods were seriously considered, as capacitance is directly proportional to the relative permittivity and thus the moisture content. A capacitor with the concrete as dielectric could be used as the tuning element in the same type of oscillator as used with the transmission line (see section 7.2). Most present systems measuring capacity operate at a frequency below 100 MHz, but a capacitive measurement system could probably be designed to work at a higher frequency. Even then it would not be easy to design a capacitive sensor at microwave frequencies because of the limitation in physical size. If the plates or the leads to the plates are of the same order of magnitude as the wavelength of the frequency used, the effect of phase difference between various parts of the sensor must be taken into account. The relatively large capacitor plates and the lower frequency used meant that this type of measurement is presently limited to the surface of the concrete. Being exposed to rain and possibly running water means that there is very little information that can be gathered from a reading of moisture on the surface of the structure only.

6.2. Methodology. The use of different materials to test ideas

One of the difficulties in working with concrete is the time scale involved in conducting experimental work. It is common practice to allow 28 days for the cement to harden to the design hardness (Taylor, 1997). Some cement hydration can go on for months, depending on factors like temperature and type of cement. Additionally the diffusion rate of moisture through concrete is extremely slow (see section 3.3.1). Equilibrium conditions, which means that there is no further diffusion of moisture between a sample and the environment, will only be reached after a considerable time, depending on the size of the sample. There was therefore a need during this investigation to get an indication of trends and to test the methodology within the time limitation imposed by the research framework, without using cement as the basic material for the initial work. Although this

method did help, it also took the investigation and development into a direction that turned out to be a dead end. However, it is deemed important enough to report as some valuable information was gathered in the process and essential experience gained in the study of moisture in porous solids.

6.2.1. The change from 2-wire to 5-wire (cage-coaxial) transmission line

Figure 6-1 Two-wire transmission line embedded in acrylic.
The sharp point was used to facilitate insertion into sand.

The simple 2-wire transmission line was mounted in an acrylic surround with a sharp point to penetrate sand (Figure 6-1). This transmission line configuration was initially used with and without the acrylic cover to measure the apparent ε_r for sand, gypsum and water. End effects were observed, as TDR measurements in air indicated a longer transmission line than the physical length of the transmission line. Objects in the near vicinity also affected the readings due to the stray EM fields and it became clear that calibration of the two wire transmission line in terms of moisture content would be subject to errors. Tests with gypsum brought about a change in ideas. If the EM field could be restricted to a region inside a coaxial transmission line, the effect of stray fields would not be a factor. Figure 4-5 and Figure 4-6 show the transmission line that was designed with a central conductor and 4 radially spaced outer conductors to act as a shield. Because of the appearance of a cage, it is called the 'cage-coaxial' transmission line. TDR tests with this transmission line in air showed a much better agreement with the physical length and gave confidence in results with this design. It was possible to touch the outer conductors by hand or bring other objects to close proximity with negligible affect on the readings. Considering the high frequencies involved, it was indeed a surprise that the screening was so effective. The cage-coaxial

transmission line was then used for all further investigations and the calibration on different materials. The tests on water (see section 4.2) were done using this transmission line in both bare conductor and insulated (painted) conductor forms.

At first this cage-coaxial transmission line was only intended for calibration of different materials into which the transmission line could be cast. Section 6.2.3 will describe how it led to the idea of using a gypsum ($CaSO_4$) dielectric transmission line to measure the moisture content.

6.2.2. Sand as a dielectric medium for convenient control of moisture content

In order to do some quick exploratory tests, sand was used as the medium to measure moisture instead of a 'solid' porous material. Sand can be mixed with an exact amount of water to obtain a mix with a required moisture level. It should be emphasised that dry sand is a mixture of solid sand grains and air, so that the permittivity of the dry sand would be reduced by the presence of air. Damp sand is a mixture of sand, air and water.

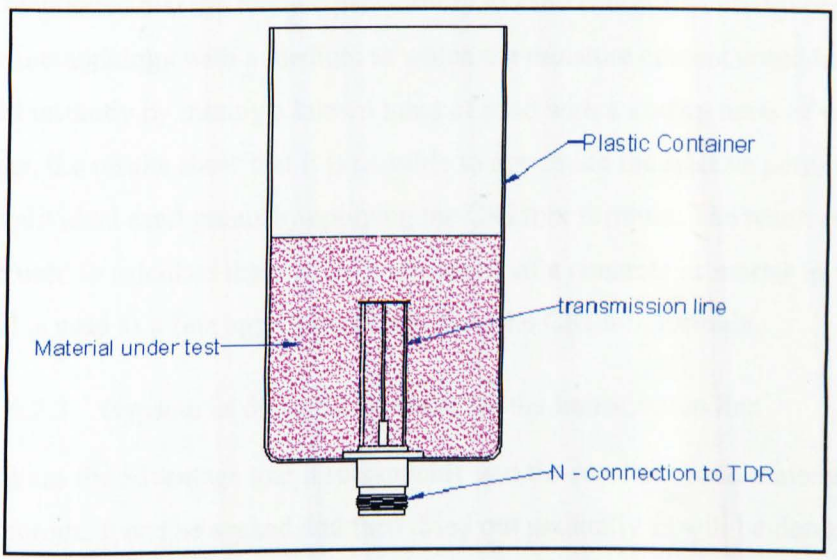

Figure 6-2 Cage-coaxial transmission line in container to measure the permittivity of various loose (sand or grain) and liquid substances

Figure 6-2 shows the experimental arrangement. The container could be used for a loose material like sand (or grain) and for the measurement of the permittivity of bulk water (section 4.2). This set-up has the advantage that the apparent length of

the transmission line could be measured using TDR with and without the material under test. The HP 8572C displayed the apparent transmission line length directly in mm (see section 4.5.1). From that ε_r could be calculated from Equation 4-17.

The relative permittivity of dry sand, which is a mixture of solid and air, was measured to be between 2.4 and 2.5. Although the relative permittivity increased with addition of moisture, the problem was that the adhesion force of the water in damp sand tends to 'tie' the grains together making it difficult to obtain the same density of solid material per unit volume (compaction) as with dry sand. The results could therefore only be used to test the effect of moisture on the apparent transmission line length qualitatively and not be used to test for example the formula for mixed dielectrics in section 5.3. If the CRI formula is applied (see Table 4-1) and the percentage of solid sand grain is 60% (measured by adding sand to a water and measuring the increase in volume and the volume of sand added), an overall relative permittivity (sand grains and air) of 2.5 gives a relative permittivity of the solid sand grains of 3.9.

It was mentioned that the relative permittivity of sand was done initially only to test the methodology with a medium in which the moisture content could be changed instantly by mixing a known mass of sand with a known mass of water. However, the results show that it is possible to determine the relative permittivity of the individual sand grains by applying the CRI mix formula. The result can then be used to calculate the relative permittivity of a concrete or mortar in which the sand is used as a fine aggregate by applying the CRI mix formula.

6.2.3. Gypsum as dielectric medium for the transmission line

Gypsum has the advantage that it sets quickly and the resultant solid material is highly porous. It can be soaked and then dried out gradually as will be described later. It can also be mixed with sand or some other aggregate to reduce the porosity in the same way as mortar. These properties suggested that gypsum would be an excellent material to test the methodology and the transmission line could be embedded in gypsum or a gypsum/sand mixture. Moisture content was changed by first soaking the sample in water, letting it dry to a required level (determined by mass) and then sealed in PVC film ("cling film") to enable the

moisture to reach a homogeneous distribution throughout the volume of the sample. This procedure was repeated for different levels of moisture content. The moisture content was determined by subtracting the dry mass (after oven drying) from the mass at every moisture level and dividing it by the volume of the gypsum.

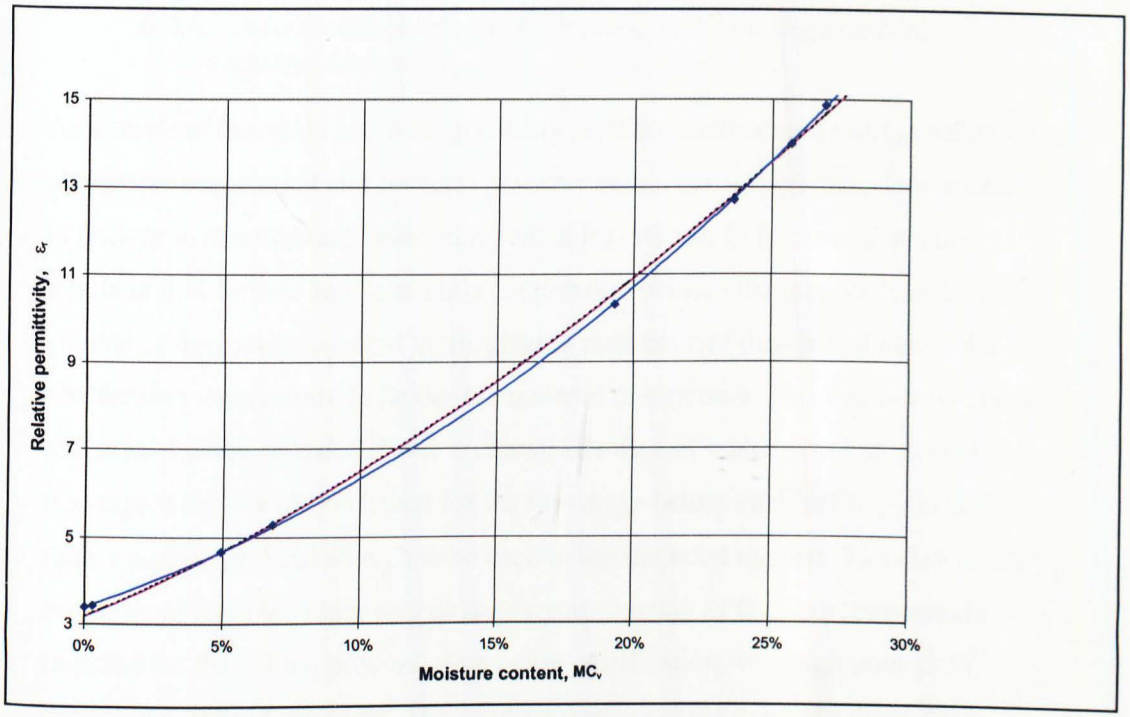

Figure 6-3 Result of Gypsum/Sand TDR measurements of relative permittivity versus moisture content.
Detail as in Figure 5-8

The experimental results, shown in Figure 5-8, is shown again in Figure 6-3 for convenience. There is an excellent agreement between measured and calculated data. In fact the results were so reproducible that it was considered using the gypsum embedded transmission line as the final moisture probe. The material was easy to mix and cast in any required form. Setting is quick compared to cement so that calibration could be done very soon after being cast. The sensor could be mounted in a drilled hole in the concrete under test and when the moisture in the gypsum and the concrete reached equilibrium, the moisture in the gypsum would give a measure of the moisture in the concrete. At this point it was thought that all that was required was to find the relationship between the moisture contents in

two porous materials in close contact and in equilibrium. Unfortunately further investigation (Dunster A, telephonic communication, 4/11/1999) revealed that gypsum would react with the cement paste in the concrete and could not be used in this manner. Gypsum can still be used as a filler medium when the probe is used in a material where this incompatibility is not a problem.

6.2.4. Porous ceramic clay as filler material for the cage-coaxial transmission line

As a result of the chemical incompatibility problem encountered with gypsum, an alternative was sought and found in porous ceramic clay (clay). The clay is used in pottery to manufacture baked clay (ceramic) articles. In its normal use the article is first formed and baked at a temperature below vitrification. It is then painted or decorated, covered in the glazing material and then baked above the vitrification temperature to render the material non-porous. The clay is very stable and investigation revealed that it is chemically neutral with respect to cement. At the stage when the clay is baked for the first stage below vitrification, it is still highly porous yet hard enough to be used in the intended manner. The clay could not be handled in the same way as the gypsum casting as the high temperature required for the baking process, even below vitrification, was high enough to destroy the transmission line. The solution was to cut the clay into discs, then drilled to allow the conductors to be inserted. The discs were then stacked to form the complete transmission line as shown in Figures 6-4 and 6-5.

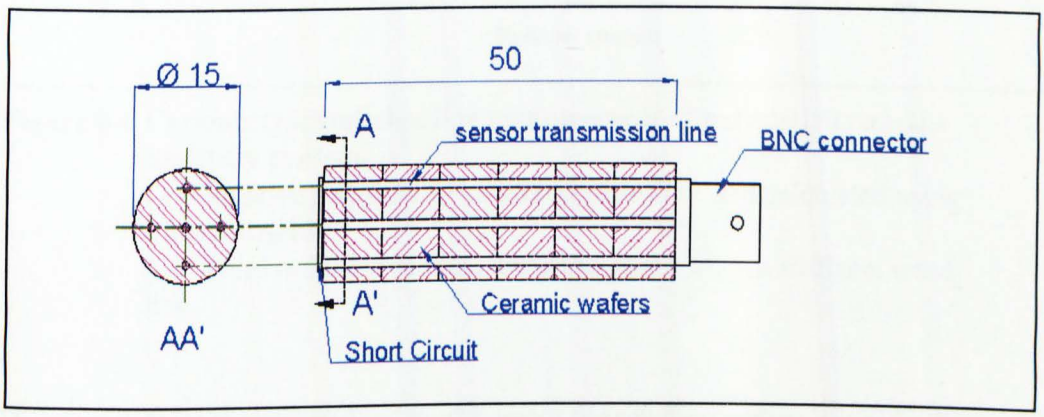

Figure 6-4 Transmission line with ceramic wafers (dimensions in mm)

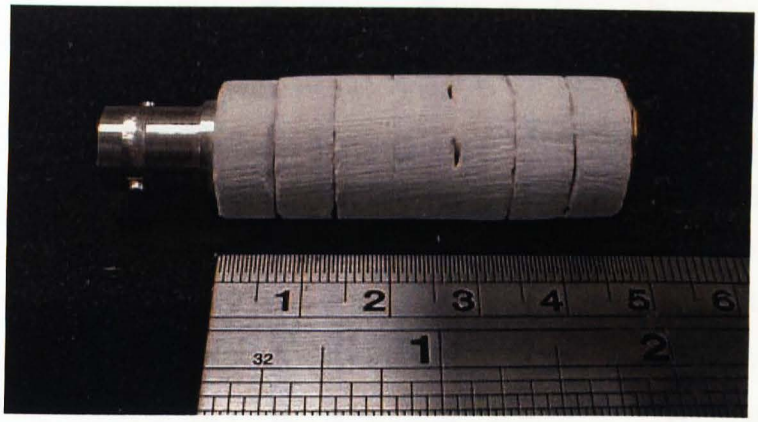

Figure 6-5 Photograph of transmission line with ceramic wafers

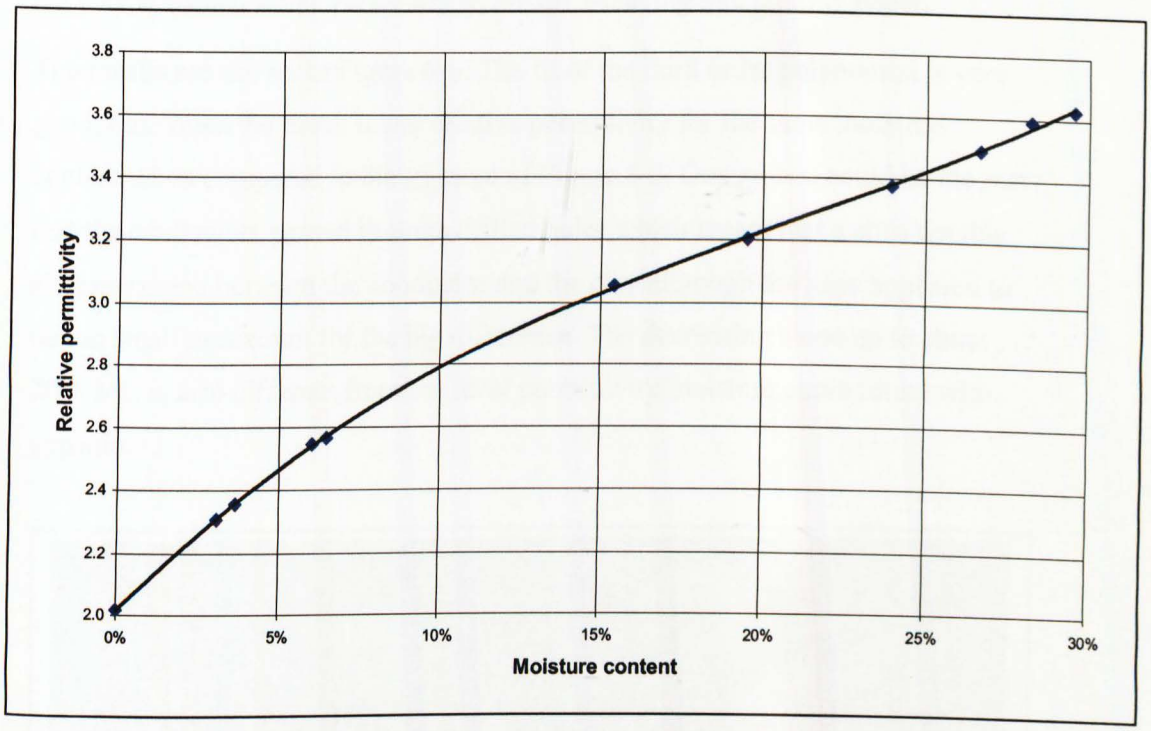

Figure 6-6 Ceramic transmission line measurement of permittivity versus moisture content.
(♦) Relative permittivity measured with TDR and calculated using Equation 4-18.
(—) Third order polynomial trend line using Microsoft Excel trend line.

Moisture content was determined by following the same procedure as used with gypsum. In all cases the TDR measurements were taken with the transmission line wrapped in PVC film to prevent evaporation during the test. It was found that

there was a drift in the readings with time with no apparent change in the mass, due to movement of the moisture to one side under the influence of gravity. To counter this, the transmission line was mounted on a shaft that was rotated with an electric motor at about 20 rpm to counter the effect of gravity (see Figure 6-7). This turned out to be a very effective solution to avoid drift and no further drift was experienced. It was not realised at the time that this gravitational effect could only be experienced if the pores in the clay were relatively large and/or that the adhesion force between water and solid was weak, otherwise the capillary force would have been strong enough to counter the gravitational force. Another indication of large pore size and high permeability for moisture was the fact that the clay absorbed water very quickly, almost behaving like blotting paper.

The results are shown in Figure 6-6. The fit of the third order polynomial is very good, but notice the much lower relative permittivity for the same moisture content when compared to the gypsum of Figure 6-3. One reason could be the fact that the conductors passed through drilled holes which meant that a considerable air gap existed between the conductor and the clay although the gaps appeared to be too small to account for the big difference. The decreasing slope up to about 20% MC is also different from the ideal permittivity/moisture curve found with gypsum.

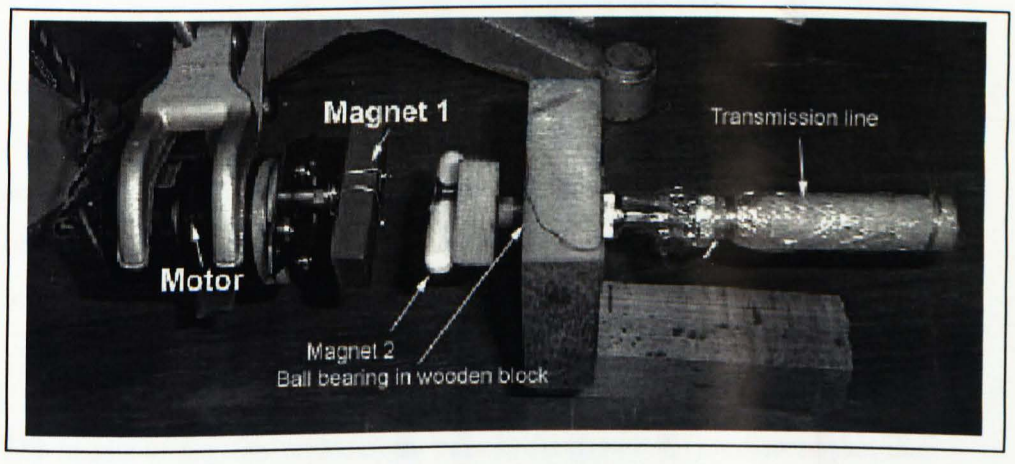

Figure 6-7 "Anti-gravity" jig.
The transmission line is rotated continuously to counter the effect of gravity on the flow of moisture.

The transmission line results with the clay in terms of transmission characteristics were promising and it appeared to be an excellent solution to use this clay as the filler material (dielectric) for the transmission line. What remained was to determine the final moisture equilibrium conditions when the clay was placed in contact with moist concrete. This experiment was described in section 3.4.1, which clearly showed that the clay would not take up any moisture and therefore was not suitable for measuring moisture in concrete.

6.3. Transmission line designs as a sensor for measuring moisture in concrete

Thus far the two transmission lines discussed were the simple two-wire and the cage-coaxial transmission lines. The two designs represent completely different approaches to the measurement of moisture. The two-wire transmission line is closer to the conventional approach with a more direct measurement of the permittivity of the surrounding medium, allowing the EM fields to penetrate into the concrete under test. The cage-coaxial transmission line on the other hand restricted the material volume that affected the transmission line to the small volume inside the cage. The more indirect method employed with the cage-coaxial transmission line is justified by the uncertainty of the exact characteristics of the surrounding concrete, which introduces an unknown error into the calibration. The fact that both the effect of moisture and that of temperature on the filler material can be measured before insertion into the concrete, plus the screening effect from the influence of steel reinforcement and other unknown objects, makes the use of a cage-coaxial transmission line with filler material highly attractive.

6.3.1. Porous filler material in the cage-coaxial transmission line

The results of the tests on moisture transfer (section 3.4.1) indicated that the choice of material to fill the space inside the cage (filler material) was of paramount importance. For the filler material to represent the conditions in the surrounding material it must be as close as possible in terms of porosity and

capillary pressure to the surrounding material. For concrete the obvious choice is to use cement paste or a fine aggregate mixed with cement paste as a filler material. The difference in porosity between the filler cement paste and the cement paste in the surrounding concrete (the MUT) would be minimal and mainly due to a difference in water cement ratio. The discrepancy in moisture content due to this difference would be less than the differences due to unknowns in the nature of and quantity per unit volume of the fine and coarse aggregate used in the MUT. Depending on the type of sand used the mortar has less porosity than the cement paste alone. This was tested by measuring the porosity of the cement paste and mortar in the test blocks that were used for the moisture equilibrium tests described in 3.4.1, see Table 3-2.

The relatively long time needed for the material in the cage to reach moisture equilibrium with the surrounding concrete (typically about one week) remains a disadvantage of the cage-coaxial with filler material design. Although its use is fully justified if the moisture sensor based on this principle is to be left in situ for long periods.

6.3.2. Side-looking transmission line.

There is no doubt that a moisture sensor that is less material sensitive and can measure the moisture content instantly would be very attractive. Therefore a design was considered which had the advantage of the two-wire transmission line but with a less widely spread EM field through the material under test (concrete). Figure 6-8 shows the design principle of a transmission line called the 'skew transmission line'. It is an effect a quasi-coaxial transmission line with the centre conductor only partly screened to allow some of the EM field lines to "leak" into the surrounding material. By moving the position of the centre conductor closer to the side, it tends to approach the characteristics of the two-wire transmission line. The sensitivity to the permittivity of the material under test increases as the centre conductor is moved closer to the edge, but it is affected more by nearby objects like steel reinforcement. The ideal condition would be if the fields inside the surrounding concrete could be limited to a well-controlled depth. The transmission line is very sensitive to the size of the air gap between the body of

the transmission line and the side of the hole. For this reason some mechanism must be used to ensure that it is pressed tight against the side where the central conductor is.

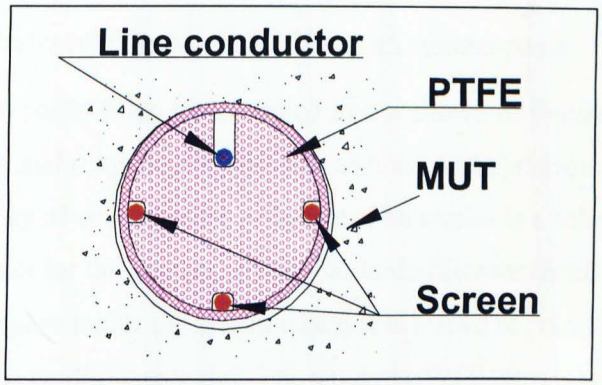

Figure 6-8 The "Skew" transmission line showing the position of the conductors.

There is much scope for further work on this design and some variations using stripline in a tubular form was considered but not investigated further. TDR measurements with this transmission line in wood and concrete looked promising, but no attempt was made to take it further as one of the effects noticed was the tendency for the EM field to be repelled by the concrete when the moisture content and therefore the conductivity was very high. The material under test started to appear like part of the screen, which meant that the EM field moved into the low loss inner dielectric. The effect was detected as a reduction of the apparent length with increasing moisture content. In spite of this, the method should be suitable for the measurement of moisture in the hygroscopic range (up to 100% relative humidity).

A solution not investigated was to use the stripline approach as described in the literature (Völgyi, 2001). It can be modified to work in a cylindrical hole by making the earth plane a solid cylinder with the stripline in an insulating sleeve or cover over the earth plane. In any design where either the "skew" transmission line or a modified stripline is used, the contact area between the active side of the transmission line and the material under test is of the utmost importance. No air gap can be allowed as the electromagnetic fields are very close to the strip and even a small variation in the distance to the material under test will affect the

calibration severely. The reason in the case of the stripline is that use is being made of the small amount of stray field on the opposite side of the stripline to the earth plain and any dielectric must be close to the strip to affect this field.

6.3.3. Partly filled transmission line with cement paste.

The design of the partly filled transmission line is shown in Figure 6-9. It is another quasi-coaxial transmission line but with the material around the central conductor made up of cement paste as shown. The screen is a solid copper cylinder with a slot for the cement or other suitable filler material. The EM field is restricted to the space inside the screen where it is forced to pass through the cement around the central conductor. The amount of moisture taken up by the cement paste in the transmission line is relatively small and should reach equilibrium much sooner than the cage-coax transmission line. This configuration was not tested. There is some uncertainty about the transmission mode and the effect on the apparent transmission line length when the conductivity of the filler material becomes high.

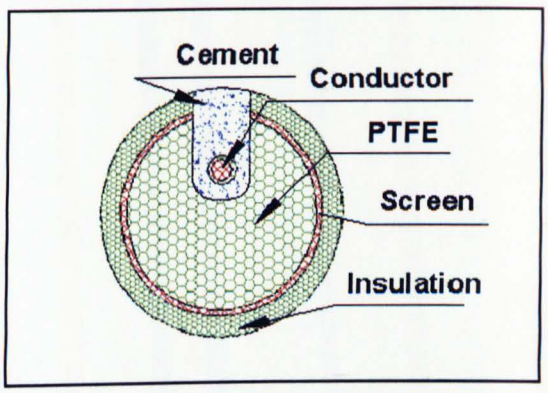

Figure 6-9 Partly filled transmission line showing the position of the central conductor surrounded by cement in contact with the MUT

Of the various configurations for the transmission investigated, the cage-coax turned out to be the best solution for a stable sensor. The electromagnetic fields are restricted to the 'cage' rendering the probe less sensitive to outside EM interference. The main criticism is that the moisture content in the concrete structure itself is not measured, but relies on known moisture equilibrium between the MUT and the filler material calibrated for moisture content. It was felt that any

possible error due to this is compensated for by the accurate calibration of the filler material compared to the uncertainty in calibration of the MUT. The disadvantage of the method is greatly reduced if the moisture content is measured in terms of saturation as will be discussed in section 8.8. The time lag until equilibrium is reached is of no importance in a system designed for monitoring over years and even decades.

Chapter 7. Electronics for the moisture sensor – Theory and design

In the previous chapters the characteristics of moisture in concrete was investigated. In section 4.4.2 the cage-coaxial transmission line design was introduced to measure the permittivity and therefore the moisture content. What is required is a suitable low cost method to measure the apparent (electrical) length, which is a function of the permittivity of the filler material of the transmission line. TDR measurement, although eminently suitable for measuring the permittivity, requires unsuitable expensive and bulky instruments or complicated electronic circuits. It was decided that the solution lies in the use of an oscillator that uses the transmission line as a tuning device to determine the frequency of oscillation. The frequency can be calibrated in terms of the apparent transmission line length and therefore the moisture content.

Most of the investigation with the cage-coaxial transmission line in Chapters 5 and 6 was done with a 50 mm transmission line filled with various filler materials. The length of 50 mm was chosen originally because it is a quarter wavelength ($\frac{\lambda}{4}$) long at 866 MHz when filled with (dry) gypsum, a suitable frequency for the purpose. It will be shown in section 7.2 that the transmission line will not be used as a quarter wavelength resonance circuit. Used as an inductance (see section 7.2) the frequency of oscillation would be 530 MHz with the 50 mm transmission line. The length was reduced to 30 mm in order to increase the oscillator frequency to 900 MHz when used as an inductance. As most of the data collected was on the 50 mm transmission line, both are used here to illustrate the methods employed.

An oscillator was built and tested to confirm the theory of operation, but the detailed circuit design of the electronic circuits for a practical probe is regarded as engineering development based on the information gathered in this research and will not be described in detail in this thesis.

7.1. General oscillator theory as used in the moisture probe

This section examines the principles of operation of suitable oscillators while section 7.2 will investigate the transmission line as tuning element for an oscillator.

At UHF and higher frequencies, the most effective transistor configuration for an amplifier is the common-base type. This type of configuration can provide higher gain, efficiency, and stability at higher frequencies. Because an oscillator may be considered as a regenerative feedback amplifier, these conditions also apply to the oscillator under well-designed conditions. The basic microwave oscillator circuit being considered here is the common base feedback oscillator shown in block form in Figure 7-1.

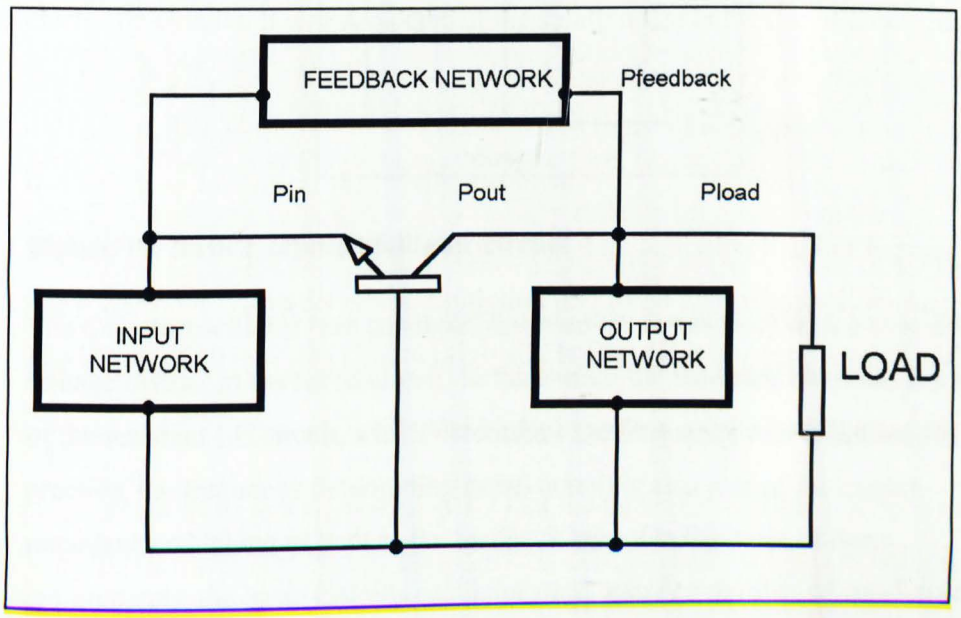

Figure 7-1 Basic configuration of a Common Base Oscillator Circuit

The feedback network can be an external loop, an internal loop, or a combination of internal and external elements. Although many variations of the feedback networks are possible, three general families of oscillators are found to be effective at microwave frequencies. These are the Colpitts, the Hartley and the Clapp circuits (Malvino, 1979). The Hartley oscillator requires a split inductance and the Clapp additional components so that only the Colpitts is considered and shown in basic form in Figure 7-2.

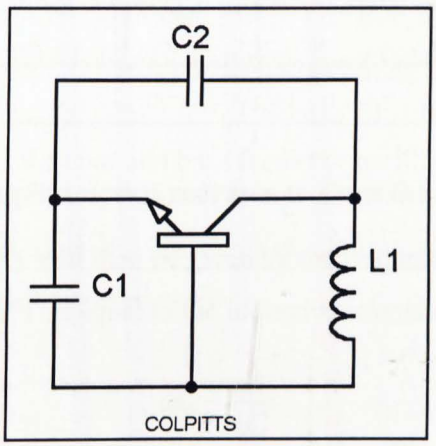

Figure 7-2 Basic Colpitts oscillator circuit

The Colpitts oscillator uses an amplifying element (transistor) with a capacitive voltage divider in the tuned circuit. In this circuit the feedback elements form part of the resonant LC circuit, which determines the frequency of oscillation. In practice, the frequency determining tuned circuit is also part of the output impedance matching as well as the feedback loop. On the basis of these requirements, the basic Colpitts oscillator must satisfy a number of conditions simultaneously if the circuit is to be an efficient oscillator. To see how the various capacitors shown form part of a parallel tuned circuit, the circuit is redrawn in Figure 7-3. The capacitor $C3$ is the equivalent of stray capacitance across the inductance plus the collector to base capacitance. The total capacitance C of the tuned circuit is the series combination of $C1$ and $C2$ in parallel with $C3$.

$$C = \frac{C1 \times C2}{C1 + C2} + C3$$

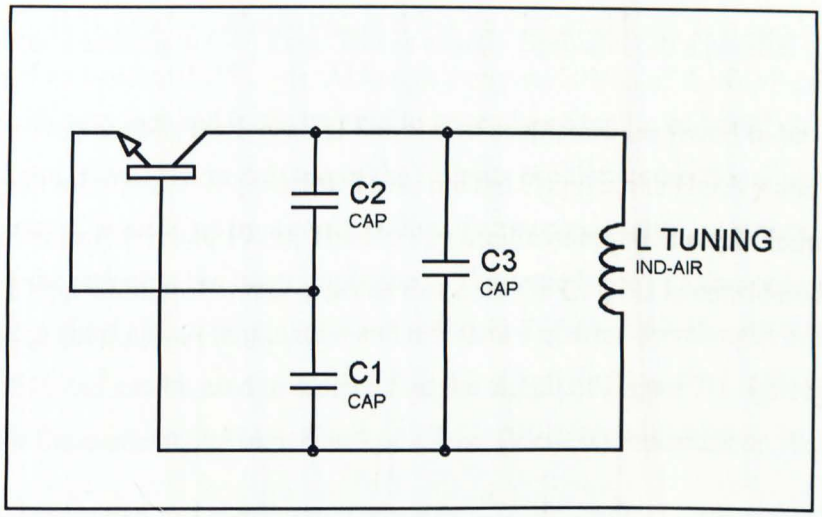

Figure 7-3 Colpitts circuit redrawn to show the tuning circuit

The oscillation frequency will then be given by the frequency where the capacitance reactance of C is equal to the inductive reactance of L.

$$\omega L = \frac{1}{\omega C}$$

therefore

$$\omega^2 = \frac{1}{LC}$$

and

$$f = \frac{1}{2\pi\sqrt{LC}} \qquad \textbf{Equation 7-1}$$

where $\omega = 2\pi f$

7.2. Transmission line as inductance in the tuning ('tank') circuit

To illustrate how the frequency of oscillation changes with moisture content, the impedance of a transmission line and its use as an inductance will next be examined. A short-circuit terminated lossless transmission line will appear as an open circuit (infinite impedance) at a frequency where the transmission line length

is a quarter wavelength ($\frac{\lambda}{4}$) long. This is exactly equivalent to a parallel tuned circuit with zero loss and it can be used in general as a tuning or 'tank' circuit for an oscillator. However, in the case of the Colpitts oscillator considered here, the capacitance C is made up by a combination of stray capacitance, plus those added to match the output to the input impedance. The impedance of a transmission line, with a short circuit termination and less than a quarter wavelength in length, is inductive and can be used to replace L in the circuit of Figure 7-3. Ignoring losses for the moment, the impedance of a short (lossless) transmission line, length l, terminated in a short circuit when $l < \frac{\lambda}{4}$, is given by (Jordan, 1962):

$$Z_l = jZ_0 \tan \beta l \qquad \textbf{Equation 7-2}$$

where

Z_0 = characteristic impedance of the transmission line (ohm)

Z_l = input impedance of the transmission line (ohm)

β = phase constant (rad m^{-1})

l = length of the transmission line (m)

The input impedance is thus directly proportional to the tangent of the phase change βl, which increases rapidly as the 90° angle (and the quarter wavelength length) is approached. The oscillation will be at a frequency where the modulus of the inductive reactance given by Equation 7-2 is equal to the modulus of the capacitive reactance of the effective capacitance C.

$$\frac{1}{\omega C} = Z_0 \tan \beta l$$

$$f = \frac{1}{2\pi C Z_0 \tan \beta l} \qquad \textbf{Equation 7-3}$$

As an example take the impedance versus frequency graph of a 50 mm transmission line (obtained as will be explained in section 7.2.1) and the modulus of the reactance of a 3.8 pF capacitor (a typical value in a practical circuit), and note where they cross in Figure 7-4. The frequency of oscillation in this case would be at 530 MHz according to the graph. By replacing these values in Equation 7-3 for the 50 mm transmission line and Z_0 = 50 ohms [8], β can be calculated.

$\beta = 20.133$ rad m^{-1}

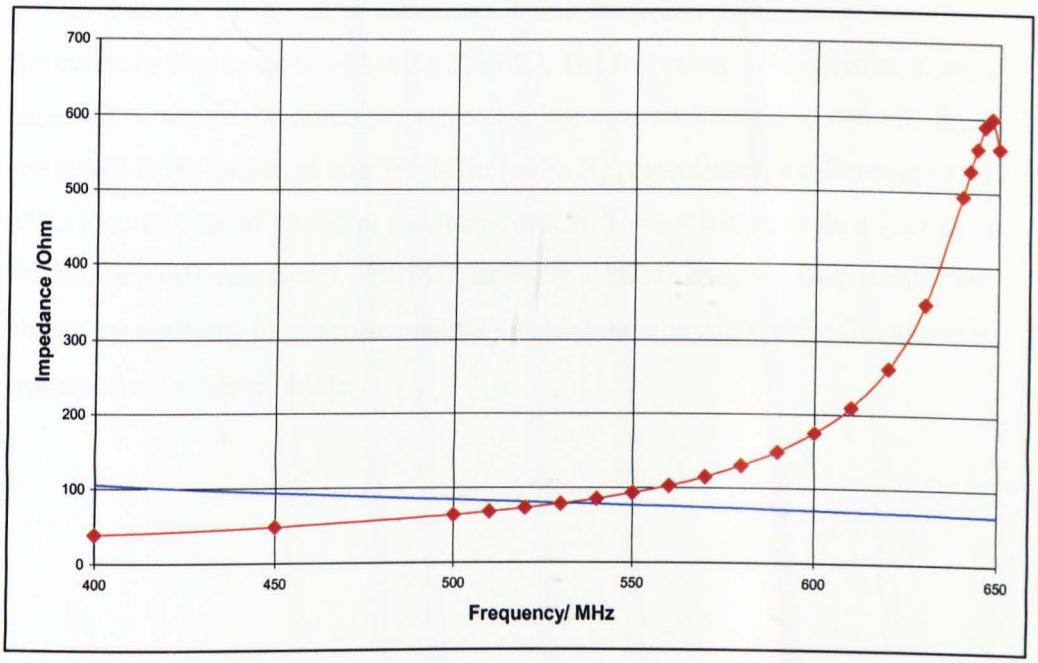

Figure 7-4 Impedance of a 50 mm mortar filled transmission line

(—◆—) Reactive impedance (positive imaginary i.e. inductive) measured on the Smith chart of the network analyser.
(—) Modulus of the capacitive reactance of a 3.8 pF capacitor.

Use Equation 4-16 and 4-17 to obtain ε_r.

$\varepsilon_r = 4.128$

This shows that the frequency of oscillation can be used to determine the relative permittivity ε_r at that frequency and can thus be calibrated against the moisture content.

[8] Obtained by measuring the phase and the impedance on the HP 8752 C and calculating Z_0 with Equation 7-2

Note: It is unfortunate that the value for ε_r obtained by TDR measurements ($\varepsilon_r \approx 5$ for 0% MC in Figure 5-6 and Figure 5-7) cannot be used in a graph of permittivity versus moisture content to calibrate the oscillator and thus determine the moisture content. TDR measures the average relative permittivity over a wide bandwidth whilst the above result is the relative permittivity at 530 MHz. The moisture calibration must therefore be done at the appropriate frequency. Next the method used to determine the frequency of oscillation will be discussed.

The effect of moisture on the frequency of oscillation is demonstrated in Figure 7-5 for a mortar filled transmission line 30 mm long. The 'oven dried' transmission line is taken as having 0% MC. The frequency of oscillation in each case will be where the capacitive reactance line cuts the 0% and 15.4% MC lines are at 903 MHz (point A) and 791 MHz (point B) respectively, a difference of 112 MHz for a change of 15.4% in moisture content. The sensitivity is thus 7.27 MHz /% MC or a difference of 0.14% MC for every 1 MHz change in frequency. This shows the accuracy of moisture content measurement possible if the frequency is measured to within ±1 MHz.

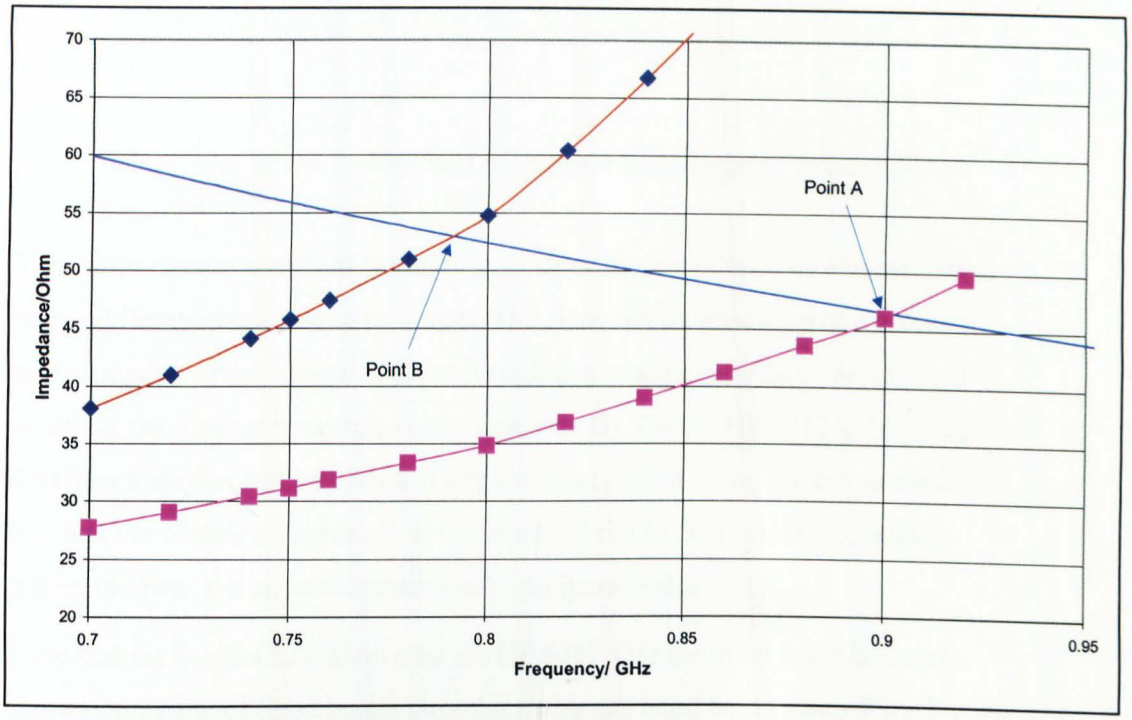

Figure 7-5 Reactive inductive impedance of a 30 mm mortar filled transmission line exposed to different moisture contents

(—◆—) Moisture content 15.4%. Inductive impedance measured directly on the HP 8752C network analyser.

(—■—) Moisture content after oven drying and assumed to be 0%. Inductive impedance measured directly on the HP 8752C network analyser.

(—) Calculated modulus of capacitive reactance of a 3.8 pF capacitor

7.2.1. Use of the Smith Chart to measure impedance of a transmission line

The Smith chart is a convenient method to show the impedance of a transmission line at different points along its length. The chart can be used to give a visual representation of the change of input impedance of a transmission line of fixed length as the frequency changes (see Appendix D). On the HP 8752 C Network Analyser a marker can be placed at any frequency point along the transmission line and the complex impedance at the marker point is then displayed, both as values in ohms and as an inductance or capacitance value.

Note that the Smith Chart shown on the HP 8752 C is the input impedance of a transmission line of fixed length over the frequency band being swept (See Figure 7-6). The HP 8752 C shows impedance directly and not in a format normalised to the characteristic impedance ($Z_0 = 1$) as is customarily shown on a Smith chart.

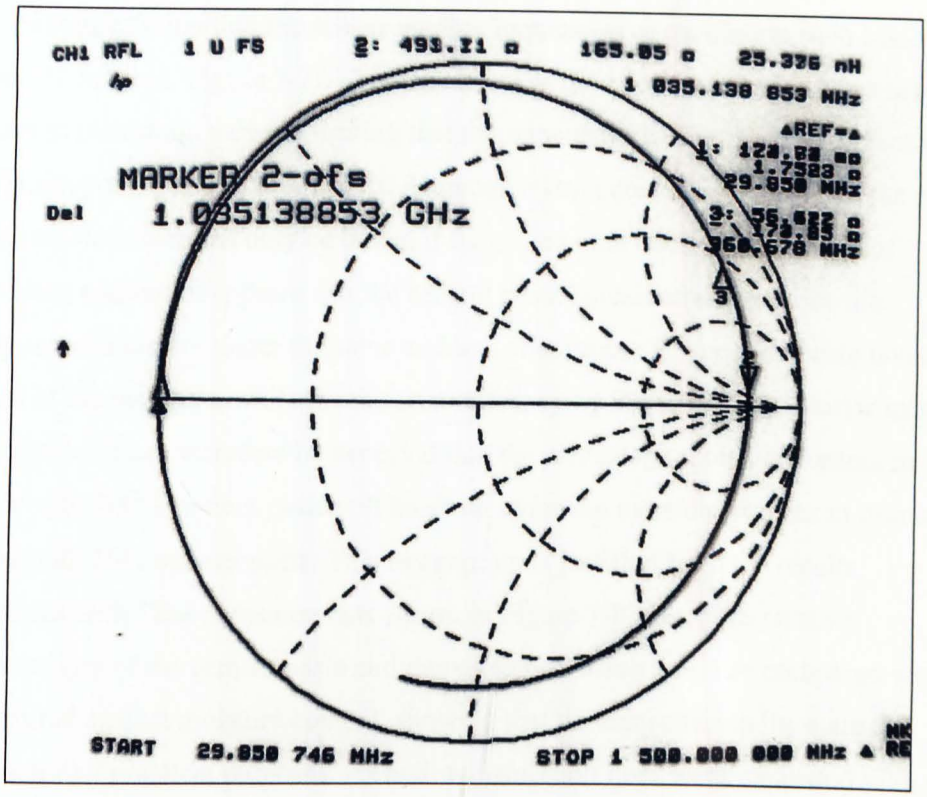

Figure 7-6 Impedance locus as shown on the HP8752C screen.

The impedance locus with a frequency sweep between 30 MHz and 1.5 GHz for a 30 mm transmission line with 50% sand and cement mortar dielectric

The effect of transmission loss means that the real part of the impedance, R, is greater than zero. The transmission line impedance will move away from the outer circle, which is the locus of zero resistance. As the loss tends to increase with frequency the locus of the impedance of a 'lossy' transmission line of fixed length will tend to follow a spiral locus around the centre. The spiral effect is seen in Figure 7-6. Note that the locus is not necessarily a concentric spiral.

The graph in Figure 7-7 is a plot of the imaginary part of the impedance of two 50 mm transmission lines, one filled with cement paste and the other with mortar containing 50% sand. Measurements were taken under the same ambient conditions. The reactance of a 3.8 pF capacitor ($X_c = \frac{1}{\omega C}$) is again shown as a positive value or modulus. If 3.8 pF is the total effective capacitance C of the tuned circuit of the oscillator, the frequency where the plot of X_c crosses the plots

of the transmission line reactances are the frequencies of oscillation (493 MHz and 530 MHz in Figure 7-7). The impedance of the two transmission lines also differ in maximum value indicating that the impedance loci cross the horizontal at different points on the Smith chart. Although a strict comparison between the two transmission lines can only be drawn if they were both calibrated in terms of moisture content, it appears that the cement paste contained about twice the amount of moisture under the same ambient conditions. The cement paste takes up most of the moisture, while the moisture taken up by the sand in the mortar mix is negligible. It can therefore be expected that the percentage moisture content in the filler with 100% cement paste will be about twice the moisture content in mortar filler with 50% cement paste. This assumption is justified from the results obtained with TDR measurements shown in Figure 7-8 where the relative permittivity of the cement paste and mortar transmission lines are compared when measured against moisture content, showing that the transmission lines are the same for all practical purposes. As both transmission lines were measured with the filler material to a maximum moisture content (close to saturation with the surface moisture removed with blotting paper), the results indicate that the porosity of the cement paste is indeed twice that of the mortar, which justifies the assumption that the sand component in the mortar did not take up any moisture.

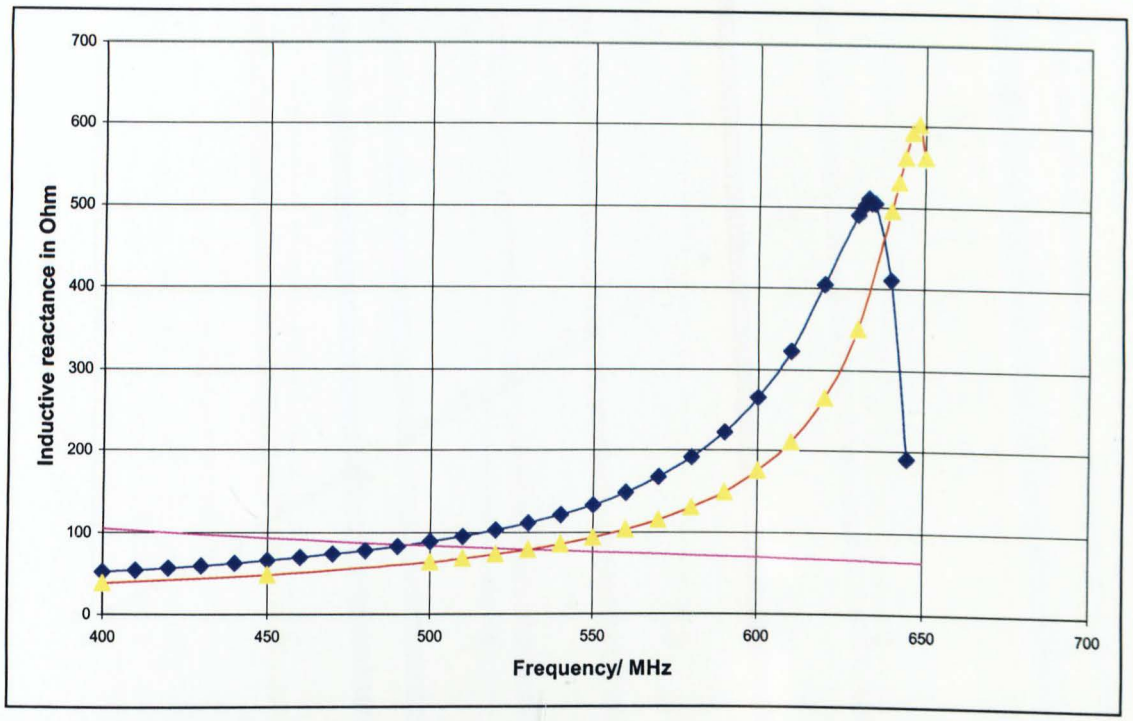

Figure 7-7 Inductive reactance of 50 mm transmission lines with cement paste and mortar dielectric.

(—◆—) Inductive reactance of 50 mm line with cement paste dielectric as read off the HP 8752C network analyser screen.

(—▲—) Inductive reactance of 50 mm line with mortar (50% sand) dielectric as read off the HP 8752C network analyser screen.

(—) Modulus of capacitive reactance of a 3.8 pF capacitor.

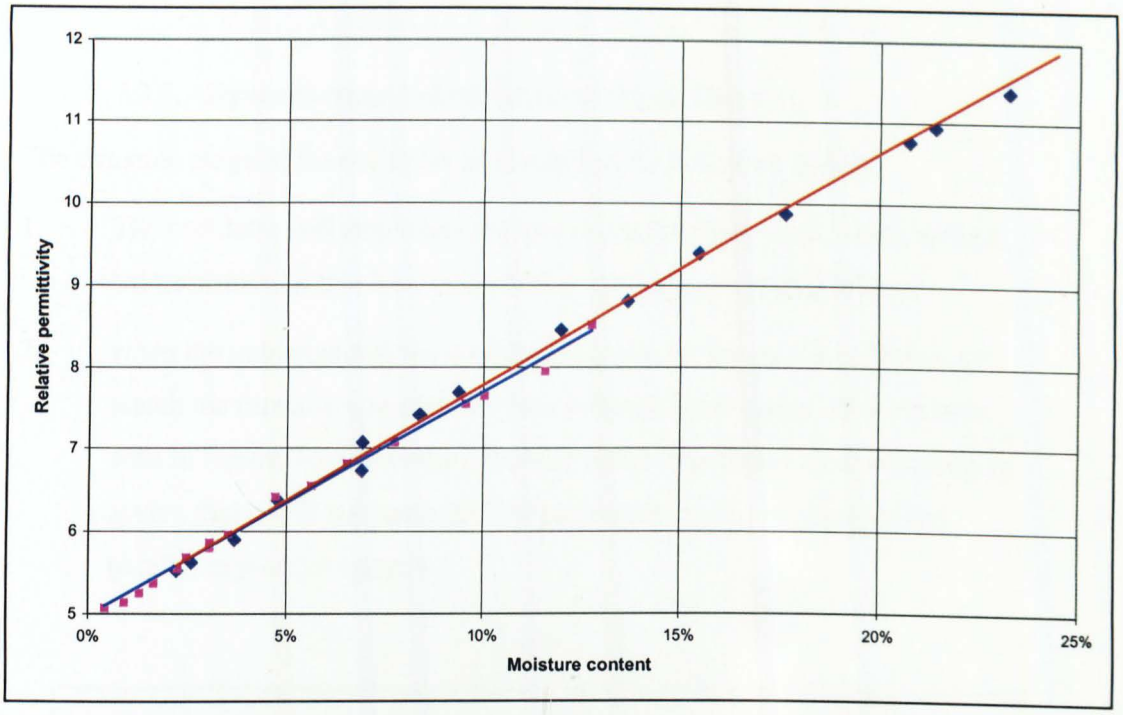

Figure 7-8. Comparison of relative permittivity versus moisture content for 50 mm mortar and cement paste dielectric transmission lines.

(♦) Relative permittivity measured with TDR on the cement paste filled transmission line using Equation 4-18
(■) Relative permittivity measured with TDR on the cement paste filled transmission line using Equation 4-18.
The relative permittivities of the two filler materials follow a straight line with nearly the same slope and constant value.
(—) Linear trend line as indicated by Microsoft Excel for cement paste.
(—) Linear trend line as indicated by Microsoft Excel for mortar.

7.2.2. Dynamic range and resolution of the oscillator

The dynamic range of the oscillator is determined by two main factors.

1. The oscillator will stop when the loss in the feedback loop, which include the transmission line loss, exceeds the loop gain of the amplifier or
2. when the inductive reactance of the transmission line is not sufficient to match the capacitive reactance of the external capacitance. This effect is seen in Figure 7-9 where the curvature of the impedance locus becomes so severe that it will not reach the reactance value required to match the parallel capacitive reactance.

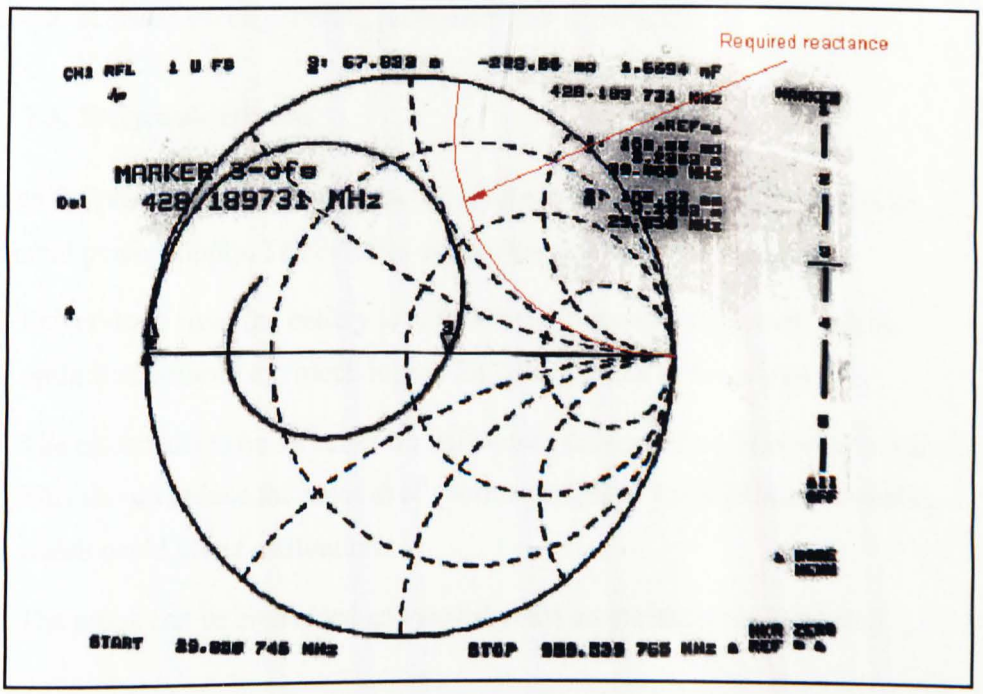

Figure 7-9 Locus of a high loss transmission line as seen on the HP 8752C network analyser

In the transmission line used as a moisture sensor there are two main factors that should be considered:

a. The moisture content range to be covered and thus the range of ε_r to be measured.

b. The resolution in terms of moisture content.

Factors a and b are mutually exclusive. The only way in which both a high resolution and a wide range can be achieved is to place probes with different and overlapping dynamic ranges in close proximity in a structure.

To measure very high moisture content such as that experienced under saturation conditions or in freshly poured concrete, the transmission line must be designed to be less sensitive to higher dielectric losses. If the value of the parallel capacitance for the oscillator circuit used is known, the impedance plot (for example in Figure 7-4 and Figure 7-5) will indicate if the capacitive and inductive reactance lines will intersect. The question of loop gain versus loss must however be calculated or tested using a "Spice" simulation programme such as the *Workbench 5.0* used in this study, or it must be tested with a real oscillator. Any margins allowed will have to be based on engineering judgement and experience.

7.3. Electronic circuits

Since the probe has to be left in situ for long periods it is imperative to use an external power supply. The external supply has numerous advantages.

1. Power drain from the battery is of less importance and the circuit can be optimised without too much regard for conservation of battery power.
2. The circuit has to be switched on only while the (occasional) reading is taken. This should reduce the amount of parameter drift in the oscillator transistor, which could affect calibration.
3. The probe can be embedded and sealed since no maintenance is needed.

7.3.1. 'Down conversion' of test frequency

Using the 30 mm transmission line, the measuring oscillator will operate between 750 MHz and 900 MHz. Although a frequency to voltage converter could be employed to change this frequency directly to a voltage for measurement purposes, it is advantageous to mix it with a local oscillator and monitor the

change in the 'beat' frequency between the two. The percentage change in the beat frequency is $\frac{f_1}{f_2 - f_1}$ times more than the percentage change in the oscillator frequency. Therefore with down-conversion the sensitivity to change in the test oscillator frequency f_1 can be increased or decreased as circumstances demand by adjusting f_2. The practical limitations will be discussed in the following sections.

Another important advantage of using down-conversion is that frequency drift in the test oscillator f_1 can be tracked by a similar frequency drift in the local oscillator f_2, and f_1-f_2 would be unchanged. This aspect will be discussed in more detail in section 7.3.2 and 7.3.3.

7.3.2. Factors affecting frequency drift of the oscillators

Any free running oscillator will experience some drift in frequency due to changes in circuit parameters (due to temperature, ageing, supply voltage etc.). In the Colpitts oscillator circuit envisaged the frequency is determined by the characteristics of the transmission line tuning element as well as the other capacitors making up the total tuning capacitance *C*. Temperature, which affects various circuit elements, is the most important source of drift in the short term. The probe may be placed in an environment where it will experience wide temperature variations and the effects of temperature cannot be ignored.

As the components age, some parametric drift due to gradual changes in transistor characteristics must be expected. In the author's experience there is relatively little parametric drift due to charge diffusion through the semiconductors in a 5 to 10 years period, provided the components are not continuously subjected to a voltage difference across the junctions. This illustrates the reason why the probes should only be powered when a reading is taken.

7.3.3. Local oscillator tracking of the sensing oscillator frequency.

To compensate for parametric drift the local oscillator should be as similar as possible to the test oscillator. The component values and transistors types must be the same in the two circuits. In principle any parametric drift in the test oscillator should then be tracked by similar changes in the local oscillator. The importance

of using the same type of tuned circuit (a transmission line rather than a fixed inductance) can be demonstrated by comparing the change in frequency with a transmission line as inductance in the tuned circuit with that of the same circuit with a fixed inductance.

The impedance plots of an oscillator with a fixed inductance (8.2 nH) in the tuned circuit is compared with a sensing oscillator using the 30 mm transmission line as inductor. The oscillators are identical except for the inductor used. Say the capacitance *C* changed from 3.8 pF to 4.0 pF in both the sensor oscillator and the local oscillator circuits (due to a supply voltage change for example). For the transmission line the point of oscillation changed from point A (903 MHz) to point B (890 MHz) in Figure 7-10. The frequency of the local oscillator with the inductance of 8.2 nH however, although at the same frequency (point A) for 3.8 pF, moved to point C (880 MHz) for the 4.0 pF. It shows that the difference in slope of the impedance-frequency curves made it impossible for the local oscillator to track the sensing oscillator. Clearly the local oscillator must also use a transmission line as tuning device to ensure proper tracking. A stripline on the printed circuit board can be used as a transmission line for this purpose to ensure that the reactance is a tangent function that will track the sensor oscillator.

A change in the supply voltage will change the transistor junction capacitances, affecting the tuned circuit directly. Provided the above precautions are taken, the changes in the two oscillators due to voltage variations should track each other closely. However it is still prudent to keep the supply voltage constant to reduce possible tracking errors between the two oscillators.

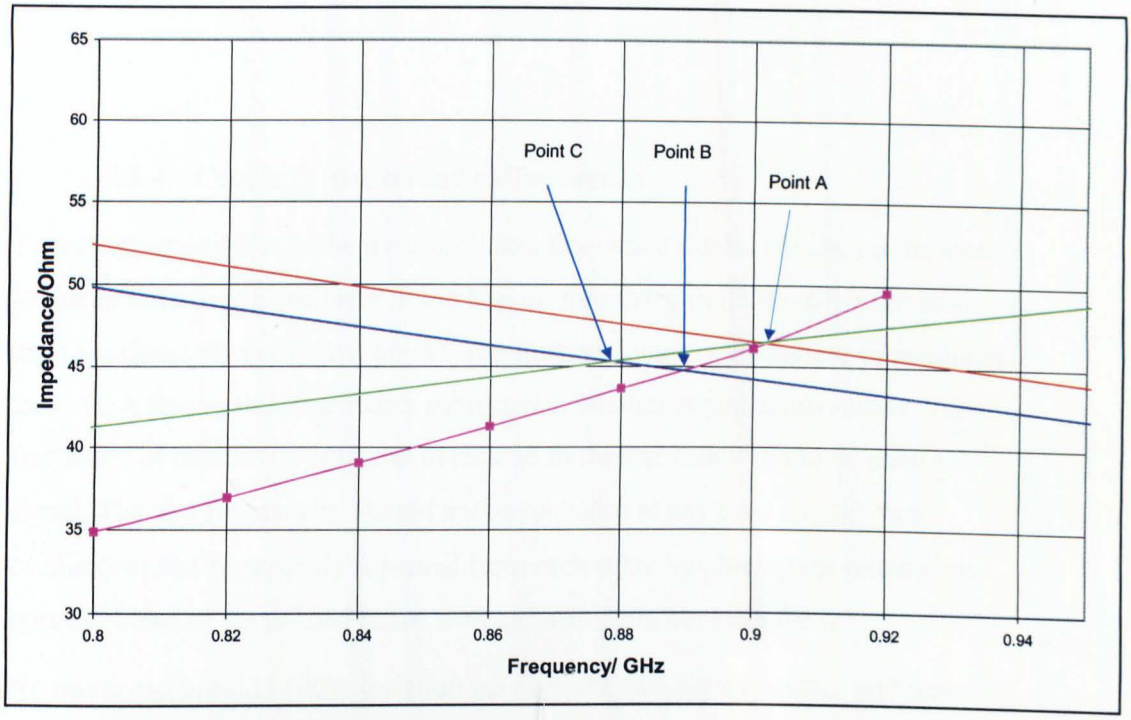

Figure 7-10 Comparison of the effect of a change in capacitance on oscillator frequency with the 30 mm mortar filled transmission line and a fixed inductance.

(—■—) Measured impedance of oven dried mortar filler on the HP 8752C network analyser (0% MC).

(—) Modulus of capacitive reactance (impedance) of a 3.8 pF capacitor.

(—) Modulus of capacitive reactance (impedance) of a 4.0 pF capacitor.

(—) Inductive reactance of 8.2 nH inductance.

7.3.4. Oscillator lock-on and buffer circuits

To maximise sensitivity, the local oscillator frequency can be adjusted to be close to that of the sensing oscillator at the highest frequency (with the filler material dry i.e. effectively at 0% MC point). The limiting factor is the danger of oscillator lock-on. A free running oscillator subjected to another signal source close to the frequency of oscillation will tend to lock on to the frequency of the external signal. The two frequencies should not be too close at any time and the two oscillators must be properly screened from each other by placing the circuits on opposite sides of the printed board with an earth plain between them.

No mixer can provide 100% isolation between the two signal sources and there will always be some coupling via the mixer from the one oscillator to the other. To isolate them, both oscillators can be fed through buffer amplifier stages to the mixer. With good screening and buffering the two frequencies can be within less than 100 kHz from each other, but should probably not be closer than about 1 MHz in practice.

7.3.5. Frequency to Voltage conversion

The beat frequency can be converted to a voltage in a number of ways in order to monitor it on a data collecting system like a voltage data logger. This conversion should be done externally to keep the component count and cost of the embedded sensor as low as possible. By using an external converter the options are kept open to update or renew the interface circuitry as required.

The beat frequency can be passed through a number of divider stages that will reduce the frequency to a value that can be handled by a frequency to voltage integrated circuit like the LM2907, or to a digital counter to obtain a readout of moisture content.

7.4. Future development

It is apparent that there are a number of options open for further development. To ensure that the method investigated could be used in practice a Colpitts type oscillator with the transmission line as tuning device was built and tested using an external signal generator as local oscillator. As mentioned in section 7.3.4 the effect of the close physical proximity of two oscillators must be tested and adequate screening provided to prevent locking between the oscillators. Temperature tests were carried out at constant humidity on the transmission line (see section 8.7) and the results indicated that there is no need for a temperature compensating circuit, depending on the accuracy and resolution required. It is feasible to fit an integrated temperature sensor to provide both moisture content and temperature information to a data logger. Various integrated circuit temperature sensors are available that will give a voltage output proportional to temperature. The output of the temperature sensor could be read directly or used to correct the data automatically.

7.4.1. External monitoring equipment

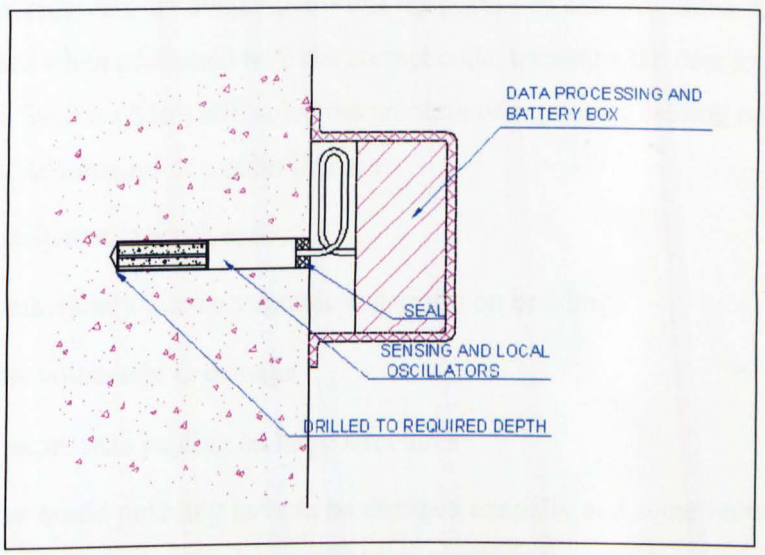

Figure 7-11 Proposed outdoor installation.
The interface box helps to seal the entrance to the drilled hole

The interface circuits are mounted externally in a separate housing containing the batteries (if power is not to be supplied over a cable) (see Figure 7-11). It is

normal practice to use a voltage to current conversion (4 to 20 mA for 0 to 10 volt) for remote sensing purposes. The current signal is less prone to change over distance as there would always be some voltage drop in a sensing lead. Instead of a voltage to current converter, the beat frequency can be fed to a counter to give a digital output of moisture level. With a digital system the different sensors may be connected by means of one data/power cable and the sensors addressed individually in sequence to obtain the data. With the data in digital form more sophisticated monitoring systems can be used. As sensors are addressed individually the calibration data of individual sensors can be used to correct the data if required. The clock frequency can be changed to compensate for temperature changes if required. Externally mounted equipment can be replaced over time if damaged, or it can be updated as the technology and/or requirements change. With a digital system optical cable can be used to reduce the problem of electromagnetic interference. The use of an external digital circuitry opens up the possibility of doing away with cable connections to the sensors from the central data-gathering unit. Provided the external units are accessible, batteries can be fitted in the external unit and the data transmitted by radio link. Standard radio transmitter/receivers are available for this purpose. The external unit acts as a receiver and when addressed with the correct code, transmits the data in a short data burst. Such a system will solve the problem of expensive cabling on structures. Advantages of a radio link are:

(a) Installation is much easier

(b) Aesthetically more acceptable especially on buildings

(c) Less vulnerable to damage

(d) Cheaper than cabling on large structures.

As batteries would probably have to be changed annually and some units may be difficult to reach, the battery box could be mounted in a more accessible position with a relatively short power lead to the remote unit.

7.4.2. Electromagnetic Compatibility (EMC)

In terms of EMC regulations (In the UK this comes under British Standard BS 6527:1988) the sensor may have to be tested by a contractor with the required calibration equipment. One of the advantages of the cage-coaxial transmission line is that the EM fields are restricted to the inside of the cage. With a good design of the EMC characteristics the amount of radiation will be low enough not to warrant restrictions in terms of frequency. A restricted narrow frequency band will render the sensor useless.

In conclusion this chapter looked at the practical applications of the results to design and build a sensor that will meet the requirements of low cost, high reliability, ruggedness and capability to function for decades without re-calibration. An oscillator will use the inductive reactance of the sensing transmission line as part of the tuned circuit. The moisture content in the filler material of the transmission line will change the reactance of the transmission line and thus the frequency of the oscillator. A method to calibrate the sensing transmission line was discussed as well as a method by which the oscillator frequency, and thus the moisture content, can be monitored.

Chapter 8. Results and Analysis of Experimental Data

This chapter will re-examine some of the results to highlight the important findings. Most of the findings were discussed under their relevant headings, but some are reiterated here.

a. The suitability of the cage-coaxial transmission line to measure relative permittivity.

b. The precision with which moisture content can be measured with the transmission line as tuning (inductive) element of the sensing oscillator.

c. The moisture equilibrium condition between two and more porous materials in close contact, of importance here because of the use of a separate filler material to measure moisture content.

d. The boundary effect on the water molecules in a solid matrix affecting the relative permittivity of water and how is can be accounted for in a dielectric mix formula of overall permittivity in a porous material.

e. The effect of insulated conductors on the permittivity of bulk water.

f. The variation in apparent ε_r at discrete frequencies as measured with the cage-coaxial transmission line.

g. The effect of temperature on the relative permittivity of a mortar (cement and sand) and the relatively low sensitivity of the moisture content probe to variations in temperature.

h. An important new moisture parameter proposed to measure moisture as a percentage of full saturation.

The wide scope of the above findings highlights the multi-disciplinary nature of this investigation.

8.1. The suitability of the cage-coaxial transmission line to measure relative permittivity

As an example of the accuracy of measurement of the relative permittivity with the cage-coaxial transmission line, consider Figure 8-1, a graph of relative permittivity versus temperature for bulk water using uninsulated (bare) transmission line conductors. The deviation of the individual points from the trend straight line, given by $R^2 = 0.9952$, is due to the relatively 'flat' peak that the TDR curve has on the HP 8752C, owing to dielectric losses and conduction in water. The flat curve introduces an error in the determination of the maximum point. The relative permittivity measured (79.1 at 20 °C and 80.9 at 15 °C, when using the trend line) compares well with the values obtained in the literature with other methods (Hobbs, 1974). The consistency of the results provided confidence in the use of the cage-coaxial transmission line to measure relative permittivity. In a dielectric material like gypsum with lower loss than water, the peak (maximum) of the reflection point is better defined (see Figure 4-9) and the points on the curve follow a smooth line as shown in Figure 6-3.

8.2. The suitability and accuracy of moisture content measurement using the transmission line as inductive tuning element for the sensing oscillator

The results of calibration tests showed conclusively how suitable the transmission line sensor is to measure moisture content. The final resolution that can be achieved depends on the dynamic range to be covered. As an example in section 7.2 it is shown that with a resolution of ±1 MHz, the moisture content is measured to ±0.14% MC. In fact the resolution can be reduced to ±100 KHz, which would give a resolution in MC of 0.014%. In practice such high resolution will not be required and very small changes in relative permittivity due to temperature and oscillator tracking errors will introduce greater errors than the resolution. Such errors will have to be eliminated before such accuracy is meaningful. On the other

hand, if measurements are taken under well-controlled (laboratory) conditions, a resolution of ±0.01% MC can be achieved. Note that a resolution of ±0.14% MC in concrete is about ±0.056% gravimetric moisture content.

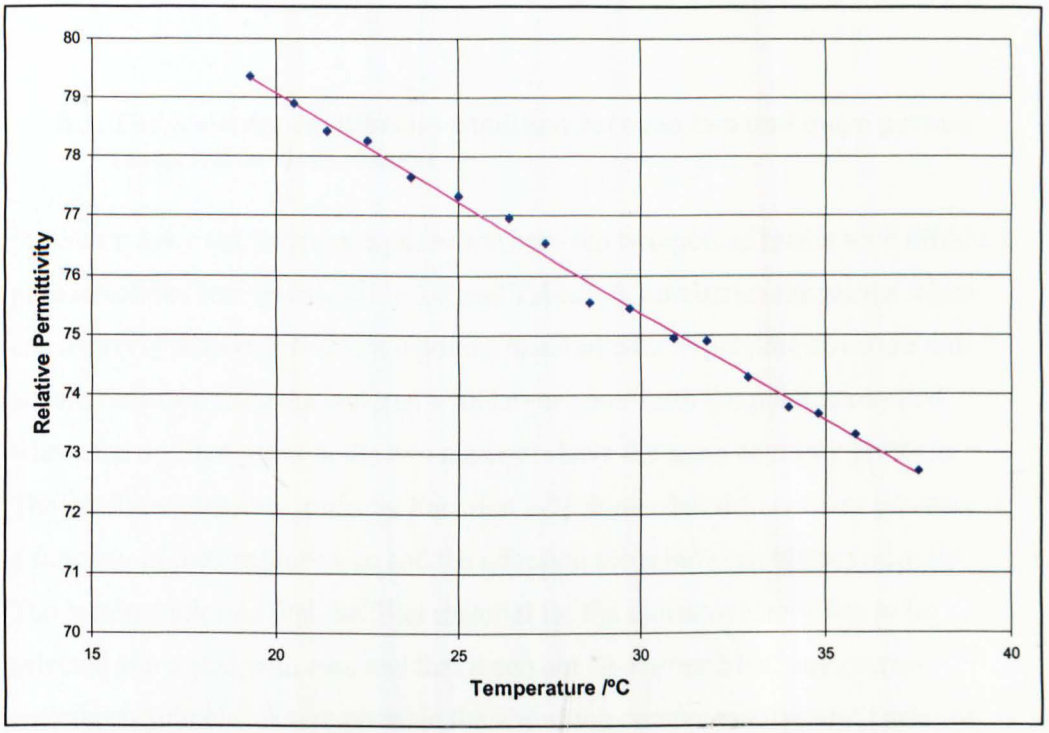

Figure 8-1 Measurement of relative permittivity as a function of temperature for bulk water using TDR.

For details refer to Figure 5-1

8.3. The moisture equilibrium condition between two and more porous materials in close contact

In section 3.4.1 the moisture equilibrium between two porous media with different pore structures was tested. Table 3-2 and Table 3-3 summarise the results which conclusively demonstrated that a porous material with a fine pore structure will absorb moisture from the material with larger pores until the point is reached where the unfilled pores in the two materials have the same capillary pressure. The capillary pressure, given by Equation 3-7, shows that the capillary pressure is a function of the capillary size and the adhesion force between water and solid. The results indicated that the filler material for the moisture sensor has to be selected and tested with care and that it can not be assumed that any porous material is suitable. Where possible the absorbing component (cement paste) of the material used as filler in the transmission line should be the same as the absorbing component of the MUT. Apart from moisture measurement in concrete and provided that the necessary calibration and moisture equilibrium tests are carried out, the moisture probe with a suitable filler material for each case can be used for measuring moisture in a range of materials like timber, masonry and soil.

8.4. The boundary effect on the water molecules in a solid matrix, and how it can be accounted for in a dielectric mix formula.

Equation 5-19 is a formula for calculating the total relative permittivity in which the boundary effect is accounted for in a logical manner into the Complex Refractive Index (CRI) formula for mixed dielectrics. The author extended the CRI formula to three materials to include the fundamental ingredients in a porous solid namely solid, air and water. Calculation based on this formula fitted the experimental results of permittivity versus moisture content for a gypsum-sand mix extremely well as shown in Figure 5-8. The excellent match can be attributed to the relatively simple pore structure of the gypsum. The relative permittivity versus moisture content graph for cement paste and mortar however shows a

different tendency (Figure 5-6 and Figure 5-7), possibly due to the complexity of the pore system that does not allow a simple mathematical representation as in the case of gypsum. However a third order polynomial provides a near perfect fit and can be approximated by a linear trend line. An empirical formula was then derived for the linear line based on the CRI formula with the second order term removed. There is no theoretical basis for doing it, but it gave a good agreement with the experimental results. Some future work can be done on the search for a theoretical basis for such a formula, preferably a third order polynomial instead of a straight line.

A possible explanation of this trend that closely follows a third order polynomial fit, is as follows: At low moisture content more than 28% of the gel pores are already filled (non-evaporable water). Water entering the pore system will quickly fill the smaller open pores. This is the region up to 2% MC seen in Figure 5-9. The slightly larger pores start to fill above 2% MC but the high adhesion force of the water/solid, concentrates the water on the surfaces of the pores where the boundary effect reduces the ε_r (MC of 2% to 9% in Figure 5-5 for mortar and 4% to 18% in Figure 5-6 for cement paste). After this point an increasing number of water molecules are not affected by the boundary effect and the curve starts to follow the CRI function. Note again the factor of two in the comparison between mortar and cement paste, which is a clear indication that the moisture is concentrated in the cement paste only.

8.5. The effect of insulated conductors on the permittivity of bulk water.

The reduction in the relative permittivity of water when the conductors of the transmission line were insulated with a thin lacquer is more of academic than practical interest for this application. However, the difference in apparent permittivity of in bulk water measured with and without insulation, raise the question of how such insulation will affect a cage-coaxial transmission line when a porous solid like cement paste or mortar filler is used. Two transmission lines, one with and one without lacquer, were embedded in cement paste early on in the test program. The results showed no meaningful difference in relative permittivity

between the two. The situation is expected to be different if the thickness of the insulation is increased to say 0.2 or 0.5 mm. The thicker non-porous insulation acts like another ingredient in the dielectric mix formula and is expected to have quite an important impact on the total permittivity. This is the method proposed to reduce the sensitivity of the moisture probe transmission line under very high moisture content conditions (above the hygroscopic range and close to saturation).

8.6. The variation in apparent ε_r at discrete frequencies as measured with the cage-coaxial transmission line.

The difference in ε_r between measurements with TDR and measurement at discrete frequencies was shown in section 7.2 where ε_r at 430 MHz was calculated to be 4.128 under ambient conditions against $\varepsilon_r = 5$ for the dry mortar filled transmission line measured with TDR (see Figure 5-6 and Figure 5-7). However, provided the calibration is done at the relevant frequency, as is the case in the method described in Chapter 7, the calibration is perfectly valid. It is suspected that this variation is due to the non-ideal short circuit termination of the cage-coaxial transmission line rather than a real difference in ε_r in cement paste or mortar. Until ε_r is measured at this frequency in a different way, for example by testing the velocity of propagation using microwave antennas on both sides of a sample of the MUT, the difference will be assumed to be due to the characteristic of the cage-coaxial transmission line. No correction due to this difference is needed if the sensor is calibrated as described in Chapter 7.

Figure 4-10 shows the difference in relative permittivity when measured at discrete frequencies and using the phase change at each point relative to the angle of a transmission line in air to calculate the relative permittivity. The measured relative permittivity starts to drop quite sharply towards the lower frequencies, probably due to a change in the transmission mode of the EM wave at lower frequencies and therefore a characteristic of the transmission line used.

8.7. The effect of temperature on the relative permittivity of a mortar with 50% sand as fine aggregate.

The temperature of a medium affects the relative permittivity and has to be taken into account if the measurement of oscillator frequency is to be used to determine the moisture content. The effect of temperature on the permittivity of bulk water was shown in section 4.2.2. In the case of bulk water the temperature coefficient is negative, decreasing with increase in temperature (Figure 5-1 and Figure 5-2). The effect of temperature was measured by sealing a mortar filled transmission line to keep the moisture content constant (Figure 8-2), then the frequency was determined where the equivalent inductance on the network analyser was 8.2 nH, over a range of temperatures (Figure 8-3).

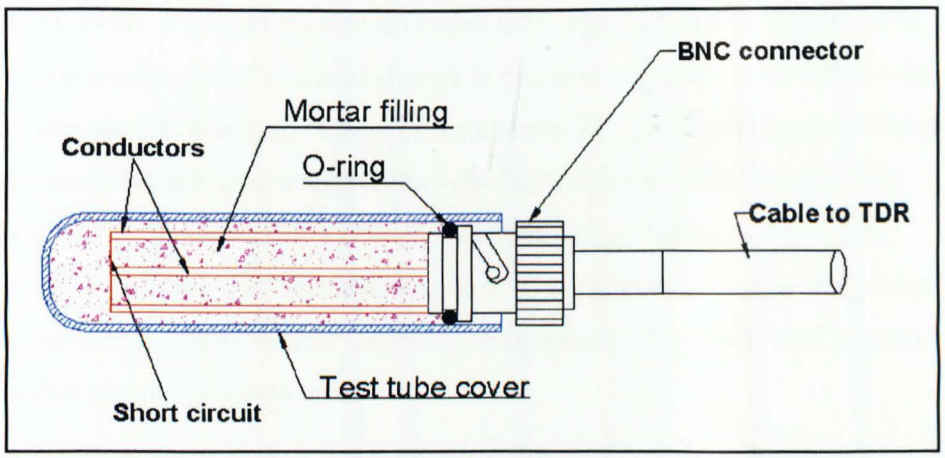

Figure 8-2 Sealed transmission line for testing temperature effect on relative permittivity without changing the moisture content.

Measurement with air as dielectric was carried out before casting the transmission line. After the initial test without a casting, the transmission line was cast in a mould with a mortar filling, then cured (hardened) in 100% relative humidity for 5 weeks before it was dried and inserted into the non-porous tube. The end was sealed with an O-ring (Figure 8-2). The results shown in Figure 8-3 indicate a decrease in frequency and therefore an increase in permittivity with temperature (positive temperature coefficient). Compare the result with Figure 5-1 and Figure 5-2, which show that bulk water has a negative temperature coefficient for permittivity.

Although it would have been better to measure the impedance over the frequency band as was done in section 7.2, the time to complete each test series for every temperature point meant that due to rapid cooling the temperature would have changed during the test. The method chosen enabled the investigator to take a single reading before any detectable change in temperature. Ideally the more direct impedance test should be done in a temperature chamber through a cable connected to the network analyser.

In Figure 8-3 the frequency for an inductance of 8.2 nH indicated on the Smith chart of the network analyser, changed from 881 MHz to 879.4 MHz, with a change in temperature of 20°C (from 10°C to 30°C). Referring to section 7.2, this difference of 1.6 MHz is equivalent to a change in moisture content of 0.224% (1.6 × 0.14%). A note of caution is needed with regards to the variation due to temperature changes. The test of change in frequency with temperature was done with one specific moisture content of the sample. The combination of dry material and water having opposite temperature coefficients for permittivity probably means that at higher moisture content, the trend can go the other way as the permittivity of the water becomes dominant. The variation of permittivity with temperature and thus the error caused by temperature differences may be even less at higher moisture content levels.

The relatively small change in permittivity with temperature, and thus the accuracy needed, made TDR unsuitable to measure the effect of temperature on relative permittivity.

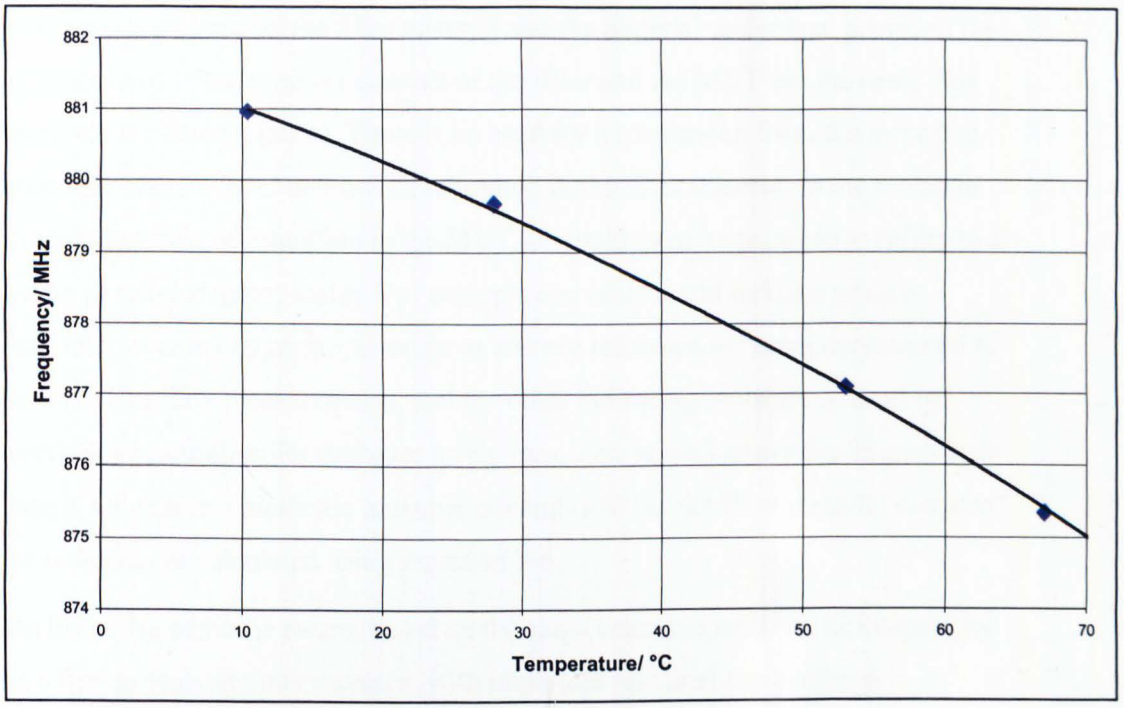

Figure 8-3 Change in frequency with temperature for the 30 mm mortar filled transmission line at constant moisture content.

(◆) The frequency where the input impedance showed an equivalent of 8.2 nH on the network analyser was recorded for each temperature. The inductance was chosen as the approximate point where the oscillator frequency would be with the transmission line under test as tuning element.
(—) Second order polynomial trend line with Excel.

8.8. Moisture content as a percentage of saturation

The method employed in this study to measure moisture content leads to an important conclusion namely, moisture content can be measured as a percentage of saturation. Such measurement is of great value in building materials in general as it gives a real indication of the level of moisture content in terms of the maximum that can be achieved. It is of special importance if used as an early warning of potential frost damage (see Figure 3-9 and section 3.3.4) together with a temperature sensor (built into the probe, or separately). Note that a measurement as a percentage of saturation is independent of the difference in ratio of porous to

non-porous material in the filler material and the material under test, provided the pore systems in the porous materials of the filler and the MUT are the same (for example the cement paste). There is no need for a conversion from the indicated moisture content level in terms of saturation in the filler material to the moisture content in terms of saturation in the MUT. It would even be possible to calibrate a probe in two (or more) scales. For example one scale could indicate relative humidity over the hygroscopic range as an easy reference for users accustomed to relative humidity measurements, and the other indicating moisture content in percentage saturation for moisture levels from zero to well above the hygroscopic range. Of course, volumetric moisture content (MC) in the filler material can also be indicated or calculated using Equation 3-6.

As far as the author is aware, based on thorough literature reviews, this capability is a first in moisture measurement with important practical implications.

8.9. Calibration and operation of the moisture sensor

8.9.1. Calibration

The following is a suggested method of calibration. The variation in internal capacitance values between different transistors plus the strong effect of small differences in physical lengths of transmission lines means that the frequency of oscillation cannot be derived reliably from measurements of relative permittivity versus moisture content. It was shown in section 4.6 that the apparent relative permittivity as measured with the transmission line varies with frequency due to transmission line characteristics (see Figure 4-10). In essence calibration will therefore have to be a direct measurement/calibration of beat frequency, discussed in 7.3.1, against gravimetrically measured moisture content. Further conversion of this beat frequency to a monitoring output depends on the design of the external or interface circuits as discussed in section 7.3.5 and 7.4.1. Calibration will be done on a batch of sensors manufactured to facilitate quality control of the material and processes. Ambient temperature should be maintained at a convenient level and recorded.

Steps:

1. A batch of filler mortar mix is prepared for a batch of sensors to be manufactured and calibrated. The mix ratio of cement, fine aggregate (sand) and water is weighed within close tolerance limits (within say ± 1% of the prescribed amount) and one mix is used for all the sensors in a batch. The fine aggregate must be washed and graded in sizes and the correct combination of grades (to be determined) used.

2. Before encapsulating the sensor transmission line in the filler material and with the transmission line permanently connected to the oscillator circuit (sensor oscillator frequency f_{air}), adjust the reference oscillator frequency f_r to obtain the correct beat frequency f_b ($f_b = f_{air} - f_r$) as measured on a frequency counter by changing the length of the reference oscillator tuning transmission line, which is in the form of a strip line on the printed circuit board (see section 7.3.3). A sliding short circuit is used for this purpose, soldered permanently into the final position. The frequency f_b must be determine beforehand on a number of sample sensors by measuring the difference between the sensor oscillator frequency obtained with the transmission line before encapsulation (f_{air}) and after encapsulation with zero moisture content filler material (f_{dry}). The reference oscillator frequency f_r is then set to obtain a beat frequency f_b, which is this difference in frequency ($f_{air} - f_{dry}$) minus say 1 MHz to ensure it will run at a slightly higher frequency than the sensing oscillator at zero MC[9]. The adjustment compensates for variations in the internal capacitances of the oscillator transistors. It also compensates for small differences in transmission line dimensions. It is important to note that before transmission line encapsulation, the sensor oscillator frequency f_{air} (1 GHz for example) will be higher than the reference oscillator frequency f_r (950 MHz for example). Check that the reference oscillator is not adjusted to the frequency higher than the sensor oscillator frequency (to 1050 MHz in this example) for the same beat frequency f_b (50 MHz in the example). If the

[9] Due to ambient atmospheric moisture the moisture content of the sensor should never reach zero in practice and the beat frequency $f_{air} - f_{dry}$ may even be set to f_b.

reference oscillator's line length is reduced (frequency increased), the beat frequency should decrease.

3. The sensor transmission lines are encapsulated in the filler mix in a mould and allowed to set, then placed in water after 24 hours to harden for one week and mature (cement hydration complete) in a 100% relative humidity enclosure for 28 days. After 28 days the sensors are kept under ambient conditions for another month to dry slowly before calibration.

4. Samples of the sensor (a sampling scheme based on results should be used to determine the correct sampling size) from the batch are tested for quality control and calibration purposes by oven drying. Some control samples are cast in the same mould without a transmission line or electronics and used as references to determine moisture content when placed in the same environment as the sensors. It is assumed that the moisture content in the sensor filler material will be the same as the moisture content in the control samples. The control samples are weighed immediately after removal from the oven to determine the dry mass and then allowed to cool off together with the sensor samples in a desiccator.

5. Add moisture in steps[10] to the control samples and the sensors and measure the beat frequency at each level of moisture content starting from the driest condition, allowing for equilibrium to be reached at each step (no change in the frequency for a constant mass i.e. when there is no change). Three moisture levels should be enough to calibrate the batch. The volume of material and the mass just after oven drying are known and therefore the volumetric moisture content. Moisture content is determined by weighing before and after each test, as there may be some change in moisture content during the test except if a test rig can be used to test the samples inside the conditioning chamber. Note that the first reading before adding moisture may

[10] Moisture can be added by placing the sensors in constant RH enclosures above the appropriate saturated salt bath, then move to the next higher RH enclosure for each step. For calibration above the hygroscopic range, water will have to be added directly and sensors must be weighed individually to determine MC.

not be at the zero moisture point due to hygroscopic absorption of moisture during the test.

6. During the month after treatment in 100% relative humidity (maturing stage) the beat frequencies of all the sensors in the batch are checked regularly and compared with the calibration data from the sample sensors and the moisture content of the control sample cylinders. Sensors that deviate outside predetermined margins (to be ascertained) are then rejected.
7. From the above data the final external interface circuit is adjusted to give the required output (analogue or digital) in terms of moisture content.

8.9.2. Operation

Suitable monitoring points and depths are selected on a structure to be monitored. Holes are drilled to the required depth and the sensors inserted. Assuming that the final sensor has a diameter of 15 mm, the holes should be drilled with a 15 mm masonry drill. The sensor should be a snug fit in the drilled hole. If not, the sensor should be forced to one side of the hole by means of a suitable spacer. Ensure that at least one side of the sensor is in close contact with the material under test. The connecting cable is then brought out and connected to the external unit and the hole sealed with a bitumen or other suitable sealing compound (Figure 7-11).

A detailed operating procedure will have to be worked out for each application depending on the design of the interface or external circuitry and type of installation not detailed in this study. For example in a small installation the external circuitry can incorporate a timing device, battery and a local data logger. The timing device powers the sensor and external interface circuitry on a daily, weekly or monthly basis and the voltage data logger records the sensor output voltage (section 7.3.5) previously calibrated in terms of moisture content as described in 8.9.1. On a large structure like a bridge or viaduct the sensors may be connected by cable through 4 to 20 mA converters (standard telemetry voltage to current converters) to reduce noise, the sensors will be switched on periodically either in sequence or simultaneously and the data recorded on a suitable data logging system. If the output is a digital signal where the beat frequency is fed

through frequency dividers to a counter (see 7.4.1), the telemetry and data logging system (RF or cable) will be adapted for the purpose.

Chapter 9. Conclusions and Recommendations

9.1. Conclusions

The aim of the study was achieved when the basis for a practical and cost effective method to monitor the moisture in concrete was found through a range of investigations. The moisture sensor can be mounted in relatively large numbers into drilled holes at any required depth to measure and monitor the moisture continuously. With some trade-off between dynamic range and resolution it can measure the moisture content from completely dry up to saturation level. Measurements are relatively insensitive to temperature changes, but if required, a temperature sensor can be included and used to compensate for temperature variations or additional information. If required the same sensor can then be used to measure the temperature and the data fed through the telemetry system. The sensor can be used in other materials apart from concrete by selecting a suitable filler material. A good knowledge of the pore structure of both the material under test and the filler material is needed to ensure that the equilibrium conditions are known and the moisture content must be calibrated accordingly. To ensure that the moisture in the filler material tracks the moisture in the material under test, the filler material should as far as possible be the same as the material under test. The indications are that variations of the transmission line could be developed that did not use the filler material principle. Variations in the design to measure the moisture instantly could be developed by using the 'skew transmission line' or a strip line transmission line concept as sensor. The low cost potential opens up the possibility for it to be used as soil moisture monitors with suitable filler material. The sensor could also be cast with the concrete during construction and be used to monitor the drying/hydration process. It can then be left in situ for long term monitoring purposes. The moisture content, or water level in a freshly cast concrete mix, is much higher than the saturation level in the hardened concrete,

due to the fact that the hydration product has not yet filled the gaps in the mix. The filler material in the transmission line on the other hand will show saturation under these conditions and not the full water content of the concrete mix. The cage-coaxial transmission line can be used without a filler material to measure the relative permittivity of a liquid. Such a function is not necessarily for moisture measurements, but can be used to measure say density of a slurry. It has the advantage that the results are given instantaneously so that the sensor can be used in a flowing liquid. With proper protection of the conductors it can be used in a highly corrosive environment for example to measure the concentration of acids?

The transmission line sensor with a filler material lends itself to a new and novel moisture content measurement, namely moisture content in terms of the full saturation level taken as 100% moisture content. The elegance of this method lies in the fact that the transmission line sensor can read such a percentage of moisture content directly using calibration data. The same applies for measurement of relative humidity, a measurement that can be useful for comparison of results with other methods if required in spite of the author's reservations about the applicability of RH measurement to determine actual moisture content levels.

Regarding the electronics, the results in section 7.2 shows that the oscillator will be highly sensitive to changes in relative permittivity. The sensitivity can be reduced in order to increase the dynamic range by adding insulation of a required thickness to the screen conductors. The fundamental approach was to find an electronic sensor with a low component count to increase reliability and decrease material and manufacturing cost. This turned out to be the case with a circuit based on the Colpitts oscillator. Any other interface and telemetry circuits as well as power supply can be added externally and does not have to be mounted inside a cavity in the concrete where it should remain sealed. The use of external interface and telemetry circuits provides flexibility and the option to update the system as technology changes if required, without disturbing the sensor itself. The external electronic circuits can be adjusted to suit the particular application.

9.2. Recommendations for Further Study

1. The transmission line characteristics should be studied further to find answers to the wide variations in apparent permittivity at discrete frequencies.

2. More work can be done on the shaping of the EM field for instantaneous measurement of moisture. For example a strip line version of the "skew" transmission line could be used for this purpose. Computer based simulations of the electromagnetic field would be beneficial.

3. There certainly is scope for further refinement of many of the aspects covered in this study. It should again be emphasised that the study importantly and necessarily covered a relatively wide range of disciplines, which invariably reduces the depth that could be achieved in each one of the areas.

References

Ahmet K, Buenfeld N, Dill M and Hammersley G, 1999, "The Long-term Monitoring of Moisture in Concrete Structures", *Project report for the Concrete Bridge Development Group (CBDG).*

Anderson J C (1964), *Dielectrics*, Chapman and Hall Ltd

Bentz D P, Garboczi E J, Haecker C J and Jensen O M, (1999), "Effects of cement particle size distribution on performance properties of Portland cement based materials", *Cement and Concrete Research*, **29,** (10), 1663-1671.

Collin R E (1966), *Foundations of Microwave Engineering*, McGraw-Hill Physical and Quantum Electronics Series, 15-20.

Consolati G, Dotelli G and Quasso F, (2001), "Drying and Rewetting of Mature Cement Pastes Studied through Positron Annihilation Lifetime Spectroscopy", *J. American Ceramic Society*, **84,** (1).

Dai G, (1999), *Measuring and Monitoring Moisture Content of Timber and Investigation of Sorption Processes*, PhD Thesis, University of Luton.

Daschner D F, Knöchel R, Kupfer K, (2001), "Resonator Based Microwave Moisture Meter with Digital Phase Signal Processing", *Proceedings of Fourth International Conference on Electromagnetic Wave Interaction with Water and Moist Substances*, Weimar, Germany, 125-132.

Dunster A (2000), Personal communfication, Luton, September 2000.

Fagerlund G, (1999) "Service Life with regard to Frost Attack – a Probalistic Approach", *Procedures 8th Internat. Conference On Durability of Building Materials and Components*, Vancouver, **2**, 1268-1279,

Fagerlund G, (1996), "Moisture Mechanics as a Tool for Service Life Prediction", *Proc. of the 7th Internat. Conf. on Durability of Building Materials and Components*, Stockholm, **1**, 21-32.

Garboszi E J and Bentz D P, (1992), "Computer Simulation of the Diffusivity of Cement-Based Materials", *Journal of Material Science*, **27**, 2083-2092

Gartner E M, Gaidis J M, (1989), *Materials Science of Concrete,* **1**, Westerville.

Glay D, Lasri T, Mamouni A and Leroy Y (2001), "Free space Moisture Profile Measurement", *Proceedings of Fourth International Conference on Electromagnetic Wave Interaction with Water and Moist Substances*, Weimar, Germany, 235-242.

Göller A, (2001), "Getting 2D and 3D Moisture Distribution by Microwave Measurements", *Proceedings of Fourth International Conference on Electromagnetic Wave Interaction with Water and Moist Substances*, Weimar, Germany, 282-290.

Halse M R and Strange J H, (1999), "Broad-Line MRI & MAS NMR Characterisation of Portland Cement: Water & Chloride Mobility & Control", Summary Report Grant GR/K71660.

Hammersley G P and Dill M J (1998), "The long-term monitoring of civil engineering and building structures- development in techniques for monitoring corrosion in reinforced and post-tensioned concrete", *Proc of Inst of Mech Engineers*, 212, Part 1.

Hedenblad D (1996), "Moisture Properties of Some Building Materials". *Proc. Of the 7th Internat. Conf. On Durability of Building Materials and Components*, Stockholm.

Hobbs P V (1974), *Ice Physics*, Oxford University Press.

Jachowicz R S (1999), "Moisture Content Measurement in Solids – Limitations and Improvements with Modern Technology", *Collection of papers, Third workshop on Electromagnetic Wave Interaction with Water and Moist Substances*, Athens, Georgia, 32-41.

Jazayeri S, (1999), *Measuring and Monitoring of Moisture Content in Timber and Investigations of Moisture Gradients Using Dielectric Measurements*, Doctoral Thesis, University of Luton.

Jazayeri S and Ahmet K, (1999), "Moisture gradient studies in timber by the measurement of dielectric parameters using a multiple electrode arrangement", *Collection of papers, Third workshop on Electromagnetic Wave Interaction with Water and Moist Substances*, Athens, Georgia, 148-152.

Jordan E C (1962), *Electromagnetic Waves and Radiating Systems*, Constable and Co Ltd.

Joshi K K, Pollard R D, (2001), "Microstrip Resonator Technique for Non-destructive Moisture/Permittivity Measurement", *Proceedings of Fourth International Conference on Electromagnetic Wave Interaction with Water and Moist Substances*, Weimar, Germany, 151-155.

Kupfer K. (1999), "Methods and devices for density-independent moisture measurement", *Collection of papers, Third workshop on Electromagnetic Wave Interaction with Water and Moist Substances*, Athens, Georgia, 11-19.

Kupfer K (2001), Opening address, *Proceedings of Fourth International Conference on Electromagnetic Wave Interaction with Water and Moist Substances*, Weimar, Germany.

Lasri T, Glay D, Mamouni A and Leroy Y (1999), "Free Space Moisture Measurement of Cellular Concrete", *Collection of Papers, Third workshop on Electromagnetic Wave Interaction with Water and Moist Substances*, Athens, Georgia, 184-188.

Leschnik W and Schlemm U (1999), "Measurement of moisture and salt content of building materials", *Collection of papers, Third workshop on Electromagnetic Wave Interaction with Water and Moist Substances*, Athens, Georgia, 189-193.

Leschnik W and Schlemm U (2001), "Measurement of the Complex Permittivity of Building Materials at 2.45 GHz. Independence on Moisture Content, Salt Content and Temperature", *Proceedings of Fourth International Conference on Electromagnetic Wave Interaction with Water and Moist Substances*, Weimar, Germany, 274-281

Malvino A P (1979), *Electronic Principles*, Tata McGraw-Hill, p544.

Nelson S O (1991), "Dielectric Properties of Agricultural Products", *IEEE Transactions on Electrical Insulation*, **26**, 5, 845-869.

Nelson S O, Kraszewski A W, Lawrence K C and Trabelsi S (1999), "Fifteen years of research on moisture content determination in cereal grains", *Collection of papers, Third workshop on Electromagnetic Wave Interaction with Water and Moist Substances*, Athens, Georgia.

Neville A M (1995), *Properties of Concrete*, Pitman.

Parrott L J, (1990), "Review of methods to determine the moisture conditions in concrete", *British Cement Association*, Dec 1990.

Powers T C, Copeland J C, Hayes J C and Mann H M, (1956), "Permeability of Portland Cement Paste", *Journal of the American Concrete Institute*, **51**, 285-289.

Richards L A, (1928), "The Usefulness of Capillary Potential to Soil-moisture and Plant Investigators", *Journal of Agricultural Research*, **37**, 719-742

Rouleau J F, Goyette J and Bose T K (1999), "Dielectric Study on Dynamical Structure in Moist Materials using Dielectric Resonator", *Collection of Papers, Third workshop on Electromagnetic Wave Interaction with Water and Moist Substances*, Athens, Georgia, 97-101.

Schmugge T J and Jackson T J, (1999), "Microwave Remote Sensing of Soil Moisture", *Collection of Papers, Third workshop on Electromagnetic Wave Interaction with Water and Moist Substances*, Athens, Georgia, 42-46.

Scott B J and Or D (2001), "Thermal and Geometrical Effects on Bulk Permittivity of Porous Mixtures Containing Bound Water", *Proceedings of Fourth International Conference on Electromagnetic Wave Interaction with Water and Moist Substances*, Weimar, Germany, 46-53.

Taylor, (1997), *Cement Chemistry*, Thomas Telford ed., pp231-237.

Tsentsiper B, (2001), "One-sided Microwave Sensors", *Proceedings of Fourth International Conference on Electromagnetic Wave Interaction with Water and Moist Substances*, Weimar, Germany, 156-164

Vaz C M P and Hermann P S P, (1999), "Development of time domain reflectometry probes for combined use with a cone penetrometer", *Collection of papers, Third workshop on Electromagnetic Wave Interaction with Water and Moist Substances*, Athens, Georgia, 161-165.

Venkatesh M S and Raghavan G S V, (1999), "Dielectric properties measurement using a cavity perturbation technique", *Collection of papers, Third workshop on Electromagnetic Wave Interaction with Water and Moist Substances*, Athens, Georgia, 194-198.

Völgyi F, (1999), "Quality Forecast of Plaster Boards using a Microwave Monitoring System", *Collection of papers, Third workshop on Electromagnetic Wave Interaction with Water and Moist Substances*, Athens, Georgia, 102-106.

Völgyi F, (2001), "Microstrip Sensors used in Microwave Aquametry", *Proceedings of Fourth International Conference on Electromagnetic Wave Interaction with Water and Moist Substances*, Weimar, Germany, 135-142.

Weast R C, (1986), *CRC Handbook of Chemistry and Physics*, CRC Press, Boca Raton, FL

Weydert R and Gehlen C, (1999), "Electrolytic Resistivity of Cover Concrete: Relevance, Measurement and Interpretation", *The 8th Durability of Building Materials & Components (DBMC) conference papers*, Vancouver, 409-419.

Wisniewski A, (1999), "A practical method of measuring moisture using an insulated dipole", *Collection of papers, Third workshop on Electromagnetic Wave Interaction with Water and Moist Substances*, Athens, Georgia, 143-147.

Wolter B, (2001), "Determination of Density and Moisture Distribution in Chip Boards with One-Sided Access Nuclear Magnetic Resonance (OSA-NMR)", *Proceedings of Fourth International Conference on Electromagnetic Wave Interaction with Water and Moist Substances*, Weimar, Germany, 316-324.

Woodhead I, Buchan G, Kulasir D and Christie J, (2001), "Non-Invasive Measurement of Moisture Distribution using TDR", *Proceedings of Fourth International Conference on Electromagnetic Wave Interaction with Water and Moist Substances*, Weimar, Germany, 143-150.

Zaghloul M S, Taha T E, El-Shenawy K, Moustfa A H, (1999), "Computer Aided Design for Surface Acoustic Wave Liquid Sensors", *Collection of Papers, Third workshop on Electromagnetic Wave Interaction with Water and Moist Substances*, Athens, Georgia, 112-116.

Zhang Y and Okamura S, (1999), "New moisture measurement method for timber using two microwave phase shifts", *Collection of papers, Third workshop on Electromagnetic Wave Interaction with Water and Moist Substances*, Athens, Georgia, 47-51.

Appendix A. Derivation of the Formula for Capillary Pressure

The formula for capillary pressure can be found from first principles as follows:

Consider a capillary tube of radius r with one end in water as shown in Figure A-1.

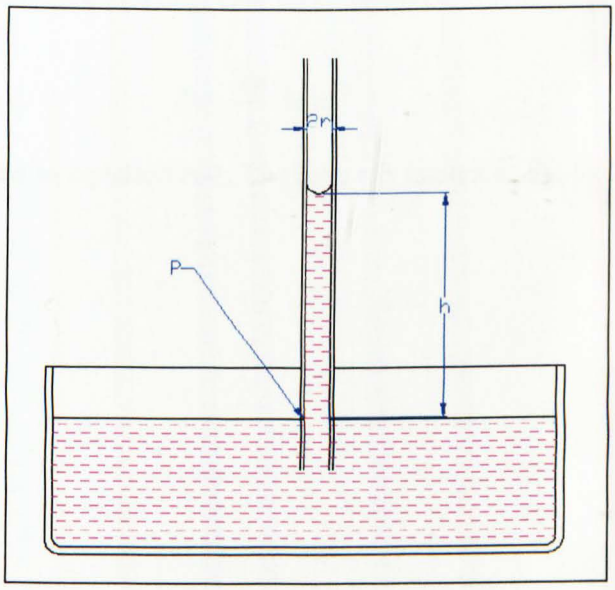

Figure A-1 Capillary tube of radius *r* in water

The pressure at point P inside the tube is at normal atmospheric pressure. The water column in the tube is subjected to a negative or 'suction' pressure drawing it up into the tube. This is caused by the adhesion force between the liquid and the solid at the liquid to solid interface at the top of the tube. The adhesion force γ is a force per unit length (N m^{-1}) of the interface, in this case $2\pi r\gamma$.

The pressure P just below the surface is this adhesion force divided by the cross sectional area of liquid in the tube.

$$P = \frac{2\pi r\gamma}{\pi r^2}$$

$$= \frac{2\gamma}{r} \text{ N m}^{-2} \qquad \textbf{Equation A-1}$$

Note that if the capillary tube was in the form of a thin vertical slit, width r and any length d, the capillary pressure can be calculated using the same argument before as follows:

$$P = \frac{2\gamma(d+r)}{dr} \text{ N m}^{-2}$$

If $d >> r$, then $d + r \approx d$ and the value for P becomes

$$P = \frac{2\gamma}{r} \text{ N m}^{-2}$$

which is the same as equation A-1. The term r is known as the hydraulic radius.

Appendix B. Complex permittivity and the Debye equation

B.1. Complex permittivity

Ignoring for the moment the effect of the relaxation time τ, any capacitor with a non-ideal dielectric will have some conductivity. The resultant leakage current is entirely due to the characteristic of the dielectric and therefore the dielectric constant is characterised by an in-phase component of the dielectric in addition to the normal 90 degree out of phase component of the capacitive reactance. This effect can be represented by a complex permittivity (Anderson J C, 1964).

$$\varepsilon_r = \varepsilon' - j\varepsilon'' \qquad \textbf{Equation B-1}$$

When an alternating EMF v is applied across a capacitor, the electric current i will be given by:

$$i = j\omega\, \varepsilon_r C_0 v \qquad \textbf{Equation B-2}$$

The complex permittivity from Equation 4-6 will make this

$$i = j\omega\,(\varepsilon' - j\varepsilon'')C_0 v \qquad \textbf{Equation B-3}$$

Converting it into real and imaginary parts by multiplying out,

$$i = \omega\varepsilon'' C_0 v + j\omega\varepsilon' C_0 v \qquad \textbf{Equation B-4}$$

The ε'' component is then defined as the in-phase or "loss" component of the complex permittivity.

It is conventional to describe the performance of a capacitor in terms of its loss angle δ, which is the phase angle between the total current I, and the quadrature component of the current. The tangent of this angle is known as the loss tangent. The smaller the loss tangent, the lower the losses because the real part is smaller. Therefore

$$\tan\delta = \frac{\text{real part}}{\text{imaginary part}}$$

$$\tan \delta = \frac{\varepsilon'}{\varepsilon''} \qquad \textbf{Equation B-5}$$

A more rigorous treatment of complex permittivity is given by Collin R E (1966) that requires no assumed conduction (leakage) current in the capacitor. Consider an atom with total charge of the electrons $-q$ appearing as a cloud around the nucleus of charge q. If an electric field E_x in the x direction is applied there will be a distortion of the atoms to create effective electric dipoles as shown in Figure 4-1

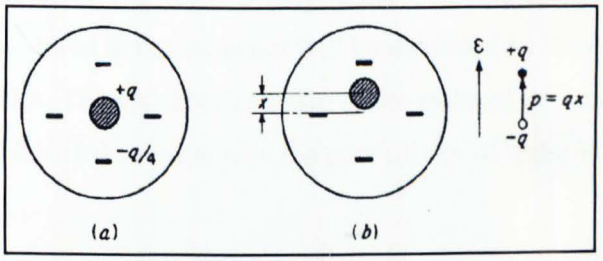

Figure B-1 Model for determining the polarisation of an atom
(extracted from Collin, 1966)

The electric field E_x will displace the electron cloud a distance x and it is resisted by a restoring force kx proportional to the distance. If m is the effective mass of the electrons, the dynamic equation of motion will take into account the inertial effect proportional to the acceleration $\frac{d^2x}{dt^2}$ and the viscous force $m\eta$ proportional to the viscosity η, and the velocity $\frac{dx}{dt}$, the dynamic equation of motion becomes,

$$m\frac{d^2x}{dt^2} + m\eta\frac{dx}{dt} + kx = -q\mathcal{E} \qquad \textbf{Equation B-6}$$

when $\mathcal{E} = E_x \sin\omega t$, the solution for Equation 4-11 is in the form $x = -A\cos(\omega t + \phi)$.

The phase difference indicated by ϕ is therefore present even in the absence of a conduction current (zero conductivity).

B.2. Relaxation Processes in Dielectrics

Anderson (1964) divides dielectric materials into three main types.

1 Non-polar materials which show variations in permittivity in the optical region.

2 Polar materials that show variation in permittivity in the infrared as well as the optical region.

3 Dipolar materials which also show orientational polarisation.

An expression for the relaxation time of a water molecule was derived in section B.1. If a dipolar material like water is used as the dielectric of a capacitor, the amount of charge stored in the capacitor will be increased by the charged needed to orient the dipoles. The dielectric constant of the material will increase significantly and this is the reason why the permittivity of water is relatively high ($\varepsilon_r \approx 80$ at 25 °C).

The orientation of the dipole in a changing electric field is not a step function after a time lag equal to the relaxation time. Debye proposed that this time lag would be in the form

$$\varepsilon_t = \varepsilon_s \, e^{\frac{-t}{\tau}} \qquad \textbf{Equation B-7}$$

where

ε_t is the relative permittivity at a time t

ε_s is the static relative permittivity

τ is defined as the relaxation time of the material

The term 'relaxation time' is used because it is regarded as the time taken from the moment the applied field is removed until all the dipoles are again orientated randomly (relaxed). According to Debye's proposed model the reorientation will be an exponential function and the relaxation time will be the time constant of the exponential function (time taken if the initial rate of change was maintained).

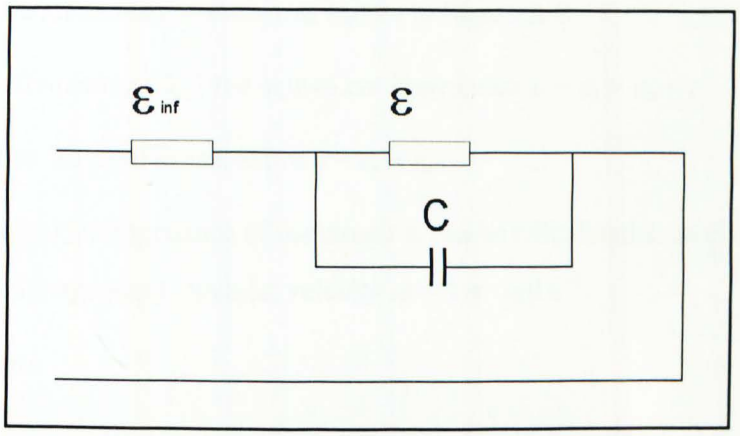

Figure B-2 Equivalent circuit of relaxation phenomena in a dielectric

Consider a theoretical capacitor with water as dielectric. The moment a voltage is applied, the water molecules will still be in a random position and the permittivity will be ε_∞ as this will be the permittivity at a frequency too high for the molecules to change orientation. As the water molecules align themselves with the electric field, the charge stored increases considerably and the apparent dielectric constant or relative permittivity will increase by an order of magnitude to the value ε_s, the static relative permittivity. The relaxation time τ is similar to the time constant in an RC circuit and an equivalent circuit shown in Figure B-2 can be drawn.

B.3. Equivalent Circuit Model of Complex Permittivity and the Debye Equation

The model proposed by Debye leads to an equivalent circuit consisting of a capacitor C where the instantaneous impedance (voltage divided by instantaneous current) at any moment is proportional to the relative permittivity. When a voltage (electric field) is applied across a dielectric the permittivity changes from ε_∞ initially to ε_s in the steady state condition. It can be regarded as equivalent to a change in instantaneous impedance of a circuit containing a capacitor that changes from an initial value equivalent to ε_∞ to a steady state value equivalent to ε_s. The relative permittivity ε_s is the steady state impedance and ε_∞ is the impedance at an frequency high enough for the impedance of the capacitor C to be negligible.

This is equivalent to a circuit with a resistor ε_∞ in series with a capacitor C in parallel with another resistor ε as shown in Figure B-2.

At zero frequency (DC) the equivalent impedance $\varepsilon_r = \varepsilon_s = \varepsilon_\infty + \varepsilon$

Therefore the parallel resistance $\varepsilon = \varepsilon_s - \varepsilon_\infty$

The equivalent impedance of the circuit ε_r can be calculated assuming an applied signal of frequency f, angular velocity $\omega = 2\pi f$ rad s^{-1}.

Therefore

$$\varepsilon_r = \varepsilon_\infty + \frac{1}{\frac{1}{\varepsilon_s - \varepsilon_\infty} + j\omega C}$$

$$= \varepsilon_\infty + \frac{(\varepsilon_s - \varepsilon_\infty)}{1 + j\omega C(\varepsilon_s - \varepsilon_\infty)} \qquad \textbf{Equation B-8}$$

In the equivalent circuit, the relaxation time must be the equivalent of the time constant (RC) of the parallel part of the circuit where the resistance $\varepsilon = \varepsilon_s - \varepsilon_\infty$ and the time constant τ is given by:

$$\tau = (\varepsilon_s - \varepsilon_\infty)C \qquad \textbf{Equation B-9}$$

Equation B-8 becomes

$$\varepsilon_r = \varepsilon_\infty + \frac{(\varepsilon_s - \varepsilon_\infty)}{1 + j\omega\tau} \qquad \textbf{Equation B-10}$$

Equation B-10 can be written as a complex permittivity (Debye equation)

$$\varepsilon_r = \varepsilon' - j\varepsilon'' \qquad \textbf{Equation B-11}$$

where

$$\varepsilon' = \varepsilon_\infty + \frac{(\varepsilon_s - \varepsilon_\infty)}{1 + \omega^2\tau^2} \qquad \textbf{Equation B-12}$$

and

$$\varepsilon'' = \frac{(\varepsilon_s - \varepsilon_\infty)\omega\tau}{1+\omega^2\tau^2} \qquad \textbf{Equation B-13}$$

The graph of real and imaginary relative permittivity as calculated from equations B-12 and B13 can be plotted for water taking $\tau = 9.2\times10^{-12}$ s. The graph is shown in Figure B-3

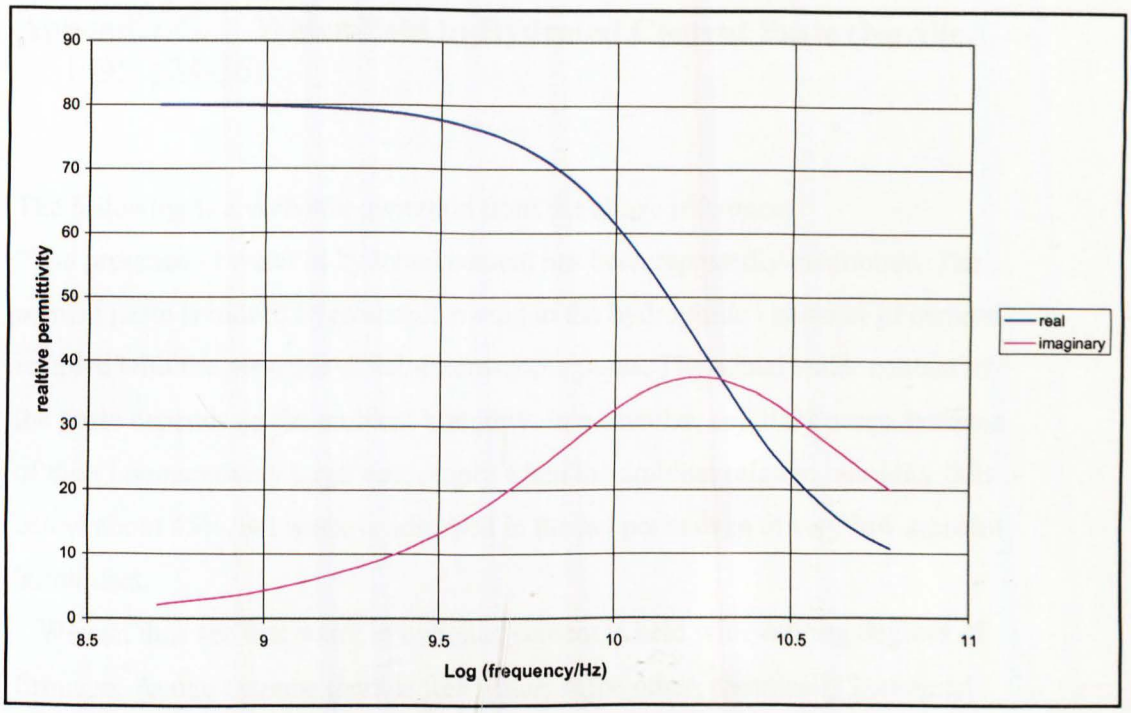

Figure B-3 Calculation of the relative real and imaginary permittivity of water.

Refer to **Figure 4-2** for details.

Appendix C. Water Held in Hydrated Cement Paste (Neville, 1995, p34-36)

The following is a *verbatim* quotation from the above reference.

"The presence of water in hydrated cement has been repeatedly mentioned. The cement paste is indeed hygroscopic owing to the hydrophilic character of cement coupled with the presence of sub-microscopic pores. The actual water content of the paste depends on the ambient humidity. In particular, capillary pores, because of their comparatively large size, empty when the ambient relative humidity falls below about 45%, but water is adsorbed in the gel pores even at very low ambient humidities.

We can thus see that water in hydrated cement is held with varying degrees of firmness. At one extreme there is free water; at the other, chemically combined water forming a definite part of the hydrated compounds. Between these two categories there is gel water held in a variety of other ways.

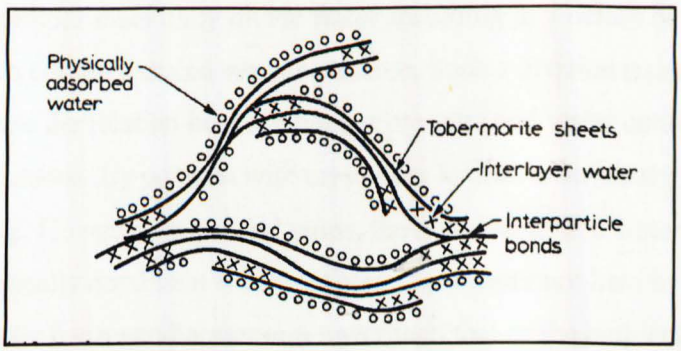

Figure C-1 Probable structure of hydrated silicates
(extracted from Neville, 1995)

The water held by the surface forces of the gel particles is called adsorbed water, and that part of it which is held between the surfaces of certain planes in a crystal is called interlayer or zeolitic water. Lattice water is that part of the water of crystallisation associated with the principal constituents of the lattice. The diagrammatic representation of Figure C-1 may be of interest.

Free water is held in capillaries and is beyond the range of the surface forces of the solid phase.

There is no technique available for determining how water is distributed between these different states, nor is it easy to predict these divisions from theoretical considerations as the energy of binding of combined water in the hydrate is of the same order of magnitude as the energy of binding of the adsorbed water. However, recent investigations using the nuclear magnetic resonance technique suggest that gel water has the same energy of binding as interlayer water in some swelling clays; thus the gel water may well be in interlayer form.

A convenient division of water in the hydrated cement, necessary for investigation purposes, though rather arbitrary, is into two categories: evaporable and non-evaporable. This is achieved by drying the cement paste to equilibrium (i.e. to a constant weight) at a given vapour pressure. The usual value is 8×10^{-3} mm of mercury. More recently, drying in an evacuated space which is connected to a moisture trap held at –79 °C has been used. Alternatively, the evaporable water can be determined by the loss upon drying at a higher temperature, usually 105 °C, or by freezing out, or by removing with a solvent.

All these methods essentially divide water according to whether or not it can be removed at a certain reduced vapour pressure. Such a division is performed arbitrary because the relation between vapour pressure and water content of cement is continuous. By contrast with crystalline hydrates, no breaks occur in this relationship. However, in general terms, the non-evaporable water contains nearly all chemically combined water and also some water not held by chemical bonds. This water has a vapour pressure lower than that of the ambient atmosphere and the quantity of such water is in fact a continuous function of the ambient vapour pressure.

The amount of non-evaporable water increases as hydration proceeds, but in a saturated paste non-evaporable water can never become more than one-half of the total water present. In well-hydrated cement the non-evaporable water is about 18 % by weight of the anhydrous material; this proportion rises to about 23 per cent in fully hydrated cement). It follows from the proportionality between the amount of non-evaporable water and the solid volume of the cement paste that the former volume can be used as a measure of the quantity of the cement gel present, i.e. of the degree of hydration.

The manner in which water is held in a cement paste determines the energy of binding. For instance, 1670 Joules (400 calories) are used in establishing the bond of 1 gram of non-evaporable water, while the energy of the water of crystallisation of $Ca(OH)_2$ is 3560 J g^{-1}. Likewise, the density of the water varies; it is approximately 1.2 for non-evaporable, 1.1 for gel, and 1.0 for free water. It has been suggested that the increase in the density of the adsorbed water at low surface concentrations is not the result of compression but is caused by the orientation of the molecules in the adsorbed phase due to the action of the surface forces."

Appendix D. The Smith Chart

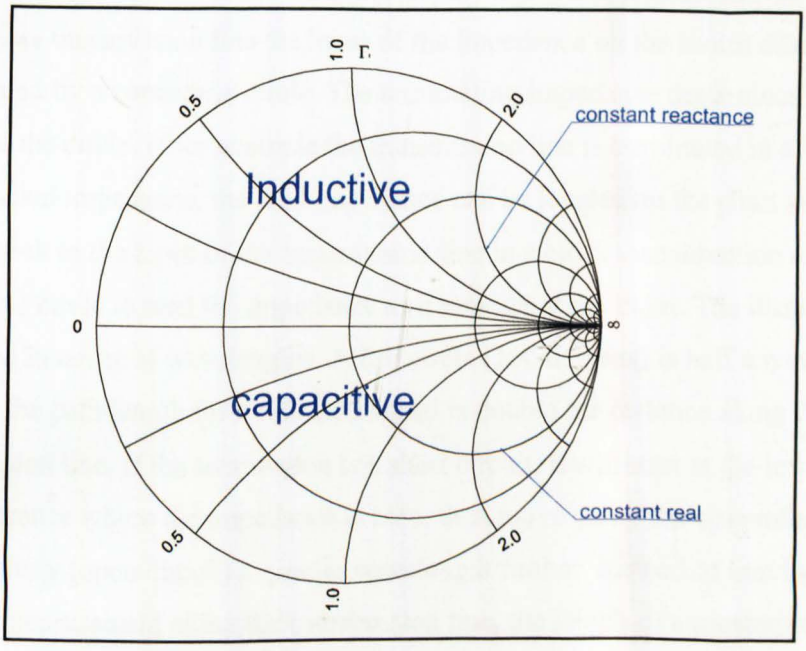

Figure D-1 Smith Chart
showing the inductive and capacitive regions as well as the lines of constant real and imaginary impedance

The Smith chart shown in Figure D-1 is designed to indicate the impedance of a transmission line at any point along the line as the point of interest is moved from source to load or vice versa. The impedance, which can go from zero to infinity, is limited to a finite area inside a circle and any complex impedance can be read off inside this circle. Impedance is shown as inductive above the diagonal line and capacitive below the line with the constant reactive lines as shown in the Figure D-1. The reactive lines are sections of circles inside the main circle with centres on the vertical line running through the point of infinity with radii decreasing with increasing reactance. Infinite reactance will thus be on the point of infinite impedance as shown. The real part of the impedance changes from zero on the outside circumference and is a family of circles as shown with decreasing radius

as the resistance increases. The family of circles all touch the right hand infinity point so that at infinite resistance (open circuit) the circle will have a zero radius and will be on the point of infinite impedance as shown in Figure D-1. A normal Smith chart will indicate the impedance normalised to the characteristic impedance of the transmission line with 1, the normalised characteristic impedance, at the centre of the main circle. As the point of interest moves along the lossless transmission line the locus of the impedance on the Smith chart is represented by a concentric circle. The terminating impedance determines the radius of the circle. If for example the transmission line is terminated in a load of some known impedance, the load impedance can be located on the chart and then moved back to the input of the transmission line in a clockwise direction along a concentric circle to read the impedance as it appears at the input. The distance is measured in terms of wavelengths. A full circle (360 degrees) is half a wavelength because the path length for a reflected signal is double the distance along the transmission line. If the termination is a short circuit, it will start at the left on the circumference where the impedance is zero, then move along the circumference to reach infinity (open circuit) a quarter wavelength further. Instead of moving the point of measurement along the transmission line, the length of a transmission line terminated in a fixed load (short circuit for example) can be changed in order to change the impedance at the input. This input impedance is read off the chart for varying lengths of transmission line.

Appendix E. Transmission line characteristics of the cage-coaxial line in air

The cage coaxial transmission line is used directly in the collector circuit of the oscillator transistor as a "tuning stub" in the short circuit termination mode at a frequency where the line length is less than $\lambda/4$ long. It is thus only used in short-circuit terminated mode. The input impedance will therefore be given by:

$$Z_{in} = Z_0 \tan\phi \qquad \textbf{Equation E-1}$$

where

Z_{in} = input impedance (ohm)

Z_0 = characteristic impedance (ohm)

ϕ = phase difference (radians) between the input of the transmission line and the phase at the termination (load) and equal to βl in Equation 7-2 where l is the length of the line in metre and β the phase constant in rad m^{-1}.

The phase change due to the reflected signal from the termination can be measured on the HP 8752 C network analyser at any required frequency as shown in Figure E-1. Note that the required phase angle ϕ in Equation E-1, is the compliment of the angle indicated on the HP 8752 C network analyser (about 123° at marker 2 for example) divided by 2. At marker 2 the required angle will therefore be,

$$\phi = \frac{180 - 123}{2} \text{ degrees}$$

$$= 28.5°$$

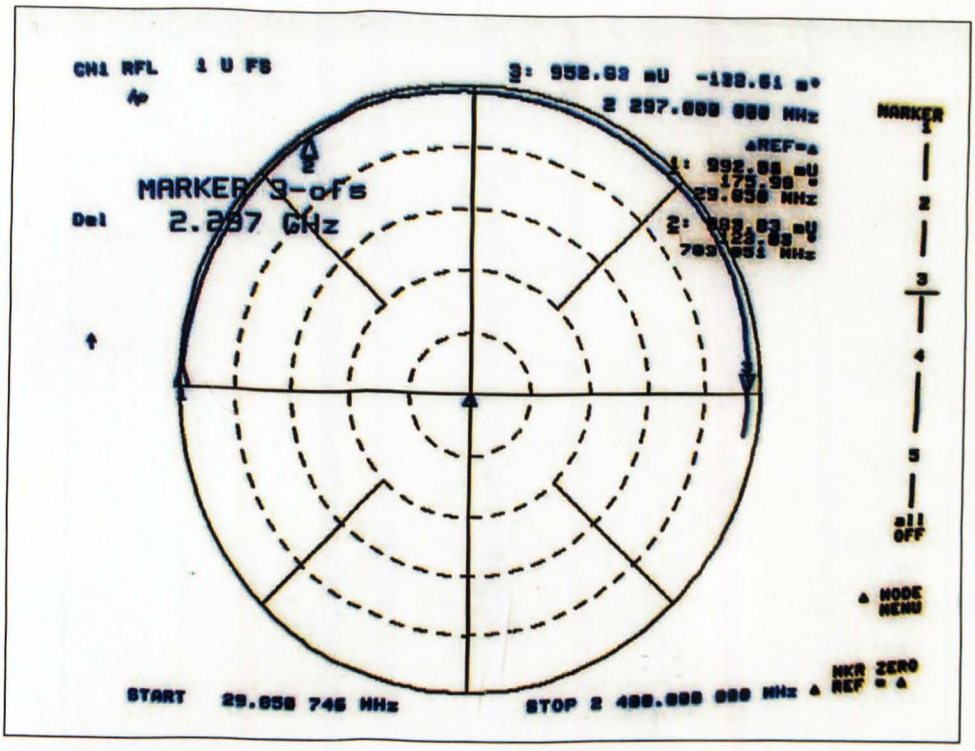

Figure E-1. Phase and amplitude display of the reflected signal on the HP 8752C of a 30 mm cage-coaxial transmission line in air.

Marker 3 is at the $\lambda/4$ point at 2.297 GHz. The standing wave ratio at this point is 1/(1-0.953) = 21.3 due to the short circuit termination and even higher at the lower frequencies.

The standing wave ratio at the input of the transmission line at the quarter wavelength frequency is determined from the amplitude of the reflected signal indicated as 952.8 mU or 0.9528, from which the standing wave ratio is calculated as follows:

$$\text{Standing wave ratio} = \frac{1}{1-0.953} = 21.3.$$

From Figure E-1 it is clear that the standing wave ratio will be even higher at frequencies below 2.297 GHz and is due to the fact that the line is permanently terminated in a short circuit and not the characteristic impedance that will give a standing wave ratio of 1.

The input impedance determined by Equation E-1 can be measured directly on the HP 8752C network analyser as shown in Figure E-2.

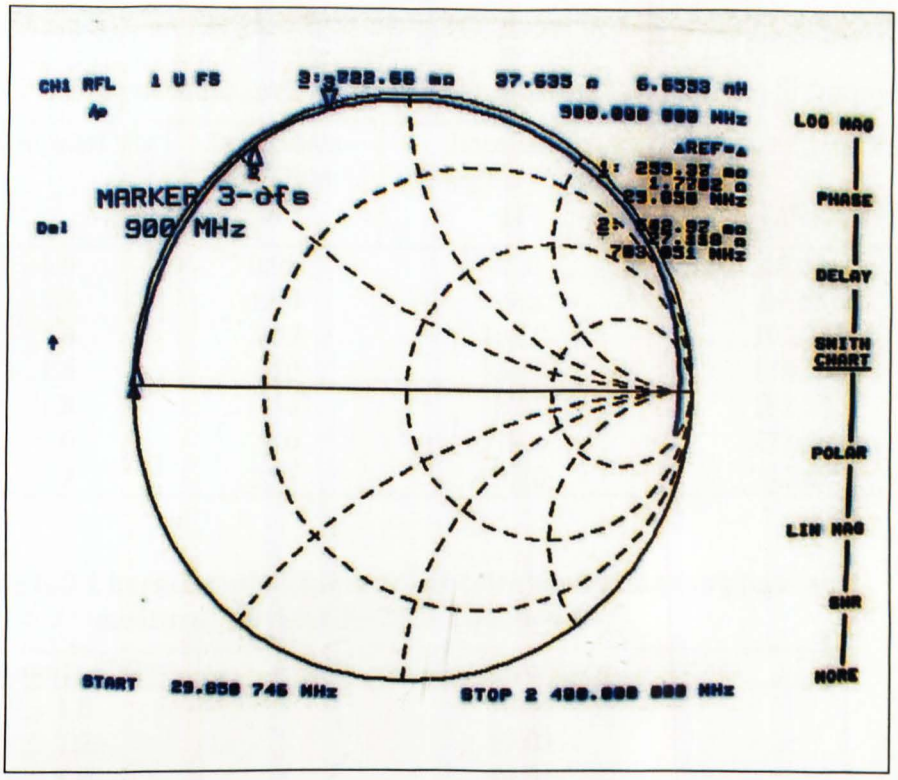

Figure E-2 Impedance locus of input impedance of the 30 mm cage-coaxial transmission line in air on the HP 8752C network analyser.

For example the impedance at 900 MHz (marker 3) can be read off directly as 0.72 + j37.6 or an inductance of 6.6553 nH.

The effective length of the line can be determined from the results shown in Figure E-1. With the transmission line a quarter wavelength long at 2.297 GHz, the effective line length l in air, assuming a propagation velocity of 3×10^8 m s^{-1} is:

$$l = \frac{3\times10^8}{4\times2.297\times10^9} \text{ m}$$

$$= 32.65 \text{ mm}$$

The measured electrical length in air is thus slightly longer in than the physical length of 30 mm, probably due to end effects at the short circuit termination. Table E-1 shows the impedance as measured at discrete frequencies (see Figure E-2). From the phase angle measurements (Figure E-1), the impedance from Table E-1 and using Equation E-1, the characteristic impedance of the transmission line can be calculated.

Table E-1 Input impedance of 30mm transmission line at discrete frequencies

Frequency/GHz	Impedance real/Ohm X	Impedance imaginary/Ohm jY	modulus Z_{in} in Ohm $\lvert Z_{in}\rvert=(X^2+Y^2)^{1/2}$
1.0	0.98	46.0	46.01
1.2	1.90	69.6	69.63
1.4	3.50	102.7	102.76
1.6	4.50	138.3	138.37
1.8	8.50	182.0	182.20
2.0	24.0	270.0	271.06
2.2	230	695.0	732.07

Table E-2 Characteristic impedance as calculated using the phase angle measured (divided by 2) in Equation E-1

Frequency/GHz	Characteristic impedance Z_0 in ohm
1.0	50.04
1.2	50.03
1.4	50.01
1.6	49.95
1.8	50.19
2.0	49.75
2.2	47.98

The results of the characteristic impedance calculations are shown in Table E-2.

The characteristic impedance starts to deviate from the ideal $Z_0\tan\phi$ (Equation E-1) close to the quarter wavelength point ($\phi=\pi/2$) in a physical transmission line due to the more pronounced effect of even small transmission losses. For example at the quarter wavelength point $\tan\phi\rightarrow\infty$ when $\phi=\pi/2$, whilst the locus of the impedance of the physical line as seen in Figure E-2 does not go through the point of infinite impedance on the Smith chart.

Appendix F. Worked example of typical data conversion to graphs (Figure 5-7 in the example)

F.4. Calculation of moisture content

Net volume of mortar filler in transmission line: total measured volume – volume of conductors = 9.9 cm^3

Oven dried gross dry mass of mortar filled transmission line M_d = 30.925 g

Gross mass of line with moisture M_m g.

Net mass of moisture = ($M_m - M_d$) g = volume of water (moisture) with SG of water = 1

Percentage moisture content (volumetric) $MC_v = \frac{M_m - M_d}{\text{net volume of mortar}} \times 100\ \%$

F.4. Calculation of relative permittivity

Measured TDR delay with 50 mm transmission line without filler (air) t_0 = 334 ps

Measured TDR delay with filler and moisture t_r

From equation 4-18, $\varepsilon_r = \left(\frac{t_r}{t_0}\right)^2$

Table F-1 Data and calculated values for graph of Figure 5-7.

Gross mass M_m /g	Mass water $M_m - M_d$ /g	Moisture content MC_v	Delay measured t_r /ps	Relative permittivity ε_r
32.187	1.262	12.75%	975	8.52
32.069	1.144	11.56%	942	7.95
31.916	0.991	10.01%	924	7.65
31.869	0.944	9.54%	918	7.55
31.69	0.765	7.73%	889	7.08
31.57	0.645	6.52%	872	6.82
31.481	0.556	5.62%	855	6.55
31.391	0.466	4.71%	846	6.42
31.273	0.348	3.52%	816	5.97
31.228	0.303	3.06%	805	5.81
31.17	0.245	2.47%	797	5.69
31.148	0.223	2.25%	787	5.55
31.088	0.163	1.65%	775	5.38
31.053	0.128	1.29%	766	5.26
31.015	0.09	0.91%	758	5.15
30.967	0.042	0.42%	753	5.08